



Chair:
Prof. Marco Finazzi

DOCTORAL PROGRAM IN PHYSICS

The Doctoral Program in Physics at Politecnico di Milano aims at attracting bright students with good scientific background and clear interest towards development and applications of new ideas and technologies. It offers a wide range of opportunities in the fields of advanced applied physics, such as photonics and optoelectronics (lasers, ultrafast optics), biomedical optics (optical tomography), vacuum technologies (thin film depositions), material technologies (microelectronics and nanotechnologies, micromechanical processing), and advanced instrumentation (electronic and atomic microscopy, nuclear magnetic resonance).

Scientific education and training to develop general research abilities in all areas of applied physics is increasingly needed by advanced technological companies. Through a general education in the basic areas of applied physics and a specific knowledge in condensed matter physics, as well as optics and lasers, the PhD Program aims at the development of an experimental approach to problem solving techniques and at the attainment of a high level of professional qualification.

The Doctoral Program has strongly experimental character. The contents are strictly related to the research activities carried out in the laboratories at the Department of Physics. They can be divided into two main areas:

- a) Condensed Matter Physics, including photoemission; spin-resolved electronic spectroscopy; magneto-optics; X ray diffraction; magnetic nanostructures for spintronics; synchrotron radiation spectroscopy, positron spectroscopy, semiconductor nanostructures.
- b) Photonics and Quantum Electronics, including ultrashort light pulse generation and applications; UV and X optical harmonics generation; biomedical applications of lasers; diagnostics for works of art; laser applications in optical communications; time domain optical spectroscopy and diagnostic techniques.

All research activities rely on advanced experimental laboratories located at Politecnico di Milano (Milano-Leonardo Campus and Como Campus) and are performed in collaboration with several international Institutions. Consistent effort is devoted to experimental research, development of

innovative approaches and techniques, and design of novel instrumentation.

The educational program can be divided into three parts: 1) Courses specifically designed for the PhD program as well transdisciplinary courses; 2) Activities pertaining to more specific disciplines which will lay the foundation for the research work to be carried out during the Doctoral Thesis; 3) Doctoral Thesis. The thesis work is the major activity of the Program. It has a marked experimental character and will be carried out in one or more laboratories at the Department of Physics.

The students are also encouraged to perform part of their thesis work in laboratories of other national or foreign Institutions. Collaborations that may involve the PhD students are presently active with several national and international research and academic Institutions, such as: ETH-Zürich, EPL-Lausanne, Lund Institute of Technology, University of Paris-Sud, Ecole Polytechnique-Paris, University of Berkeley, University of Cambridge, University College London, Massachusetts Institute of Technology, Harvard University, European Space Agency, ENEA, Elettra-Ts, PSI-Villigen, Agenzia Spaziale Italiana, European Synchrotron Radiation Facility (ESRF-Grenoble), IFN-CNR, IIT-Istituto Italiano di Tecnologia.

At present, the number of students in the three-year course is 106, and 100 of them have a fellowship.

The PhD Program Faculty, who takes care of organizing and supervising teaching and research activities, consists of members (listed here below), who are all highly qualified and active researchers covering a wide spectrum of research fields. This ensures a continuous updating of the PhD Program and guarantees that the students are involved in innovative research work.

FAMILY NAME	FIRST NAME	POSITION*
BASSI	ANDREA	AP
BERTACCO	RICCARDO	FP
BRAMBILLA	ALBERTO	AP
CAIRONI	MARIO	ST
CERULLO	GIULIO	FP
CICCACCI	FRANCO	FP
COMELLI	DANIELA	AP
CUBEDDU	RINALDO	FP
DALLERA	CLAUDIA	FP
D'ANDREA	COSIMO	FP
DELLA VALLE	GIUSEPPE	AP
DUÒ	LAMBERTO	FP
GAMBETTA	ALESSIO	AP
FINAZZI	MARCO	FP
GHIRINGHELLI	GIACOMO	FP
ISELLA	GIOVANNI	FP
LANZANI	GUGLIELMO	FP
LAPORTA	PAOLO	FP
MARANGONI	MARCO	FP
MORETTI	MARCO	AP
NISOLI	MAURO	FP
PETTI	DANIELA	AP
PICONE	ANDREA	AP
POLLI	DARIO	AP
RAMPONI	ROBERTA	FP
SCOTOGNELLA	FRANCESCO	AP
STAGIRA	SALVATORE	FP
TARONI	PAOLA	FP
TORRICELLI	ALESSANDRO	FP
ZANI	MAURIZIO	AP

*Position: FP = Full Professor; AP = Associate Professor.

DATA ENCODING AND PROCESSING FOR QUANTUM COMPUTING APPLICATIONS IN FINANCE

Gabriele Agliardi – Supervisor: Enrico Prati

Quantum computers have the potential to outperform classical computers in many problems. Their exploitation in practical applications, though, requires strong developments. We are in the so-called Noisy Intermediate-Scale Quantum Computing era, characterized on one hand by a number of qubits not allowing quantum circuits to be simulated on classical computers in reasonable time, but on the other hand by a limited quantum hardware scale and significant noise level. Consequently, current devices do not enable the exploitation of full error correction protocols and hence of the algorithms promising the highest speedups. Nevertheless, while hardware and algorithmic improvements proceed at an unprecedented rate, applicative users pursue the quest for practical use cases, that can run despite error, accepting a partial speedup.

In computational finance, quantum computers are considered promising for diverse workloads: from portfolio optimization to transaction settlement, from option pricing to risk analysis. Most of works in the scientific literature either focus on solutions implementable on current hardware, often

leading to unrealistic hypothesis or oversimplified models, or design long-term, bold use cases, assuming perfect hardware and neglecting the troubled path of current practical experiments.

In our work, we contribute to bridging such gap, starting from algorithms providing proven theoretical speedup on real-world problems, moving such applications from the abstract modeling level to the circuit implementation, and addressing the main challenges that arise at such level. Indeed, the state of the art in quantum computing does tolerate any inefficiency

accumulating along abstraction levels, but on the contrary demands circuit optimization across the full stack.

A major challenge that we tackle, is efficient data loading. It is known that in absence of specific data structures, the exact loading of a classical dataset requires a linear time in the dataset size, thus undermining the speedup of some quantum algorithms, and becoming the bottleneck in others. This opens the door for approximate data loading techniques, that typically accept a one-time costly pre-processing, in favor of an efficient loading

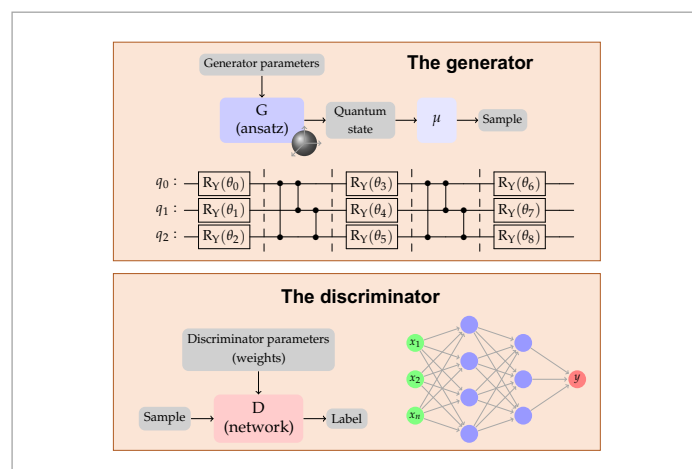


Fig.1 - Logical representation of a QGAN for data loading. The generator is a variational quantum circuit interchanging parametric rotations and entanglement layers. The discriminator is a classical neural network. The training process alternates a step of refinement of the generator parameters, and one of the discriminator weights. Source: Agliardi, G.; Prati, E. Optimal Tuning of Quantum Generative Adversarial Networks for Multivariate Distribution Loading. *Quantum Rep.* 2022, 4, 75-105.

circuit, under the hypothesis that the same input is reused multiple times. Among many proposed approaches, we focus our investigation on quantum artificial intelligence, and specifically on quantum Generative Adversarial Networks. We tune the hyperparameters of the network obtaining a 43-64% improvement compared to the state of the art. We pay close attention to multivariate distributions, of practical relevance in advanced financial use cases, and show that gradient free optimization (SPSA) methods cannot achieve results comparable to that of gradient-based methods (Adam AMSGRAD), thus calling for new advancements to support the scaling capability of qGANs.

The second challenge is efficient arithmetic manipulation. We propose a novel data representation that achieves sharper representation of floating-point random variables under a limited number of qubits, and reduces the circuit

depth needed for addition and multiplication. We achieve a circuit depth reduction up to 89% against prior representations.

The third contribution is about circuit compilation for real hardware. Before execution, a logically synthesized circuit needs to be adapted to the specific constraints given by the target hardware, such as available gates, topology, etc. Recent announcements of commercial companies introduced the future possibility to resort to multiple quantum chips connected by quantum communication channels, allowing for distributed quantum computing. Such opportunity, that opens disruptive scenarios in quantum processing capabilities, requires for specific compiling techniques, keeping into account the specific nature of distributed hardware, and the fact that the most critical resource becomes the creation of a remote entanglements. In this context, we formalize the problem

as a dynamic network flow, and exploit specific parallelization capabilities to further enhance results.

The work concurs in drawing the applicability of quantum computing to real-world problems closer. The results are applicable for instance to the financial problem of American option pricing, consisting of finding the fair price of a contract which allows the owner to buy or sell an underlying asset, such as a stock, at fixed price, in any time in the future before expiration. The possibility to exercise the option at any time represents a computational challenge, requiring intensive Monte Carlo simulations on classical computers. It is known that the execution time of Monte Carlo techniques can be quadratically improved on quantum devices by recurring to the so-called Quantum Amplitude Estimation and its variants. Our results also have implications beyond the boundaries of finance: we show that the same techniques can be exploited for other tasks that classically resort to Monte Carlo models, such as in particle physics.

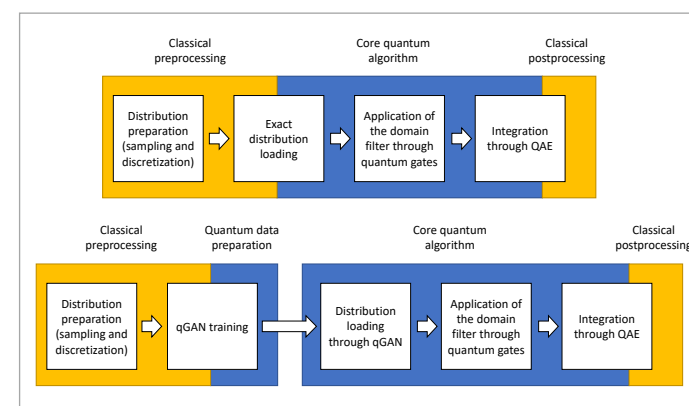


Fig.2 - A common framework for the application of distribution loading (with or without qGANs), data manipulation, and Monte Carlo sampling via Quantum Amplitude Estimation; here, the application is in particle physics. Source: Agliardi, G., et al. "Quantum integration of elementary particle processes." *Physics Letters B* 832 (2022): 137228.

ORTHOGONAL STACKING OF LIGAND MOLECULES FOR THE REALIZATION OF IN-VACUUM SUPRAMOLECULAR STRUCTURES

Guglielmo Albani – Supervisor: Alberto Calloni

In the last few decades, the scientific community has deeply focused on the realization of supramolecular complexes. This interest stems from the possibility to couple molecular sub-units in order to realize a more elaborated structure, which displays some specifically desired properties. Although the first reports regarding the realization of these complexes in solution date back in time, in the last few years much effort has been devoted to grow these supramolecular compounds in-vacuum on top of an inorganic surface. The purpose of my research is to build such kind of structures, at the same time exploiting the structural, electronic and magnetic properties of selected substrates, which are interesting for their application in electronic devices, such as Fe(001). The main issue relates to the influence of the substrate in the chemical, electronic and structural behavior of the molecules. This, in particular, affects the capability of the molecules to coordinate one another, either enabling or hindering the possibility of realizing any supramolecular structure. A long-standing expertise developed in the Physics department of Politecnico di Milano has demonstrated that the molecular

decoupling can be obtained by passivation of the Fe(001) surface in an O₂ atmosphere. Indeed, deposited molecules on the passivated iron surface can arrange themselves in an ordered array, whose symmetry is driven by the substrate below. During my PhD activity, I have mainly focused on the deposition onto the passivate iron surface [namely Fe- $\rho(1 \times 1)O$] of specific molecular ingredients, such as metal tetraphenyl porphyrins (MTPP, where M is a transition metal ion). These molecules are characterized by a planar tetrapyrrolic macrocycle, which is bounded to four peripheral phenyl groups, and which holds an inner metallic ion in its centre. It is widely reported that, in solution, MTPPs can be employed for the realization of supramolecular structures, since they can coordinate ligand molecules with the metal ion, in a direction which is strictly orthogonal with respect to their macrocycle. In order to investigate the feasibility for MTPPs deposited onto the Fe- $\rho(1 \times 1)O$ surface to coordinate other molecular species, I have added to the system a ligand molecule, namely dipyrindyl naphthalene diimide (DPNDI), which is composed by a naphthalene diimide group bounded to two pyridyl

terminations whose nitrogen atoms can be used as “hooks” to drive the molecular coordination. By a designed ordered deposition of MTPPs and DPNDIs, I was able to finally grow the in-vacuum supramolecular structure presented in Figure 1. The in-vacuum supramolecular structure is composed by a plane of ZnTPPs, which are displayed in an ordered array in a flat lying configuration, representing the “floor” of this organic building. Then, DPNDIs are grown on top of this basal plane of porphyrins, relying only on coordination chemistry. As predicted by the in-solution behaviour of these molecules, the pyridyl termination of DPNDI forms a covalent bond with the inner metallic ion of

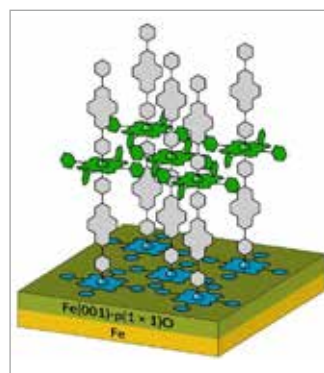


Fig.1 - In-vacuum supramolecular structure grown onto the Fe- $\rho(1 \times 1)O$ substrate, obtained by subsequent deposition of ZnTPP (blue) and CoTPP (green) linked by DPNDI ligands (grey).

ZnTPP. DPNDIs stand orthogonal to the tetrapyrrolic macrocycle and thus behave as pillars of the molecular structure. The stacking can be continued with another “floor” of porphyrins, followed by a subsequent deposition of DPNDIs and so on. In order to allow the growth of the supramolecular structure, the floating layer of porphyrins must be constituted by CoTPPs since these molecules can coordinate a DPNDI from both sides of their macrocycle, differently from ZnTPPs, according to the theoretical predictions of coordination chemistry.

To investigate the growth of this supramolecular structure, I have studied the crystallographic and electronic properties of the system by Low Energy Electron Diffraction (LEED) and Photoemission Spectroscopy (PES), both performed at the VESI laboratory of the Physics department of Politecnico di Milano. Complementary low temperature Scanning Tunneling Microscopy (LT-STM) images were acquired during a few months’ stay in Germany at the Technische Universität München. The main evidence of the formation of such

an ordered superstructure was provided, however, by means of Near-Edge X-rays Absorption Fine Structure spectroscopy (NEXAFS), a technique that I had the opportunity to master during several beamtimes granted at the ALOISA beamline of the ELETTRA synchrotron in Trieste. The basic concept behind a NEXAFS experiment is to send grazing *p*- or *s*-polarized light towards the sample and to measure the dichroism in their absorption, thus getting information about the orientation of aromatic compounds. A massive absorption of *p*-polarized light (*s*-polarized light) in empty π states is associated with the presence of flat(standing) aromatic rings. A strong dichroism in the adsorption features is representative of a high degree of order of the molecular layer. An example of the NEXAFS characterization of the first two layers of the supramolecular complex presented above is reported in Figure 2.

The most evident features in between 398 and 406 eV are related to X-ray adsorption into empty π states. When only

porphyrins are present on the substrate, the NEXAFS spectra are characterized by a massive absorption of *p*-polarized light, indicative of the presence of flat lying molecules. However, the dichroism is completely reverted when a single layer of DPNDI is added to a basal plane made of ZnTPP: a strong absorption of *s*-polarized light is instead observed. This is the experimental proof of the presence of standing DPNDI molecules, coordinated with the Zn²⁺ ion of the porphyrins below, thus demonstrating the realization of the in-vacuum orthogonal supramolecular structure.

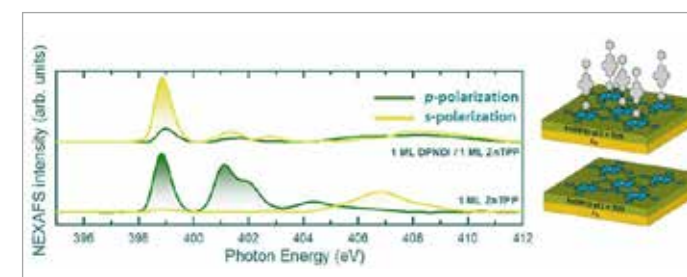


Fig.2 - NEXAFS spectra acquired at the N K-edge for the system 1 ML DPNDI on 1 ML ZnTPP / Fe- $\rho(1 \times 1)O$. The spectra acquired with *p*-(*s*-) polarized light are shown with green (yellow) lines. Only the contribution from the topmost layer is shown, as obtained by subtracting the (attenuated) signal from the film underneath.

ENGINEERING PEROVSKITE-BASED MATERIALS FOR HIGH-PERFORMANCE LASING: A STUDY OF OPTICAL GAIN PROPERTIES

Ada Lili Alvarado Leños - Supervisor: Annamaria Petrozza

In the nineteenth-century, a metallic cube-like crystal was found in the southern Ural Mountains. The newly discovered crystal was CaTiO_3 , a material that has come to be referred to as a perovskite. Nowadays perovskites represent a huge family of materials, which share a crystal structure that resembles that of CaTiO_3 . Perovskites are an extremely diverse group of materials with notable properties, which have made them stand out in a variety of fields including superconductivity, spintronics, and energy storage. Perovskites can be defined by their unit cell composition ABX_3 , and can be represented as $[\text{BX}_6]$ octahedra, organized in a corner-sharing 3D network, with the A cations at the corner positions (Figure 1). Recently, interest in metal halide perovskites surged when their efficient photovoltaic performance was discovered, rivalling state-of-the-art materials. These renewed enthusiasm in perovskite research has also fuelled an increase in research to study their light emitting properties. As of now, the developed incoherent and coherent light emitters have shown encouraging results, indicating that perovskites possess promising optoelectronic properties. In particular, it

is expected that perovskites could be used to fabricate versatile and efficient solution-processed lasing devices, due to, for example, their high optical gain and broad spectral tunability. Nevertheless, to obtain efficient perovskite lasers, it will be necessary to understand and engineer their optical gain properties.

A main component of a laser is the gain medium, a material capable of light amplification. The figure of merit used to quantify the ability of a gain medium to amplify light is the optical gain coefficient. Accurately measuring the optical gain coefficient allows to compare different perovskites and identify the most promising ones. A widely used technique to measure the optical gain coefficient is the variable stripe length method (VSLM). In the here reported work, a meticulous experimental implementation and

numerical analysis of the VSLM was carried out to study the gain properties of the 3D perovskite, MAPbI_3 . The spectral gain evolution, as well as the fluence dependent behaviour, suggest that the stimulated emission of MAPbI_3 is governed by electron-hole bimolecular recombination, similarly to bulk GaAs (Figure 2). Reducing the dimensionality of 3D perovskites, can lead to low-dimensional perovskite-like materials, known as layered 2D perovskites. These low-dimensional systems self-assemble into a 2D bulk crystalline material, consisting of inorganic 2D corner-sharing octahedra nano-sheets, which are separated by organic cation layers. This periodic arrangement forms a quantum well-like heterostructure, where the inorganic and organic layers correspond to the semiconducting and

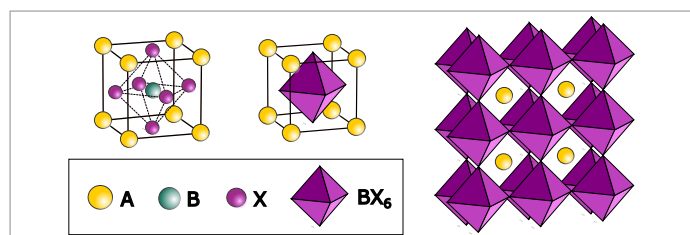


Fig.1 - Standard representation of the perovskite crystal structure, showing the unit cell with all the atoms (left), the unit cell with the $[\text{BX}_6]$ octahedron six-fold coordinated to A atoms (centre), and the repeating unit cell forming a three dimensional structure (right).

insulating layers, respectively. Layered 2D perovskites have been proposed as materials that could enhance radiative recombination, as well as improve the stability in comparison to 3D perovskites. However, their lasing performance has so far failed to meet the expectations. Thus, the currently discussed PhD project explored the possibility of tuning and improving the optical gain properties of layered 2D perovskites by changing the cation of the organic layer. More specifically, three different layered 2D perovskites were studied: BA_2SnI_4 , PEA_2SnI_4 , NMA_2SnI_4 . These materials differ from one another only by the organic cation, where the bulkiness of the molecule progressively increases from butylammonium (BA), phenethylammonium (PEA) to 1-naphthylmethylammonium (NMA). By analysing the gain

properties of these three perovskites it was revealed that the nature of the organic cation plays a fundamental role in defining the lasing potential of the material. For instance, the flexible alkyl BA cation promotes the growth of highly defective films, which show no gain. In contrast, the aromatic cations PEA and NMA form highly crystalline films. However, the strong photo-instability of NMA_2SnI_4 hinders its lasing performance. Meanwhile, the synergetic effect of a low defectivity, high optical gain and stability make PEA_2SnI_4 an ideal material for lasing. Therefore, by using PEA_2SnI_4 as a gain medium, an optically-pumped DFB lasing device was successfully developed (Figure 3). This work emphasizes the relevance of material engineering to control the optical gain properties of perovskites and highlights relevant material characteristics

needed to develop efficient perovskite-based lasers.

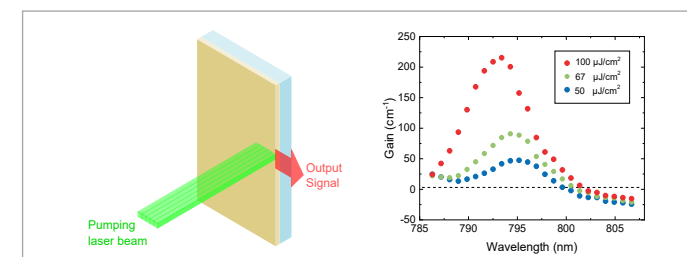


Fig.2 - Schematic of the VSL measurement (left) and the gain spectra of MAPbI_3 at different fluences obtained using the VSL method (right).

NANO-TAILORING OF THE DEWETTING INSTABILITY IN SEMICONDUCTOR THIN FILMS

Chiara Barri – Supervisor: Monica Bollani

Solid-state dewetting is the spontaneous evolution, upon time, in annealing conditions of ultra-thin solid films. We can observe that a bidimensional semiconductor layer could transform itself in tridimensional structures, well below its melting temperature, in particular condition of pressure and temperature. Minimization of the surface energy density of the wetting layer is the thermodynamic driving force that regulates the dewetting mechanism. Although this was initially regarded as a detrimental phenomenon for the CMOS technology, because it limits the thermal-budget of nanofabrication's procedures, since 30 years has been exploited in a plethora of different applications: from light management to biological filters. During my PhD, I focused my attention on the management of the controlled instability of monocrystalline semiconductor thin films like silicon and silicon-germanium alloy on a silicon oxide thermal substrate, and of amorphous germanium evaporated on native silicon oxide. It's possible to observe three different dewetting arrangements: dewetting from spontaneous void growth, controlled dewetting via edge

retraction (known as templated solid-state dewetting) and the spinodal-like mechanism. Ultra-thin silicon on insulator films show the classical dewetting features partially conducive to spontaneous void growth: in presence of defects on the crystalline films or where foreign particles are adsorbed on the silicon surface, it's possible to observe the dewetting starting point. Crystal planes guide the dewetting mechanism, elongated three dimensional structures, so called "fingers" (figure 1 a)), are formed and they evolve by breaking in ordered islands defined by the Rayleigh instability wavelength. The final shape and density of the dewetted islands, characterized by atomically flat facets, can be controlled by the variation of the initial layer thickness and by playing with the annealing parameters: time,

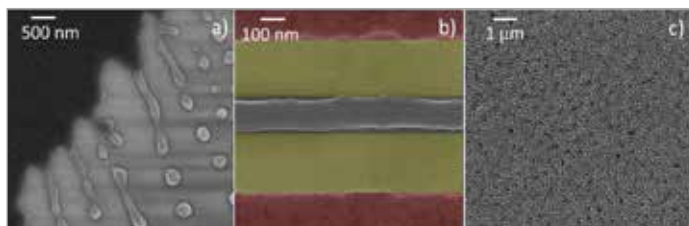


Fig.1 - Top-view scanning electron microscope images (SEM) of a) silicon fingers and islands oriented along the preferential direction obtained through solid-state dewetting (annealing temperature 650 °C - annealing time 30 min); b) zoom of one silicon dewetted wires (templated solid-state dewetting - annealing temperature 600 °C - annealing time 10 min). In yellow is highlighted the retraction area, in red the ad-hoc patterned trenches; c) connected structures obtained by the spinodal-like dewetting of 60 nm thick SiGe layer grown on silicon-on-insulator.

temperature and pressure. In order to improve the control on the final shape of the dewetted structures, pre-patterning technique could be performed. Electron beam lithography or laser writing systems followed by a reactive ion etching process create ad-hoc trenches in the initially thin semiconductor layer able to guide the dewetting front. Si wires of different aspect ratios (see figure 1 b)) and ordered Si and SiGe structures of various shape have been obtained with high reproducibility. In particular, SiGe dewetted islands, that act as Mie-resonators which are of relevance to photovoltaic applications, sensors, photo-detectors and light-sources have been implemented. Spinodal-like dewetting is observable in presence of thicker substrates of SiGe alloys pseudo-morphically grown by

molecular beam epitaxy or by low energy plasma enhanced chemical vapour deposition on silicon on insulator substrates. It gets its name from the mathematical analogy with the spinodal decomposition of heterogeneous mixtures. Spontaneous amplification of surface perturbations or height fluctuations of the dewetting film originate a dewetting mechanism simultaneous on all the sample surface that create connected structures or separated islands with a nearly-hyperuniform character (figure 1 c)). Surface perturbations, in the case of SiGe alloys that experience, due to lattice misfit, a tensile or biaxial compressive strain, are described by the Asaro-Tiller Grinfeld instability. These three different

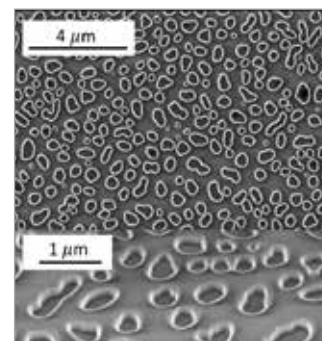


Fig. 2- SEM images (top-view - 45° tilt) of transferred dewetted pattern on silica sol-gel via degassed assisted patterning. The patterned has been obtained from dewetting of 30 nm a-Ge layer.

dewetting phenomenology has been observed thanks to various annealing experiments, based on a trial-and-error approach, performed in ultrahigh vacuum condition in a dedicated home-made annealing machine chamber opportunely developed during my PhD. A new, low-time consuming, dewetting mechanism, that doesn't require the implementation of ultra-high vacuum annealing conditions, has been developed to study the dewetting of amorphous germanium thin layer (a-Ge). The annealing has been performed by a rapid thermal annealing machine in nitrogen atmosphere. a-Ge samples on native silicon oxide, deposited via electron beam evaporator, with different initial layer thickness, have been annealed in the range of temperature 780 °C - 820 °C for a fixed annealing time of 2 minutes. Thanks to this procedure, dewetted nearly-hyperuniform disorder crystal Ge islands, with different shapes and density, has been obtained at low-cost since the optimized fabrication technique doesn't require the use of expensive GOI substrates, high-vacuum conditions and it is not time-consuming. Via degassed assisted patterning, a low-cost alternative way to

imprint resist or sol-gel, the dewetted framework has been transferred to silica layers. Considering the cost effective optimized procedure and the fact that it could be implemented on large substrates, this technique is of technological interest for light-trapping applications in solar-cells.

CONTACT RESISTANCE AND NON-QUASI-STATIC EFFECTS IN TWO-DIMENSIONAL FIELD-EFFECT TRANSISTORS

Riccardo Bona - Supervisor: Roman Sordan

The semiconductor industry set the 3 nm lithography process node as the benchmark for 2023. For long, the improvements in nanoelectronic devices have been associated to the scaling of the gate length in the field-effect transistors (FETs). The recent technological developments are linked to remodeling the traditional planar structure of a FET, therefore making the process node not directly related to the gate length. Indeed, the aggressive scaling of FETs led to unwanted short-channel effects and forced semiconductor foundries to realize new designs to cope with parasitics, mainly developing out-of-plane geometries. In principle, reducing the distance between the source and drain, reduces the latency time for carriers, consequently increasing the maximum operating frequency of the FETs. The reduction of the channel length also results in increased power dissipation due to the parasitic currents not controlled by the gate. Whenever the source and drain are too close to each other, the gate loses its efficiency in modulating the drain current, which leads to the short-channel effects.

After the isolation of graphene in 2009 by Gaim and Novoselov, a plethora of two-dimensional

(2D) materials belonging to the family of transition metal dichalcogenides (TMDCs) were discovered. They are promising materials for the post-silicon era due to their rich electronic properties and 2D nature. The possibility to employ materials, which can be ultimately thinned down to atomic planes, should allow fabrication of stacked FETs which are fully controlled by the gate, thus increasing the density of logic gates in new-generation integrated circuits. Among 2D materials, MoS₂ was recognized as an outstanding semiconductor material due to its relatively large bandgap and carrier mobility, which are similar to that of silicon. However, despite the extensive research efforts, the extrinsic carrier mobility in MoS₂-based

FETs has been limited by the contact resistance (R_c) arising at the interface between the semiconductor channel and metal contacts. State-of-the-art FETs, based on TMDCs, have $R_c \sim 1$ -10 k Ω - μ m. Many efforts have been dedicated towards the reduction of R_c , which should reach ~ 50 Ω - μ m of the conventional high-frequency FETs.

In this work, two different approaches were pursued to lower R_c . In the first approach, the edge contacts between metals and MoS₂ were investigated because they have been predicted to improve the injection of carriers. Electron-beam lithography was used to fabricate holes of radius between 50 and 100 nm in the contact area of MoS₂. The holes were filled by

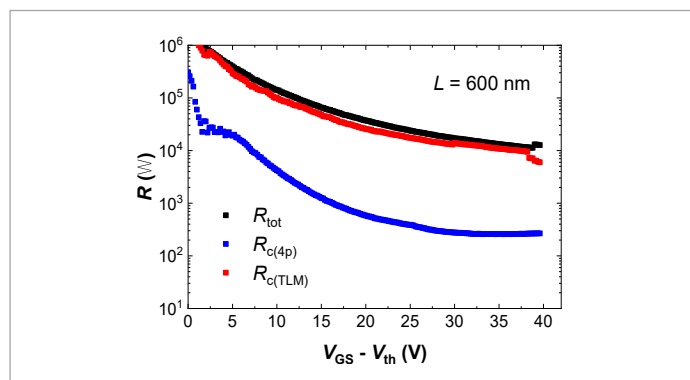


Fig.1 - Contact resistances in a MoS₂ FET, with the channel length $L = 600$ nm and channel width $W = 5$ μ m, as a function of the back-gate voltage overdrive. The 4p contact resistance $R_{c(4p)}$ is shown in blue, the TLM contact resistance $R_{c(TLM)}$ is shown in red, and the total resistance R_{tot} is shown in black.

the evaporated top source and drain contacts (Au), thus forming injection sites for carriers along the edges of MoS₂. In the second approach, a 2D semimetal WTe₂, also a TMDC, was used as a buffer layer between the contacts and MoS₂. Stacked structures comprising MoS₂ and WTe₂ were realized and characterized in a back-gated configuration. The latter approach was based on the use of Bi, a 3D-bulk semimetal, as a buffer layer between the metal contacts and MoS₂. Bi has been found to be effective in reducing the contact resistance in back-gated MoS₂ FETs as it prevents the formation of the Schottky barrier between the metal contacts and MoS₂. This is because Bi has vanishingly small density of states at the Fermi energy and lacks the induced trap states in the bandgap. All fabricated MoS₂ FETs were characterized in terms of R_c , which was measured by employing two different methodologies, namely

four-point-probe (4p) and transmission-line-measurement (TLM) methods. These methods were used in the same device structure, obtaining $R_{c(4p)}$ and $R_{c(TLM)}$ which were R_c measured by the 4p and TLM methods, respectively (Figure 1). We found that $R_{c(TLM)}$ was much larger than $R_{c(4p)}$, indicating the presence of the junction resistance $R_{jun} = R_{c(TLM)} - R_{c(4p)}$ which is a part of the contact resistance physically located in the channel next to the injecting current contact. Our results show that the contact resistance in MoS₂ FETs is dominated by R_{jun} , which should be taken into account when developing strategies for achieving good electrical contacts to 2D TMDCs. The presence of R_{jun} could also explain why the strategies adopted to reduce R_c , modifying the material below the contacts, were not successful. The non-quasi-static (NQS) effects in graphene FETs (GFETs) were also investigated in this work. Due to the carriers inertia, a

transit time is required for charge carriers to travel from the source to drain (i.e., from one side to another) of a GFETs. During this time, a difference between the drain and source currents can be measured. NQS effects are of crucial importance for devices operating at high frequencies, such as GFETs. The ambipolar nature of graphene allowed the fabrication of GFETs in which the carrier polarity was tuned by the applied gate voltage. We demonstrated that the sign of the difference between the source and drain current depends on the sign of the gate pulse. Depending on the sign of the pulse, with respect to the Dirac voltage, the electric current flowing between the drain and source comprises only electrons or holes. During the transit time, the source current changes faster than the drain current in the former case, and slower in the latter case. Typical obtained results, when a positive pulse is applied to the gate, are shown in Figure 2.

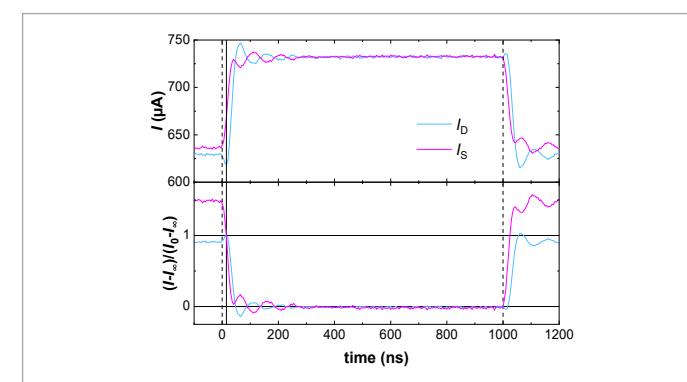


Fig.2 - Top panel: The measured drain (I_d) and source (I_s) currents as a function of time, in a GFET excited by a positive voltage pulse at the gate. The difference in the currents at the edges of the pulse is due to the transit time, needed by the electrons injected at the source to reach the drain. Bottom panel: The exponential factors of I_s and I_d as a function of time were extracted to eliminate the influence of the parasitic elements of the measurement circuit. Exponential factor of I_d is delayed with respect to that of I_s , indicating the presence of the NQS effects in the measured GFET.

APPLICATION OF ELECTRON SPECTROSCOPY TO THE STUDY OF PHOTOPHYSICS IN BIOMOLECULES

Matteo Bonanomi - Supervisor: Caterina Vozzi

My research activity mainly focuses on studying the ultrafast dynamics in biomolecules by photoelectron spectroscopy techniques. I spent most of my PhD at FERMI Free Electron Laser (FEL) in Trieste, Italy, at the Low-Density Matter beamline (LDM). In the last decades, fundamental processes of biological systems have been extensively studied on an ultrafast time scale. Particularly, the ability to track in time the energy transfer in molecules has provided new insights in the knowledge of reaction mechanisms. The dynamics of biomolecules almost invariably involve the non-adiabatic coupling of vibrational with electronic degrees of freedom, leading to the redistribution of charge and energy within the molecule. A well-established method to observe the first stages of a photochemical process is to prepare a photoexcited state with an optical laser, the so-called pump. Then a delayed probe pulse acts as the shutter of an ultrafast camera. Time-resolved photoelectron spectroscopy (TRPES) is the first-choice technique to follow the electronic relaxation processes in molecules as it is sensitive to molecular orbital configurations and vibrational dynamics.

Furthermore, it provides information on states which are not reachable by absorption methods. TRPES is an important technique for the study of non-adiabatic dynamics in polyatomic molecules and has been applied to a range of problems including internal conversion, photoisomerization, excited state proton and electron transfer, and photodissociation. Although TRPES is a commonly used technique for femtochemistry studies with table-top laser sources, applying TRPES to Free Electron Lasers (FEL) has several advantages. The use of XUV or X-ray FEL pulse for the probe step allows for site- and chemical-specific probing via inner-shell ionization. Also probing via valence ionization makes it possible to follow the molecular dynamics not just in the electronically excited state but also subsequent dynamics on the electronic ground state. In principle, both advantages are also applied to TRPES with HHG sources, but the lower photon flux of most HHG sources often poses a practical challenge for gas phase TRPES studies, both for valence photoelectron spectroscopy but especially for inner-shell photoelectron spectroscopy. I will present two topics addressed in my PhD

project: first, our results on the UV induced photodynamic in norbornadiene, a promising candidate for future application in energy storage. Then, our study on the photodynamics of the Uracil nucleobase. We studied the electronic relaxation dynamic of UV-excited norbornadiene using time-resolved gas-phase valence photoelectron spectroscopy, at LDM beamline. Norbornadiene (NBD) is a highly strained multicyclic hydrocarbon that isomerizes into Quadricyclane (QC) upon absorption in the ultraviolet (UV). QC undergoes the reverse reaction at similar wavelengths, resulting in a reversible molecular photoswitch that attracts a great deal of interest. Furthermore,

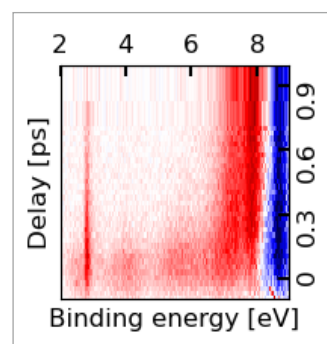


Fig.1 - Experimentally measured photoelectron binding energy spectra of UV-excited NBD as a function of the pump-probe time delay between UV (6.2 eV) and XUV (18.9 eV) pulses, plotted as the electron yield difference between spectra taken with and without the UV-excitation pulse.

the QC-NBD system, and its derivatives, constitute promising candidates for high density molecular solar thermal (MOST) energy storage, that can absorb, store, and later release solar energy as heat. The study of QC-NBD conversion mechanism has both a photochemical interest and an application perspective. The time-resolved photoelectron spectra are shown as a two-dimensional false-color map in Figure 1.

Several prominent features are apparent. A relatively narrow and long-lived feature centered at 2.8 eV is assigned as the 3s Rydberg states of NBD. A spectrally broad but short-lived structure extending from the Rydberg states to approximately 7 eV merges into two long-lived bands approximately centered respectively at 7.3 and 7.8 eV. We assigned the feature at 7.3 to QC isomerization products and the band at 7.8 to NBD photoproducts. The pronounced negative signal in the difference spectrum at

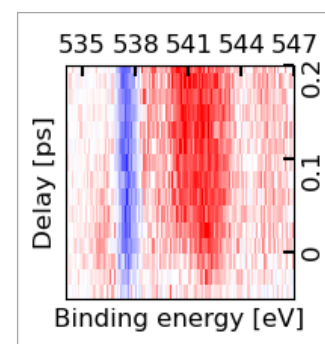


Fig.2 - Experimentally measured photoelectron binding energy spectra of UV-excited Uracil as a function of the pump-probe time delay between UV (4.7 eV) and X-ray (600 eV) pulses, plotted as the electron yield difference between spectra taken with and without the UV-excitation pulse.

8.5 to 9 eV corresponds to the depletion of the NBD ground state. Pump-probe photoelectron spectroscopy using XUV photons from an FEL reveal rich chemical dynamics, detailing the relaxation pathways of excited state NBD from highly excited Rydberg states all the way to vibrationally hot ground state products. We have identified a new fast relaxation pathway (<100 fs) that competes with the slower decay via the Rydberg states already discussed in the literature, leading to the formation of vibrationally excited photoproducts. Nucleobases are a fundamental basic building block of nucleic acids. The photoreaction mechanisms have been extensively studied over many decades by various spectroscopic techniques; however, the dynamic of these molecules remains unclear. To shed light on those mechanisms, we investigate the photodynamics of Uracil with Time-Resolved X-ray photoelectron spectroscopy (TR-XPS) at the Oxygen K-edge. We did our experiment at the SQS beamline, European XFEL in Hamburg. Like all other nucleobases, Uracil absorbs photons strongly at a wavelength of 267 nm and exhibits an ultrafast relaxation process with experimentally observed relaxation times between 50 fs and 2.4 ps. In this way, excess energy dissipates as heat, rather than bond cleavage. It is thought to be why nucleobases evolved as the "alphabet of life" in a period when the Earth was strongly

irradiated by UV radiation. The two lowest valence excited states are involved in the photoinduced dynamics of Uracil: the first $\pi\pi^*$ dark state (labeled S_1) and the first $\pi\pi^*$ bright state (labeled S_2). Since core-level spectroscopy is site- and chemical-sensitive, TR-XPS can detect an ultrafast change in the electronic distribution around a specific atom. S_1 and S_2 orbitals differ significantly around one of the oxygen atoms. Thus, we expect our probe to capture the relaxation dynamic and particularly the transition from S_2 to S_1 . This is what we observed clearly in our experiment (Figure 2). S_2 is the short-lived feature at 536 eV that decay in S_1 in a timescale of 60 fs. The signature of S_1 appears at higher binding energy as two delayed broad bands centered respectively around 541 eV and 546 eV. Calculations supporting our data demonstrate that the broad bands observed originate from different geometries of the molecules in the S_1 state. TR-XPS has enabled us to identify the different electronic states involved in the relaxation pathway with molecular structure sensitivity.

NEAR-INFRARED LOW-NOISE YTTERBIUM ULTRAFAST LASERS FOR EXTREME LIGHT GENERATION AND PRECISION SPECTROSCOPY

Francesco Canella – Supervisor: Gianluca Galzerano

In recent decades, ytterbium ion-based lasers have gained increasing importance in the scientific and technological world because of the many properties that distinguish these ions from other rare-earth elements used as active media in lasers and optical amplifiers.

Yb has a very simple electronic structure with a broad emission in the near-infrared (NIR) wavelength region ($\sim 1\mu\text{m}$), and an efficient in-band diode pumping scheme that allows reaching very high powers, ultrashort pulse durations, and broadband emission bandwidth.

Over the years, both solid-state and fiber Yb ultrafast pulsed sources have been developed that have demonstrated remarkable robustness, achievement of high power, and low noise properties. Nowadays, applications span from metrology to spectroscopy, astronomy, and more.

Within the scope of this Ph.D. work, two specific applications have been developed based on the use of Yb ultrafast sources with low phase and amplitude noise. The first of them is the generation of X-rays via inverse Compton scattering (ICS) with relativistic electrons in the framework of the INFN's BriXSinO project, while the second one is the synthesis of optical frequency

combs (OFCs) suitable for precision spectroscopy. Concerning Compton applications, since a very high average power of the infrared radiation is required (ICS electro-photon cross section is very small), the optimal starting point is a low-noise pulsed source for which high-power technology is available, namely an ultrafast Yb-doped fiber laser system. As a source, we opted for a 1030 nm mode-locked fiber laser with a repetition rate of 100 MHz and an output power of 0.2 W.

To reach the tens kW average power levels needed for the efficient interaction with electrons, the laser pulses must be first amplified by ultrafast

Yb-fiber amplifiers (a two-stage configuration) and then trapped into a high-finesse optical ring cavity. Inside the cavity, extremely high power is reached and the interaction with the electrons takes place. A sophisticated locking method has been implemented for efficient coupling of the cavity to the laser with a low-intensity noise of the trapped radiation, avoiding unwanted power fluctuations that could affect the X-ray generation. Figure 1 shows a schematic of the setup built for BriXSinO during my Ph.D. With this setup, we obtained an average power exceeding 50 W after the fiber amplifiers and ~ 20 kW of trapped power inside the cavity.

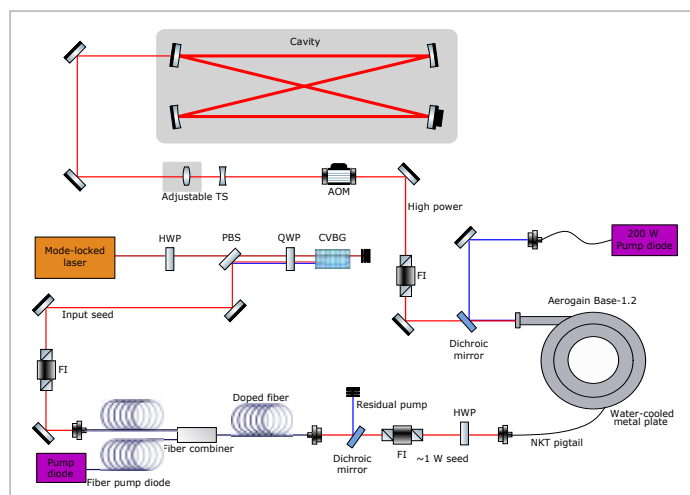


Fig.1 - Yb high-power laser system built for BriXSinO

Synthesis of optical frequency combs with extremely low phase and frequency noises is crucial in a variety of applications, for which solid-state Yb lasers are good candidates thanks to their lower noise levels compared with fiber oscillators.

During my Ph.D. we developed two NIR optical combs of deeply different repetition rate regimes, both based on Yb solid-state lasers.

The first relies on a Yb:CaGdAlO₄ (Yb:CALGO) mode-locked laser of repetition rate of 160 MHz emitting around 1040 nm. The Yb:CALGO synthesized comb covers a spectrum between 670

and 1500 nm (supercontinuum generation in a photonic crystal fiber) with particularly good low-noise properties, making it a powerful tool for spectroscopy. By using multiple optoelectronic feedback loops, we stabilized both the repetition rate and the carrier-envelope offset (CEO) frequency of the comb against an RF standard (Rb clock).

Figure 2 shows the comb's broadened spectrum and the CEO's RF spectrum. CEO free-running linewidth is narrower than 10 kHz demonstrating the extreme low-noise behavior of the Yb:CALGO comb.

The second OFC described

in my thesis has been made in collaboration with the Max Planck Institute of Quantum Optics (Garching, DE), where we demonstrated the comb-like spectrum of a low repetition rate comb at 40 kHz. The beat note spectrum of the comb against an ultra-stable 1-Hz linewidth CW reference is plotted in Fig. 3. Here the cornerstone of the setup is a Yb:KYW pulsed laser of 40 MHz of repetition rate (wavelength ~ 1030 nm). A properly driven acousto-optical pulse picker lowers the repetition frequency by suppressing a fraction of pulses. Despite the simplicity of the principle, the comb structure of picked pulses has never been demonstrated before. Moreover, our experiment shows that pulse-picking process does not introduce noise degradation. Low repetition rate combs are a potential innovative method to synthesize low-noise XUV OFCs, which are highly desirable for fundamental spectroscopy experiments (e.g. He⁺ 1S-2S transition at 30 nm).

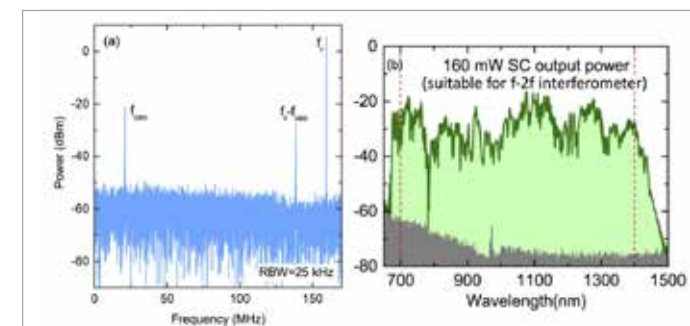


Fig.2 - (a) CEO RF spectrum. (b) Yb:CALGO broadened spectrum

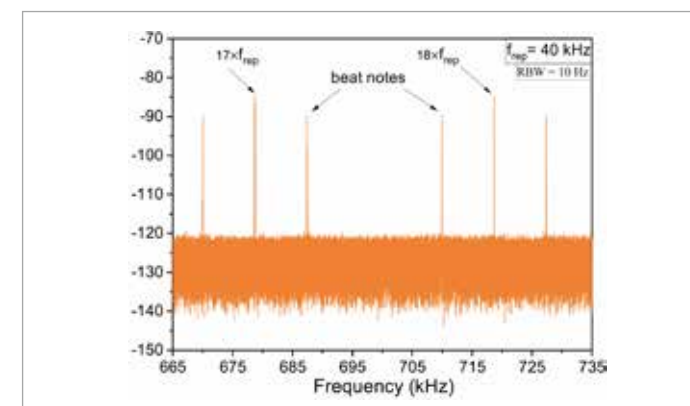


Fig.3 - Beat note spectrum of 40 kHz OFC against an ultra-stable CW reference.

HYBRID MAGNETIC INTERFACES FOR APPLICATION IN ORGANIC ANTIFERROMAGNETIC SPINTRONICS

Michele Capra – Supervisor: Alberto Brambilla

Since the discovery of the transistor in 1947 by Bardeen and Brattain, processing information become an indissoluble aspect of our modern society. As the amount of information that has to be elaborated continue to raise year after year, also the power of microprocessors must increase consequently. Currently, the solution adopted to deal with the continuous requests of faster and more efficient way to process information, is to shrink down the size of transistors, allowing a denser packing on the same chip. Despite reducing the dimension of transistors would bring many advantages, like faster frequency switching and lower energy consumption, it is intrinsically limited to the lowest possible reachable size: than of an atomic scale transistor. In the last decades, different approaches have been proposed as possible alternatives to classical semiconductor-based devices. Among the most promising ones, we can mention quantum computing and spintronics devices. While quantum computing relies on superposition states offered by quantum systems – qubits –, spintronics relies on the manipulation of the extra degrees of freedom offered by the electron spin. Many different materials possess

an ordered magnetic structure in which magnetic excitations, propagating as so-called spin-waves, can be induced. The aim of my project (that develops within a European H2020 project named SINFONIA) is to exploit spin-waves as information carriers, which could be exploited to develop unconventional computing paradigms and novel devices, such as hybrid organic spin transistors. The initial building block of my research activity consisted in studying how organic molecules can magnetically couple with an antiferromagnetic underlying crystal. The antiferromagnetic structure has been chosen because it is known that it can sustain spin-waves in the THz regime, outclassing ferromagnetic based devices, remaining moreover insensitive the external or stray magnetic fields, which may cause failure in the information transport/ computing process. Molecules would act as a transducer, able to convert external, easy to generate, signals, like electric or optical impulses, into spin-waves which can propagate in the substrate. This transducer effect is possible due to the magnetic coupling at the interface between molecules and the antiferromagnetic structure, called spinterface.

In the following, I illustrate two examples of molecular/ antiferromagnetic interfaces that have been investigated during my project.

From the molecular side, we choose to work with Iron(II) Phthalocyanine (FePc) and Cobalt(II)TetraPhenylPorphyrin (CoTPP). In Fig.1 is shown their molecular structure, with FePc on the left and CoTPP on the right. As we can see, geometrically speaking, they are very similar to each other, being planar organic macrocycle compounds with an inner transition metal ion. In particular, we have chosen to work with these molecules because they possess a non-zero magnetic moment, which may favor the magnetic substrate-molecule coupling that we are looking for, and because these molecules have been already extensively studied and are cheap to synthesize. An

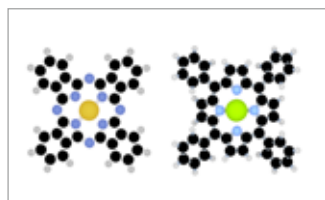


Fig.1 - Geometric structure of FePc (left) and CoTPP (right). Black, blue and white spheres refer, respectively, to Carbon, Nitrogen and Hydrogen atoms. Orange and green sphere represent, respectively, Iron and Cobalt atoms

important advantage offered by the use of molecules in hybrid magnetic interfaces lies in the fact that many different organic compounds can be synthesized, and each of them can be coupled with different magnetic surfaces, allowing for a huge number of possible choices.

The first system on which we focused on was FePc on the antiferromagnetic Cr_2O_3 . The latter was deposited on Cu(110), and from STM measurements we observed that it grows by forming islands. As the coverage is increased, we observe that also the Cr_2O_3 islands increase in size, until a full covering of the copper surface is obtained. After depositing FePc, Fig.2, we observe that FePc doesn't organize in a ordered structure above chromium oxide, resulting in a slightly disordered molecular layer, even if forming

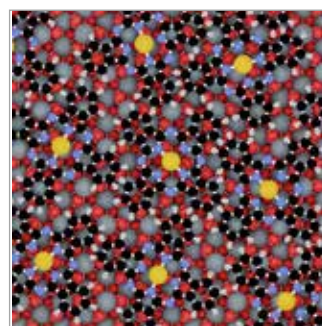


Fig.2 - Sketch of the disorder phase of FePc on Cr_2O_3

a flat molecular layer on the surface. After performing X-ray Magnetic Circular Dichroism (XMCD) measurements at the APE-HE beamline of the Elettra synchrotron facility, we managed to obtain a dichroic signal, which demonstrates the presence of a magnetic coupling between the central iron atom of FePc and the underlying Cr_2O_3 . This is a relevant result, as it can be associated to a robust long-range magnetic ordering, even in absence of a truly crystalline structure. The second system that we studied was Nickel Oxide (NiO) grown on Ag(100). Our STM measurements of NiO/Ag(100) show that they are characterized by terraces of 50 nm width. A close inspection of the crystallographic structure reveals the presence of a so call "mosaic reconstruction", meaning that each NiO terrace is not perfectly

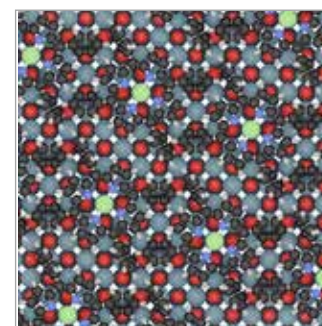


Fig.3 - Sketch of the CoTPP self-assembly above NiO surface

parallel to the other ones, but they are slightly tilted as the tiles in a mosaic. Over the substrate, one molecular layer of CoTPP is deposited, but this time the molecules self-assemble with a regular structure possessing an in-plane periodicity, Fig.3. Calculations suggest that each cobalt atom sits above a nickel atom characterized by always the same spin, which may turn out in a spin polarization of CoTPP (yet to be confirmed). In conclusion, we demonstrated that organic molecules can be magnetically coupled with an antiferromagnetic insulating substrate, opening the way to the development of antiferromagnetic organic spintronics.

RETINAL PROSTHESES/NEURON COUPLING: MATHEMATICAL MODELING AND EXPERIMENTS

Greta Chiaravalli - Supervisor: Guglielmo Lanzani

Degeneration of photoreceptors in the retina may lead to visual impairment and eventually blindness in disorders such as Retinitis Pigmentosa and Age-related Macular Degeneration. A restorative treatment is not often existing. Recently, the use of organic semiconductor-based retinal implants was proved to restore light sensitivity and visual acuity in blind rats. These implants establish tight contacts with neuronal bipolar cells in the inner layers of the retina, effectively replacing dead photoreceptors: upon illumination, the device transduces light into a bioelectrical signal that stimulates bipolar cells, thus restoring the visual path. However, the mechanisms responsible of photo-transduction and neuron coupling are still matter of debate. For all these reasons, the approach chosen to study the complex system of the in vivo retinal implant is the development of a virtual laboratory, t.i. the construction of a theoretical model, capable of reproducing the experimental findings, but also to quantify and formalize all the available data retrieved from years of study and publications. A first proposed model studied the photo-electrochemical interface of the poly[3-hexylthiophene](P3HT) material

in contact with an aqueous electrolyte, thus resembling the retinal biological environment. The model is able to catch the fundamental mechanisms responsible for the photo-voltage dynamic:

- 1) The establishment of a Photo-Dember effect secondary to the highly asymmetric transport of the charged carriers inside the material: whereas photo-generated

holes are able to redistribute across the domain of the device due to their high mobility, electrons remain trapped and virtually stacked along the Lambert-Beer generation profile, providing an asymmetric distribution of charges. In particular, a negative charge remains accumulated at the illuminated surface, thus producing a dipolar-like effect.

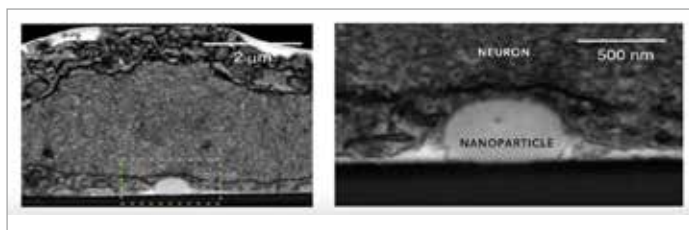


Fig.1 - Shows the image of a P3HT nanoparticle engulfed into a neuronal membrane obtained with Scanning Electron Microscopy.

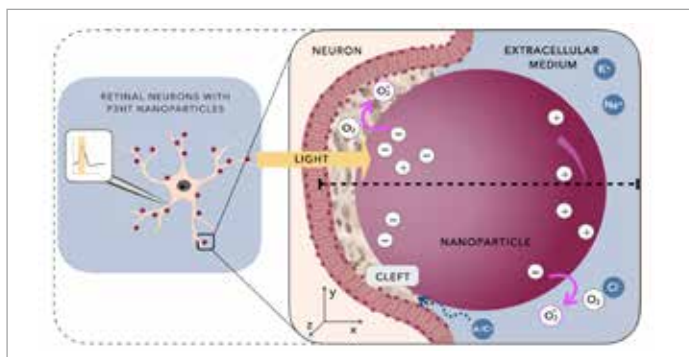


Fig.2 - Shows the schematic of the full bio-hybrid system simulated: it comprises a P3HT nanoparticle engulfed by a neuronal membrane and surrounded by an electrolytic medium. The interstitial neuron/NP interface is filled by a proteinic medium

- 2) The photo-cathodic effect at the interface with the aqueous environment: P3HT electrons in contact with an aqueous oxygenated interface reduce molecular oxygen and, exiting the bulk of the material, provide an increasing positive polarization of the device.

By introducing these two contributions in our Drift-Diffusion model, we are able to reproduce the photo-electrochemical experiments, thus validating the model which will be used as a building blocks for subsequent models. The first evolution of the P3HT model includes the description of the material as well as that of the surrounding environment, comprising of the electrolytic solution and of the neuron membrane, with the use of the Poisson-Nernst-Planck model. The goal is to study the quantitative photo-electrostatic and photo-chemical effect induced on the neuron membrane by a P3HT nanoparticle (NP) upon a physiological light stimulus.

- The electrostatic effect consists in an electrostatic coupling between the NP and the neuron. The polarization induced by the Photo-Dember effect may act as a depolarizing stimulus onto the neuron membrane, which is engulfing the NP through a proteinic-like structure named protein corona.
- The photo-chemical effect regards the production of superoxide ions by the illuminated NP, a precursor of many reactive oxygen species (ROS). ROS may interact with the neuron membrane inducing

the so called Eustress when their concentration is limited (t.i. the triggering of signaling pathway mediated by the ROS) or causing an oxidative stress when their concentration is high, thus leading to damage and, eventually, to cell death.

Simulations discard the possible relevance of the photo-chemical effect in the coupling mechanism, due to the almost negligible production of superoxide at the physiological light intensity. The accumulation of ROS onto the membrane of the neuron is estimated to modify the equilibrium concentration of just few nano-molar, a variation which is negligible with respect to concentration effectively responsible of an effective stress onto the membrane. Simulations instead support the establishment of a non negligible polarization at the neuron/NP interface, mediated by the dielectric-like cleft which inhibits ionic screening and allows a bio-hybrid electrostatic coupling. Whereas the presence of the protein does not seem to affect the concentration and the diffusion of superoxide in the cleft region, it strongly affects the electrostatic coupling, which in presence of ions, would be completely screened. The simulated electrostatic effect at physiological light conditions is of the order of 0.5 mV. Finally, a 3D model simulates the effect of different size and shape of the NP onto the final polarization effect, thus providing an optimization tool for the engineering of the prosthesis. The bigger the spherical NP the

more effective is the polarization effect, thus suggesting that aggregates of NPs (which may also reach a volume of around $1 \mu\text{m}^3$) may have a predominant role in the neuron coupling. In addition, also the effect of the shape is considered.

Overall, also upon considering preliminary experimental results on ex-vivo retinal explants, in the thesis we support the conjecture of the establishment of a photo-electrostatic effect: this effect is secondary to the formation of a dielectric-like proteinic cleft and of a tight engulfment. The effect of a single NP is not believed to be sufficient in triggering a neuron effective depolarization. Instead, it is believed that the final effect is cooperative and secondary to the simultaneous polarization of hundreds of NPs constellating the dendrites of the retinal neuron. Furthermore, the effect of clusters of NPs and the non perfect-spherical shape may provide source of more intense polarization, reaching point-like signals $> 1 \text{ mV}$.

INTEGRATION OF FUNCTIONAL MATERIALS IN NOVEL ARCHITECTURES OF MEMS DEVICES

Simone Cuccurullo – Supervisor: Federico Maspero

Functional materials (e.g., permanent magnets, soft ferromagnets, piezoelectric, photonic materials) are at the heart of many micro-electromechanical systems (MEMS), which are integrated devices that combine mechanical and electrical components. When integrated with MEMS, functional materials can enhance the performance of existing devices and can open the way to novel applications.

This PhD research activity was developed in the framework of two European projects, OXiNEMS and MetaVEH, whose goals are to introduce innovative technologies relevant to industrial applications too (magnetic field sensors and energy harvesters). The aim of the activity was the design, the fabrication and the characterization of MEMS devices integrated with magnetic materials, both permanent magnets and soft ferromagnets. Magnetic MEMS constitutes an emerging technology with a great number of potential applications; for example, magnetic storage, magnetic actuation, magnetometry, energy harvesting. On the one hand, miniaturization of permanent magnets allows to generate localized magnetic fields with no need of electromagnetic

micro-coils, which suffer losses since they are based on a dissipative process. On the other hand, microscale soft ferromagnets enables to manipulate and guide low-intensity external magnetic fields, exploiting their low coercive fields and linear magnetic response. The main challenge of the research activity was setting up a micro-fabrication process to allow the integration of the well-established silicon MEMS technology and magnetic materials. Indeed, the latter must show good adhesion, low stress, corrosion resistance and thermal stability at the fabricating and operating temperatures; however, MEMS fabrication processes comprise physical and chemical reactions (deep reactive ion etching, wet etching in hydrofluoric acid, annealing

at high temperature) which could be detrimental for the embedded magnetic materials. Therefore, the integration is not straightforward, and needs a careful optimization. In the first place, the research activity was devoted to the optimization of the deposition of magnetic materials. Concerning permanent magnets, both thin and thick films were studied. Cobalt films, with a thickness up to 200 nm, were deposited by DC and RF sputtering, and patterned through a combination of optical lithography and lift-off. The fabricated cobalt micro-magnets showed coercive fields of few hundreds of Oe, and remanent magnetization up to 1 T. Thick permanent magnets made of NdFeB and SmCo, with a thickness up to 1 μm , were deposited by RF sputtering.

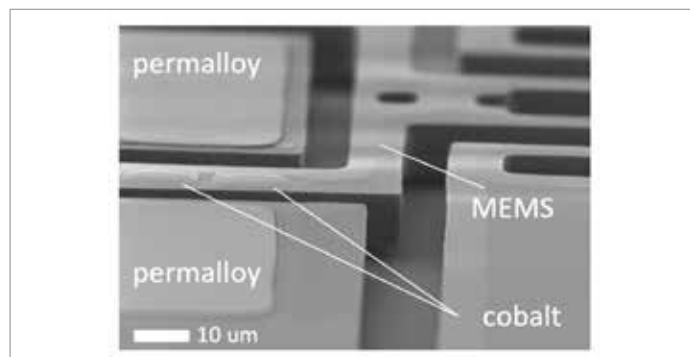


Fig.1 - Scanning electron microscope image of a fabricated silicon MEMS device, integrating thin films of two magnetic materials (cobalt and permalloy).

After a thermal treatment the films showed good hard ferromagnetic properties: in the case of SmCo, we measured coercive fields up to 12000 Oe and remanent magnetizations up to 1 T. For thick films, ion-beam etching was employed to pattern the material and obtain micro-magnets. Regarding soft ferromagnets, several alternatives were taken into consideration, going from permalloy to alloys of the NiFe family. The multilayer (Cr/MoNiFe) $_n$ gave the best performances, with coercive fields smaller than 1 Oe and high relative permeability (above 5000). The multilayered structure allows to keep a large ferromagnetic volume, reaching thicknesses above 500 nm, without having a single thick MoNiFe layer, in which the appearance of stripe domains worsen magnetic properties. This optimized soft magnetic film was employed to enhance the performance of integrated inductors in the framework of a project involving STMicroelectronics. After having optimized the growth of magnetic materials, the research activity focused on the integration of these materials in silicon MEMS devices. The main challenge was the protection of magnetic films to hydrofluoric acid, which is used to release the silicon structure from the underlying sacrificial oxide layer. To solve this issue, we tested several passivation layers (tantalum oxide, silicon carbide, silicon nitride, amorphous silicon,

CFx-polymer) to cover magnetic films and avoid direct exposure to the acid. Silicon carbide passivation layers gave the best results and were employed to fabricate magnetic MEMS devices in the framework of the aforementioned European projects.

In particular, the project OXiNEMS aims to introduce a new class of ultra-sensitive magnetometers combining N/ MEMS with superconductive and/or ferromagnetic materials. The research activity focused on the design, the simulation and the fabrication of a proof-of-concept device, namely a silicon MEMS resonator including soft and hard magnetic elements. The working principle of the device is based on the frequency modulation of a magnetized MEMS resonator, through a magnetic field gradient proportional to the external field to be measured. The first prototype of the magnetometer was fabricated and electrically measured in air, attesting the correct working of the device. To perform the device characterization in vacuum, a dedicated vacuum chamber was designed; in the future, it will be employed to characterize new prototypes, fabricated after a further optimization. The European project MetaVEH intends to introduce a new class of energy harvesters, exploiting micro-fabricated meta-structures integrated with piezoelectric and magnetic materials. The research activity focused on the study at the micrometric

scale of the effect known as "magnetic plucking". This non-linear effect is employed to convert the frequencies of human-related vibrations (<100 Hz) into the optimal working frequency of a MEMS vibration energy harvesters (1 - 10 kHz), to enhance the efficiency of the energy conversion. To do this, micro-patterned hard ferromagnets with sufficient volume (thickness > 1 μm) are needed to enhance magnetic interaction. In the first place, the activity was devoted to numerical simulations of magnetic plucking, to optimize the configuration of the magnets and the device geometry. Secondly, exploiting the development in the deposition of hard magnetic materials, a simple experiment was designed to measure the plucking effect between two SmCo micro-magnets. Due to the technological complexity and the fabrication challenges, the research activity is still ongoing. However, during these three years, in the first place, a MEMS process was set up for the first time at PolifAB, the micro- and nanotechnology facility of Politecnico di Milano; secondly, the deposition of soft and hard magnetic materials was optimized; lastly, a solid know-how was established, concerning the integration of magnetic materials and MEMS.

PHENOMENOLOGY AND PHYSICAL BASIS IN THE SPECTRAL DETECTION OF X-RAYS IN CDTE

Paolo Distefano – Supervisor: Giacomo Claudio Ghiringhelli

X-ray inspection is frequently used in quality control in industry because it is often important to check goods in opaque containers. To ensure high quality standards, new materials and new methods were introduced for real-time inspection in the production lines. An example is XSpectra[®], Xnext patent technology combining three distinct layers of innovation: a CdTe solid state detector, an integrated circuit for data acquisition and artificial intelligence algorithms to process the acquired images. The XSpectra[®] eye is a pixelated CdTe single photon counting detector that can supplement conventional radiography with spectroscopic data, enabling a chemical-physical study of the inspected goods that aids in the detection and classification of non-compliances. Despite being a potential semiconductor material for industrial X-ray inspection, because of its high absorption coefficient and wide band gap, which allow for room temperature operation, CdTe has several drawbacks, particularly because of the presence of crystal defects. The principal example regarding a CdTe Schottky diode is a time instability known as bias induced polarization. When a reverse bias voltage is applied to the detector,

the thermal population of deep levels (Cd vacancies), causes a buildup of space charge over time, that distorts the electric field degrading the detector performances. The increase of the electric field at the anode lowers the height of the Schottky barrier, so increasing the leakage current and degrading the signal to noise ratio, while the formation of a low electric field at the cathode, up to the formation of a dead layer, a region of zero electric field, reduces the counts and the charge collection efficiency. Therefore, bias-induced polarization causes the peaks to widen, shift, and lose counts. In this context we concentrated our efforts on the study of CdTe physics, particularly on the Xnext system, to find practical solutions to malfunction of the detector, like that described above, or to improve the detector output both in terms of response and stability. In reality, it is evident from the above explanation that there is a relationship between the quality of the data collected and the capacity to recognize and categorize non-compliances in the inspected products. To be more specific, our earlier work was the electrical and spectroscopic characterization of bias-induced and high-flux

polarization (which is due to the accumulation of positive charge inside the detector caused by the low mobility of holes). We electrically characterized bias-induced polarization by tracking the temporal evolution of the dark current of the unlit detector at various temperatures. We were able to determine the energy position of the deep trap level thought to be responsible for bias polarization from these data (0.59 eV above the valence band edge), but we were also able to demonstrate that if we consider long time scales, this is not the unique level in play. Using a radioactive source of ²⁴¹Am, we have also investigated the spectrum evolution of bias-induced polarization over extended periods of time. Thanks to these measurements, we have identified a new pattern that emerges after the spectral degradation and leads to a certain recovery and stabilization of the spectroscopic response. Parallel to that, we have also briefly described high flux polarization from both an electrical and spectroscopic perspective. For the electrical description of high flux polarization, we have documented the evolution of the current before, during, and after X-ray illumination using an X-ray tube.

We identified many tendencies that varied by pixel as well as an overall rise over time that eventually can also “kill” the pixel response. Lastly, by interposing the recording of ²⁴¹Am spectra between flux-increasing X-ray tube irradiation, we assessed the impact of high flux polarization on the spectroscopic capabilities of the detector. The spectral performances decline steadily with increasing X-ray flux, because of the increase of the charge accumulated in the detector. After characterizing the polarization processes, we focus on enhancing the spectroscopic capabilities of these CdTe diodes by using infrared illumination with both low and high X-ray fluxes. In fact, since CdTe is transparent to infrared light, it is possible to interact with the trap level, emptying or filling them, as reported in literature. With this method, the space charge that has built in the detector, and so the electric field, can be controlled. We examined the time evolution of the spectra of an ²⁴¹Am radioactive source while shining different near-infrared LEDs between 855 and 1450 nm on one side of the detector. Light that is close to the band gap edge can recover the detector

from polarization and produce a stronger and more interesting interaction; however, the usage of this LED is incompatible with simultaneous X-ray measurement due to the large photocurrent it generates. We demonstrated that, regardless of whether the bias voltage is applied or not, a prior illumination of several minutes with these interacting LED can accelerate the standard spectroscopic response of bias induced polarization, resulting in the stabilization of the spectroscopic performance we were seeking, but in a short amount of time. After a single infrared irradiation, CdTe remembers this illumination for several weeks. We demonstrated that this method is still effective up to an X-ray flux of about 10⁶ photons/s impinging on the pixel. We also made assumptions about the configuration of the electric field responsible for each spectrum using a simple model with a linear electric field with two distinct slopes, emphasizing the significance of the relationship between the electric field in the detector and the spectrum acquired. In this framework we developed a new way to map the electric field during the spectroscopic evolution. This is based on the temporal evolution of the charge signals generated

inside the detector: measuring the output of the charge sensitive amplifier, that is proportional to the collected charge, it is possible, applying the algorithm we developed, to extract the electric field profile. Finally, our work also focused on other ongoing projects involving the investigation and characterization of additional CdTe defects, such as Te inclusions, micrometrical precipitates embedded in the CdTe matrix. Using infrared transmission microscopy, we have 3D mapped their positions and dimensions inside CdTe crystals produced by Acrorad. Furthermore, we have participated in the testing and the development of new hardware enhancements for XSpectra[®], such as a new tungsten collimator able to improve the stability of the diode by shielding its guard ring, and a detector with a smaller pixel pitch.

FABRICATION AND CHARACTERIZATION OF DIELECTRIC NANOSTRUCTURES: FROM DEWETTED NANOISLANDS TO BICS BASED METADEVICES

Luca Fagiani - Supervisor: Monica Bollani

Nanophotonics is a branch of optics focused on studying the properties of light at the nanometer scale, and its interaction with objects of sub-wavelength dimensions. This field has become increasingly popular due to the demand for smaller photonic components for various applications, including compact optical circuits or networks. Initially, nanophotonic devices were constructed primarily using metals to take advantage of plasmonic processes such as light transport via surface plasmon polaritons. However, the drawbacks associated with metals, such as significant losses and heating issues, have resulted in a decline in interest in these materials.

Dielectric materials, such as Si, Ge, and GaAs, which possess high permittivity and high refractive index, have been proposed as a viable alternative to plasmonic materials for the fabrication of sub-wavelength objects. These materials exhibit similar optical properties to plasmonic materials, but are not affected by high absorption and losses. Additionally, they are well-suited for integration into optoelectronic based on CMOS technology. It is worth noting that Si nanostructures have the capability to support multiple

electric and magnetic Mie resonances in both the visible and infrared regions. This unique property can be utilized for various applications, including the manipulation of incoming radiation through scattering, redirection, field confinement, and control of its phase and amplitude.

Over the past few decades, extensive knowledge has been gained in the fabrication of Si structures. The most successful results in terms of fabrication quality have been achieved using expensive techniques such as electron beam lithography or focused ion beam lithography. However, due to the high cost associated with these techniques, other fabrication approaches have been developed more recently. These approaches include nanoimprint lithography

and solid-state dewetting, both of which produce structures with a lower quality than that of the state-of-the-art, but still closely approximate it.

In the first part of our study, we examined the fabrication and characterization of the morphological and optical properties of dielectric nanostructures created via solid-state dewetting. We utilized finite element method simulations to support our investigation of these structures as Mie resonators. Our study has demonstrated a high level of control over the solid-state dewetting mechanism, which we have employed as a fabrication tool in both random and patterned systems. This approach has allowed us to generate matrices of SiGe islands (as shown in Figure 1a) with Mie resonator properties that we

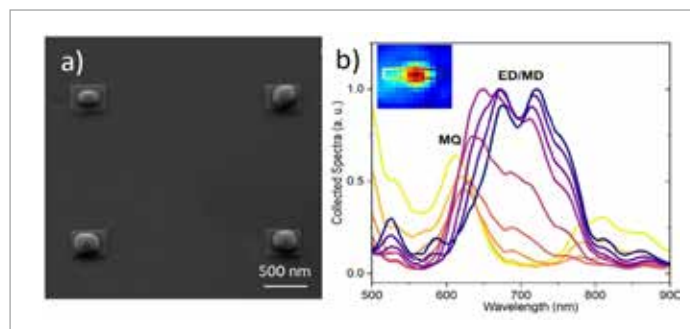


Fig.1 - a) SEM characterization of dewetted SiGe islands. b) Dark Field Scattering spectra from Hyperspectral map.

investigated through simulations and dark-field characterization using Dark-Field Hyperspectral imaging spectroscopy. Our experimental findings have shown that the dewetted SiGe islands can sustain multiple Mie resonances, as predicted by our COMSOL simulations. Additionally, with the use of a piezoelectric stage and hyperspectral mapping (as shown in Figure 1b), we were able to spatially separate the contributions of the Electric Dipole/Magnetic Dipole resonances from those of the Magnetic Quadrupole resonances. This achievement of isolating the contributions of individual resonances in a simultaneous scan is a result that has previously been accomplished only through theoretical means or experiments performed with different incoming polarizations. Combining the optical properties of individual resonators within a single dielectric nanostructure opens the door to the development of metasurfaces. This term refers to a group of engineered planar geometries consisting of a collection of dielectric nanoparticles. These innovative devices offer the possibility of enhancing the aforementioned light control properties. Additionally, it is possible to achieve higher values

of quality factor (Q) than those found in the single dielectric nanostructure resonances. Despite the challenges involved in designing the fabrication process of these complex devices, the expected benefits have motivated the scientific community to invest in them. The concept of metaphotonics, the merge of nanophotonics and metamaterials, has recently been extended to the exploitation of another physical principle: bound states in the continuum (BICs). These are localized energy states situated in the continuum spectrum of radiating waves. BICs have recently been utilized in photonics due to their ability to offer significantly higher quality factors in both single resonators and metasurfaces when compared to Mie resonances. In our study, we successfully realized a metadvice based on bound states in the continuum (BICs) using e-beam lithography and dry etching, which can selectively control the polarization of incoming light, as reported in the sketch of figure 2. We utilized finite element method (FEM) analyses to examine the sensitivity of the device to fabrication imperfections, revealing a high sensitivity to the quasi-BICs Q -factor of their modes, but the estimated

fabrication errors are within the tolerances. Afterwards, we examined the transmittance behavior of the device as a function of introduced in-plane asymmetry and incoming light polarization. An optical transmission setup was utilized to verify the optical properties of the metapolarizer. The device exhibited excellent agreement with the simulations, suppressing TM and TE linearly polarized light in specific wavelength ranges for each configuration. Furthermore, the experimental polarization extinction ratio reached values of 40 dB, which are comparable with other devices at the cutting edge of research. This is an innovative result for BICs-based devices, as it is the first time that a device has been produced that can suppress two cross-polarized components of incoming light in a unique and compact geometry.

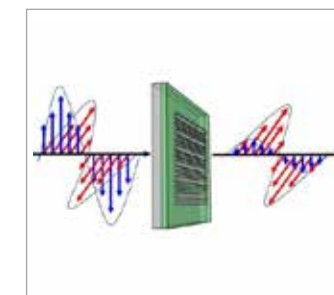


Fig.2 - 3D Sketch of the BIC-based device working principle.

A NOVEL PHOTODETECTOR PLATFORM BASED ON Ge AND Si MICROCRYSTALS FOR VIS-NIR DETECTION

Virginia Falcone - Supervisor: Giovanni Isella

The direct epitaxial growth of silicon and germanium on silicon (Ge-on-Si) has fostered the development of visible-near-infrared detectors for telecom and imaging applications. A viable route to enhance the responsivity of such photodetectors might be exploiting the micro-structuring of the absorbing layer to increase the effective volume of interaction between light and matter.

In this work we report on a new type of detectors, obtained from Si and Ge micro-crystals epitaxially grown on a patterned Si substrate. The faceted morphology and relatively high aspect ratio of the micro-crystals is seen to enhance the fraction of absorbed light and the detector responsivity as compared to conventional planar devices. This enhancement is present in the indirect regime of absorption of Ge, for the Ge micro-crystals, and in the NIR for the Si micro-crystals.

The epitaxial growth has been performed by means of Low-Energy Plasma-Enhanced CVD (LEPECVD). Micro-crystal formation is based on the self-assembly of Ge or Si crystals on a Si substrate, deeply patterned by optical lithography and reactive ion etching. 3D micro-crystals, several micrometer tall and

characterized by a limited lateral expansion, are obtained by using optimized growth parameters. Due to crystal faceting and pattern periodicity, enhanced light absorption as compared to conventional epitaxial layers is expected.

Modeling of the visible-near-IR absorption properties of Si and Ge-on-Si micro-crystals has been performed by finite difference time domain (FDTD) simulations. The simulations have been implemented also for an equivalent planar epilayer, both for Si and Ge. The results of the simulations for patterns of Ge and Si micro-crystals and their equivalent planar epilayer are represented in Fig.1. The simulations confirmed that crystal faceting and pattern periodicity lead to enhanced light absorption as compared to conventional epitaxial layers

and make Si-Ge micro-crystals promising building blocks for optoelectronic devices operating in the VIS- NIR spectral region. To experimentally confirm the FDTD results I proceeded with the electro-optical characterization of a single micro-crystal. An experimental set-up based on a nanomanipulator with a tip radius of 100 nm and a confocal microscope was used. The responsivity obtained for a single micro-crystal proved the VIS-NIR photoresponse and the enhancement with respect to an equivalent planar epilayer (Fig.2 (a)).

The Si micro-crystals have been grown with a doping profile tuned for their operation as photodetector in the linear regime but also as avalanche photodiodes (APD). For this reason, with the same set-up described above, measurements

in the avalanche regime, i.e. very close to the breakdown voltage, have been performed. Fig. 2(b) shows the measured gain as a function of the reverse bias for an incident wavelength of 900 nm. This gain reaches a maximum value of 104, comparable to state-of-the-art literature reports. After the characterization of the single as-grown micro-crystal I proceeded with the fabrication of a photodetector based on such 3D micro-crystals. The main challenge in realizing vertically illuminated photodiodes based on micro-crystals is the formation of a top transparent contact that can adapt to the surface morphology and bridge the 100-200 nm gap between adjacent microcrystals. To this purpose, I decided to use graphene as a suspended continuous top contact, with an absorption that does not exceed 2.4%. The Ge micro-crystals

fabricated devices have been characterized by electrical and optical measurements. Responsivity measurements confirm the enhanced absorption close to the germanium indirect gap (Fig.3). Simulations and measurements confirm the possibility of exploiting 3D self-assembled micro-crystals as a new class of photodetectors, exploiting light trapping phenomena in self assembled semiconductors microstructures.

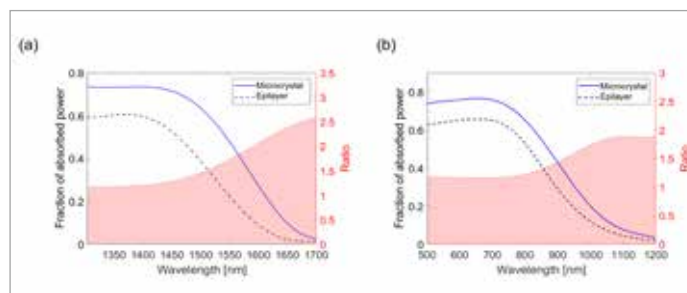


Fig.1 - Simulated fraction of absorbed power for: (a) Ge micro-crystal and Ge equivalent planar epilayer; (b) Si micro-crystal and Si equivalent planar epilayer.

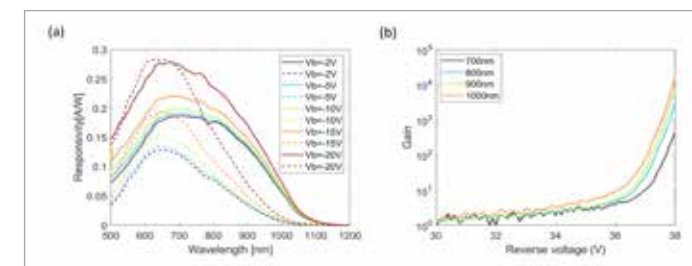


Fig.2 - (a) Comparison between the responsivity of a Si micro-crystal and a Si mesa diode. An enhancement of the responsivity is observed in the NIR region; (b) Gain of a Si micro-crystal operating as APD for a wavelength of 900 nm.

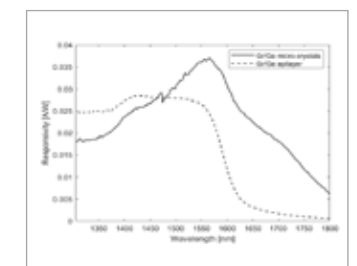


Fig.3 - Responsivity of graphene/Ge micro-crystals device and the equivalent epilayer, operating as APD for a wavelength of 900 nm.

ULTRAFAST TERAHERTZ SPECTROSCOPY OF INNOVATIVE MATERIALS

Lorenzo Gatto – Supervisor: Eugenio Cinquanta

The ability to generate and detect pulsed terahertz (THz) radiation, characterized by photon frequencies in the range 0.1 – 10 THz, gives access to a variety of excitations of great interest for condensed matter physics. In particular, THz radiation is sensitive to intraband absorption and is able to detect intra-exciton transitions. This enables us to follow the ultrafast relaxation dynamics of excited species, also when they are optically dark. Furthermore, infrared (IR)-active vibrational modes of solid-state and molecular systems can fall in this frequency range. This makes time-resolved THz spectroscopy (TRTS) a powerful tool at the interface between the high-frequency regime of electrical transport and that of low-energy excitations in condensed matter. During my Ph.D. I built a new setup dedicated to TRTS and I used it to study charge carriers and charge-phonon coupling in emerging materials, such as perovskites and transition metal dichalcogenides (TMDs). The setup includes a new home-built non-collinear optical parametric amplifier (OPA) for the generation of visible ultrashort pulses, devoted to sample photoexcitation. I explored different THz generation methods including optical rectification in ZnTe and GaSe crystals, and

two-color laser plasma in air. The THz detection scheme, based on electro-optical sampling, was also modified to measure simultaneously the pump-probe differential signal and the reference THz transient. This is important to exclude systematic errors in the evaluation of transient transmission. I also optimized the arrangement and focal lengths of the parabolic mirrors used to collimate and focus the THz radiation. This allows for the minimization of the aberrations and of the beam waist, consequently improving the signal-to-noise ratio. The new setup was used to continue the investigation of the charge-carriers dynamics and charge-phonon coupling in all-inorganic perovskites. In particular, we performed optical pump-THz probe experiments to study thermally evaporated thin films of CsPbBr_3 and we investigated the effects of specific annealing conditions in collaboration with the research group of Dr. Annamaria Petrozza (CNST-IIT). In particular, I pointed out unexpectedly faster relaxation dynamics of the photogenerated charge carriers following the annealing process. This was accompanied by a remarkable reduction of the photoluminescence intensity. Nevertheless, by scanning electron

microscopy we also observed the expected larger grain size after the annealing, which should lead instead to the increase of the relaxation time, due to the smaller concentration of grain boundaries. The combination of these complementary experimental techniques allowed us to highlight a larger contribution of non-radiative recombination channels, which counteracts the effect of the increased grain size. The fine-tuning of the annealing conditions is crucial for the improvement of the power conversion efficiency of photovoltaic cells based on thermally evaporated all-inorganic perovskites and the use of TRTS in combination with different characterization techniques proved to be an effective strategy to tune the fabrication parameters. A different class of perovskite materials is represented by

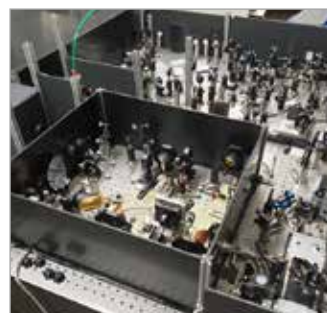


Fig.1 - Time-resolved terahertz spectroscopy setup and non-collinear optical parametric amplifier

mixed-halide perovskites. The wide tunability of their optical bandgap makes them attractive candidates for implementation in tandem solar cells. Nevertheless, differently from all-inorganic perovskites, they are also affected by a relatively low photostability, attributed to various photodegradation processes such as the halide segregation. Their low photostability represents one of the main factors hindering a more massive industrial application. I used our setup to assess the photodegradation of $\text{MAPb}(\text{I}_{1-x}\text{Br}_x)_3$ samples, exposed to a continuous-wave 532 nm radiation. This allowed us to point out a reversible change in the THz response after the irradiation. The reversibility of this change suggests that it might be related to the halide segregation process. I applied the same procedure to a

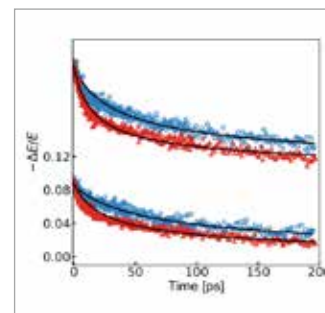


Fig.2 - 400nm pump - THz probe dynamics on as-deposited (blue circles) and annealed (red triangles) CsPbBr_3 thin-films.

sample prepared following a new fabrication protocol developed by the research group of Dr. Aurora Rizzo at CNR-NANOTEC. In this case, I did not observe any change after the irradiation by the 532 nm light. Thanks to the combination with photoluminescence mapping, we attributed our results to a higher localization of the segregated phase, which is averaged out by the large spot of our THz probe. I started then to use the capabilities of our TRTS setup to study TMDs. I specifically investigated the THz response of a few-layer MoS_2 sample, prepared by liquid exfoliation at the Trinity College of Dublin (Prof. Valeria Nicolosi) in collaboration with Prof. Christoph Gadermaier. A better comprehension of the factors limiting the charge

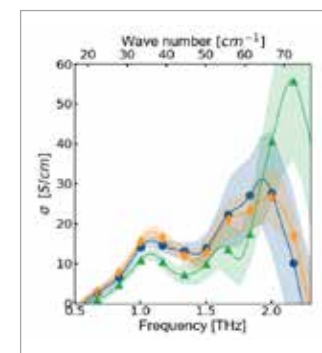


Fig.3 - Terahertz response of a $\text{MAPb}(\text{I}_{1-x}\text{Br}_x)_3$ sample before (blue circles), during (green triangles), and after (orange diamonds) the irradiation.

carriers' mobility in few-layer TMDs can be important to steer new strategies for the development of electronic devices based on these materials. At the equilibrium, I found absorption features that can be attributed to IR-active shear and layer-breathing modes. These low-frequency vibrational modes are obviously absent in the case of a monolayer and they have been usually studied by Raman spectroscopy in few-layer samples. Our technique allows us to investigate how IR-active modes couple with photoinduced charge carriers. I found indeed a photoinduced response, which cannot be simply explained in terms of free carriers in a nanostructured environment (Drude-Smith response), but requires the presence of additional features. These can be linked with the IR-active modes found at the equilibrium. The coupling between charge carriers and low-frequency interlayer phonons would have an impact on the charge transport properties of the material. Further investigations, including measurements on new MoS_2 samples fabricated through a physical deposition method, will clarify the interpretation of our result and allow a better evaluation of their impact on the charge carriers' mobility.

COMPUTATIONAL IMAGING BASED TIME-RESOLVED MULTISPECTRAL FLUORESCENCE MICROSCOPY

Alberto Ghezzi – Supervisors: Cosimo D’Andrea, Andrea Farina

Fluorescence microscopy is a powerful technique to study physical, chemical, and biological processes over a broad range of applications. It generally comprises an imaging system, but fluorescence is multidimensional and can provide a rich information by means of the emission spectrum and the lifetime. Imaging, spectrum and time (4D dataset) allow for high specificity techniques, however high dimensionality leads to a longer acquisition time, which in general should be limited when measuring a sample that has a dynamic behavior, as typically for biological samples. Multidimensionality is implemented in several manners in common fluorescence microscopy systems, whether they are scanning or wide-field. In the former case, the fluorescence is resolved with high-performance point detectors, which are available for time-resolved or multispectral measurements, however, being scanned, these schemes are slow as they proceed one pixel at a time. The latter approach, namely wide-field, is based on cameras and so allows for very fast imaging, but it provides a limited multidimensionality since common schemes are scanning in the spectral and temporal dimension.

One alternative and efficient implementation for 4D acquisitions is the single-pixel-camera (SPC): the sample is illuminated wide field with a series of patterns and the emitted fluorescence is integrated to a point by a lens, i.e., SPC measures the inner product between the image and the used patterns. When the number of patterns equals the desired number of pixels, an image can be reconstructed computationally. In the simplest case, this operation is a matrix inversion, but it is also possible to reconstruct images with less measurements than pixels by resorting to regularization methods. This is called Compressive Sensing (CS): an acquisition framework which allows to reduce the number of measurements preserving the information content. In SPC design, this is achieved through a choice of pseudorandom

patterns, e.g. based on the Scrambled Hadamard matrix. The aim of this PhD thesis is to propose and experimentally validate a system for fluorescence microscopy which allows for fast multidimensional imaging by exploiting the computational techniques of SPC and CS. One important part of this work has been the system development, which exploits a Digital Micromirror Device (DMD) as a binary reflective spatial light modulator to illuminate the sample with a pulsed laser. The system has two detection paths, one with a CCD camera and the other with a spectrometer coupled to a multichannel photomultiplier tube and to a time-correlated single photon counting (TCSPC) board. Fast measurement requires CS, but also short integration time in TCSPC. Hence, part of this thesis work was devoted in testing novel

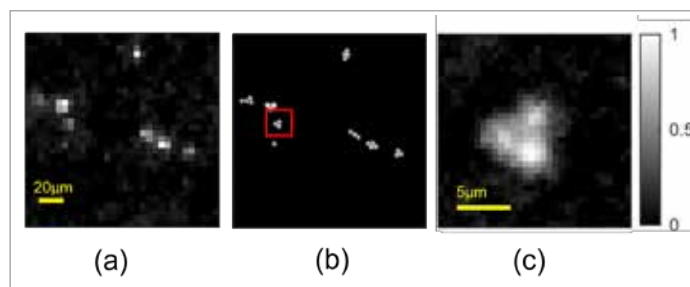


Fig.1 - (a) SPC image of a beads sample with CS (b) CCD image of the same field of view as in (a). (c) Zoomed CS-SPC measurement performed in the region of interest highlighted in red in (b).

high-performance detectors, like a multichannel 32x1 SPAD array and a silicon photomultiplier, that in future will allow for high throughput fluorescence microscopy applications. The system is validated by acquiring a 4D dataset from a fluorescent beads sample, and images (32x32 pixels) have been reconstructed from CS acquisitions. The compression level has been increased up to reconstructions with only 307 spatial measurements and result in Fig.2(a). Quantitative studies have been devoted to evaluating the optimal compression levels with a minimal impact on imaging, fluorescence spectra and lifetimes. Low spatial resolution is a well-known problem of SPC: although it is always possible to project more patterns, this is not always feasible because of the higher acquisition times. In this work I

exploited the inherent flexibility of the system to increase spatial resolution: with the help of a camera image (Fig. 2(b)), patterns can be encoded in a smaller area of the DMD, and projected into a region of interest, resulting in a higher spatial resolution only where needed, as in Fig. 2(c). A computational method to increase the spatial information without sacrificing the field of view, is called data fusion (DF), and it has been developed within this project. DF is a variational algorithm to build a high-resolution multidimensional dataset from SPC, so that the spatial dimension is constrained to the CCD image. DF has been applied to a cell dataset: starting from a 4D CS-SPC measurement with 32x32 pixels, an image with 256x256 pixels as in Fig.3(a) has been obtained after DF. Then, the multidimensional dataset has been exploited to obtain the

lifetime maps in Fig.3(b) and (c), relative to two different spectral bands. In addition to system design and reconstructions, part of the work also included the development of new methods for visualizing the acquired dataset. Indeed, CS and SPC methods allow for fast acquisitions, but often require long processing times. An algorithm for a fast fit has been designed to allow the visualization of FLIM images in real time during the measurement. In conclusion, in this PhD thesis I developed and experimentally validated a time resolved multi-spectral fluorescence microscope based on SPC and its symbiotic use with CS and DF: this integration between hardware and algorithms, at the base of computational imaging approach, resulted in an effective strategy for reducing the acquired dataset while preserving multidimensional images with high spatial, temporal, and spectral resolutions.

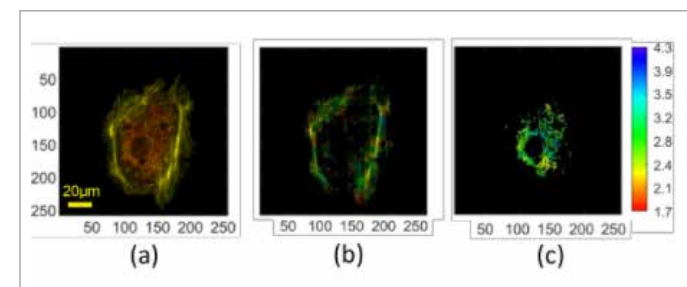


Fig.2 - (a) Image of a cell obtained from a CS-SPC dataset after DF with a CCD camera image. (b) Lifetime map within a smaller spectral band (c) Lifetime map in a spectral band complementary to (b).

ATTOSECOND CHARGE DYNAMICS IN GERMANIUM

Giacomo Inzani - Supervisor: Matteo Lucchini

A fascinating goal of many technological and research fields is the control of the electro-optical properties of a solid with light. However, we need further insights into light-induced ultrafast electron dynamics to manipulate them beyond the current limits of electronics. In the last decade, attosecond science pushed the available temporal resolution down to the sub-femtosecond (fs) time domain, unveiling several physical processes.

Among them, the light-induced injection of charge carriers from the valence to the conduction band of a solid by a strong ultrashort light pulse plays a fundamental role. This process, called photoinjection, can turn a semiconductor into a metallic state, changing its conductivity by orders of magnitude. Controlling charge injection on ultrafast time scales could have disruptive technological implications, but only a few experiments investigated this process with attosecond temporal resolution. Moreover, studies mainly focused on wide-gap dielectrics from a simplified standpoint and identified only one dominant physical mechanism for charge injection. Here we change perspective, investigating photoinjection in a prototypical

narrow-gap semiconductor: germanium.

We adopted the transient reflectivity spectroscopy technique (Fig. 1a). In this pump-probe experiment, an intense infrared (IR) field impinges on the sample, inducing electron transitions from the valence to the conduction band and dressing the band structure, acting as a pump. After a carefully controlled time delay, a single extreme-ultraviolet (XUV) attosecond pulse, the probe, impinges on the sample, probing electron dynamics. We measure pump-induced variations in the sample reflectivity close to the $M_{4,5}$ Ge absorption edge (3d levels, at 29.2 and 29.8 eV, Fig. 1b) as a function of the XUV photon energy and the pump-probe delay. We observed two types of features with distinct time scales. Long-lasting signals, unfolding within a few fs, link

with the injection of carriers between different bands. On top, reflectivity oscillations at twice the frequency of the IR pumping radiation (1.33 fs) come from the pump-induced acceleration of charges within the same band. Understanding this process is not trivial, so we resorted to our theoretical collaborators. Time-dependent density functional theory calculations spot the most relevant regions of the band structure involved in this process. Moreover, they demonstrate that single-photon absorption, multi-photon transitions, and tunnel injection concur in determining the final excited electron population after interacting with the intense light pulse. However, they unfold on different time scales within the pump envelope and involve distinct band structure regions. We assess the contribution of the

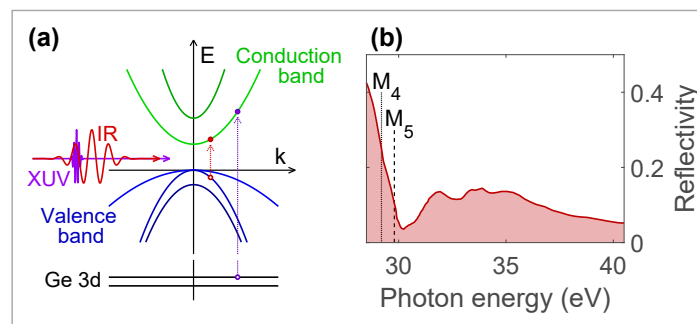


Fig.1 - (a) Scheme of the pump-probe experiment on Ge. **(b)** Equilibrium reflectivity of Ge at 66° from the literature. Dashed and dotted lines mark the absorption edge.

various multi-photon transitions by a novel dynamical projective operatorial approach. It refines the sampling of reciprocal space, further clarifying the interpretation of the experimental results. Varying the pump intensity in the calculations, we demonstrate that in the experimental conditions, two-photon transitions dominate. Instead, only single-photon absorption occurs for lower intensities, while higher-order processes become relevant at higher values. In addition, this analytical model unveils the surprising role of intra-band motion, which hinders photoinjection by disadvantaging higher-order transitions, at variance with what the literature reports for single-photon injection.

The unique possibilities offered by our experimental setup allowed further investigations. Since the beamline we developed has two focal positions, we can perform two experiments simultaneously. One is the transient reflectivity experiment we just described. The other is a two-colour photoemission measurement from a gas

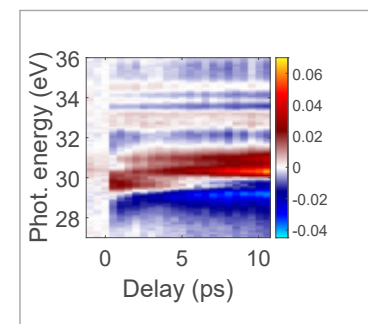


Fig.2 - Experimental differential reflectivity trace for the Ge sample.

target. Before impinging on the solid sample, the pump and probe pulses are both focused on a gas jet, and IR-dressed photoelectron spectra ionized by XUV pulses are collected. We obtain a streaking trace by measuring several photoelectron spectra for different XUV-IR delay values. From a simplistic perspective, the center-of-mass of the map corresponds to minus the IR vector potential, and the electron wavepacket contains information on the XUV radiation. We can retrieve the XUV intensity temporal profile and the IR vector potential, fully characterizing the pulses later used for the transient reflectivity experiment, by employing suitable reconstruction algorithms. However, achieving an absolute delay calibration has been difficult so far, and the reconstructed quantities were not directly related to the experimental delay axis of the transient reflectivity measurement. We developed a new approach called rACE (refined Analytical Chirp Evaluation), which allows precise calibration of the delay axis. Our method relates it to the time axis of the reconstruction, with a

resolution better than 5 as, even under non-ideal experimental conditions.

This novel approach allowed comparing the absolute timing of the reflectivity oscillations at twice the pump frequency to the squared IR vector potential inducing them. We repeated the transient reflectivity experiments on germanium samples with different doping. Including dopant atoms shifts

the sub-fs optical response of a material up to a few hundred attoseconds. Although a definitive interpretation of these experimental results is still missing, we tried to relate them to a simplified description of doped semiconductors. The shift in the optical response should link with doping-induced variations in the band structure and many-body interactions, which are strongly dependent on the carrier density. Therefore, we propose doping as a way of controlling many-body phenomena and, consequently, the optical properties of a material on the attosecond time scale. This result represents another step towards steering the ultrafast optical properties of a solid-state sample on the fs and sub-fs time scale.

SOLUTION PROCESSED ORGANIC FIELD-EFFECT TRANSISTORS FOR HIGH-FREQUENCY PRINTED ELECTRONICS

Tommaso Losi - Supervisor: Mario Caironi

The creation of an extended network of a wireless communicating and distributed electronics, known as Internet of Things (IoT), through cost-effective device integration in daily objects, is tough to be very important in the up-coming future in many application fields such as: health-care, agriculture, food industry, entertainment and energy sector. Among all the possible available technologies, organic electronics is maybe the most suitable one for this purpose. First, devices can be fabricated with simple large-area, low-cost and high throughput processes at room temperature. This is fundamental for a cheap integration of electronic components. Second, because of the mechanical properties of organic materials, devices can be flexible and conformable, highly desirable for wearable and light-weight electronics. Furthermore, because of the increased number of electronic components in our environment, recyclability and biodegradability become important requisites for IoT, and organic materials are more prone to that with respect to those used in more standard electronics. Because of all these advantages, in the last decades a lot of efforts has been put to improve the performances of organic

field-effect transistors (OFETs), which are the fundamental units of any electronic circuit and ideal components for rectifiers in the IoT field. In particular, field-effect mobility in OFETs has nowadays outclassed the one of amorphous silicon and approached the one of low temperature metal oxides ($\sim 10 \text{ cm}^2/\text{Vs}$). However, to ensure wireless communication capabilities, many challenges has to be faced. In particular, to maximize operational frequency, it is necessary the combination of downscaled device dimensions and organic semiconductors with high mobility, in order to reduce unwanted parasitism and at the same time increase channel transconductance. This is not trivial at all because, at small scales, injection phenomena start to become very relevant and can be responsible of an overall device performance degradation. Because of that, it is important to reduce the so-called width-normalized contact resistance ($R_c W$), a parameter used to quantify the efficiency of charge extraction. This is open issue for OFETs since they are usually characterized by values of $R_c W$ well above $1 \text{ k}\Omega\text{cm}$. Only few works reported values in between $1 - 0.1 \text{ k}\Omega\text{cm}$, which are essential to alleviate contact degradations and retain high mobilities

in transistors with reduced dimensions. In the first part this work the attempt of integrating a well-known high mobility organic semiconducting blend, composed by C_8 -BTBT (2,7-dioctyl[1]-benzothieno[3,2-b][1]benzothiophene) and C_{16} -IDT-BT (poly(indacenodithiophene-co-benzothiadiazole)), in downscaled transistors, is presented. Such system is among the best performing solution processed poly-crystalline organic semiconductors existing, able to display high field-effect mobilities, without the need of complicated deposition processes. However, its high performances in literature were demonstrated only in device architectures not suited for high frequency and at impractical operating voltages of 80 V . A first optimization in transistors with relaxed dimensions (long channel and overlap length) was carried out, reaching mobilities as high as $8 \text{ cm}^2/\text{Vs}$, with lowered operating voltages of 30 V . This result was achieved by processing and post-processing optimization and with the use of a thin parylen layer as dielectric material. The semiconductor has proved also a good versatility in changing substrate (from glass to plastic PEN) and contact type (from

evaporated metals to printed conductive polymers) without any relevant performance degradation. Furthermore, it shown good compatibility with solution-based patterning methods such as inkjet printing, which is ideal to make circuits. After an optimization, it was possible to demonstrate a mobility up to $6 \text{ cm}^2/\text{Vs}$ in printed OFETs on flexible substrates.

To retain high mobilities in downscaled transistors, molecular doping was used as effective strategy to reduce contact resistance. Different dopant molecules have been tried and the best results were achieved with the fullerene derivative $C_{60}F_{48}$. With doping, a value of $R_c W$ as low as $260 \Omega\text{cm}$ was obtained, which is the best result obtained so far for polymer-based OFETs. With that, it was possible to reduce both channel and overlap length down to few μm , increasing channel transconductance from 20 mS/cm to 0.250 mS/cm , together with a low gate capacitance. This first step is fundamental to develop high performing OFETs working in the high frequency (HF) and even ultra-high frequency regime (UHF).

The second part of this work was devoted to the reduction of thermal degradations in downscaled OFETs, related to the device self-heating during operation. This unwanted effect, is responsible of a continuous and irreversible performance deterioration, preventing the final frequency achievement. In this work the heat dissipation problem was tackled by decreasing the

dielectric thickness, which allowed to work at very low operating voltages (important also for real applications). The original parylen dielectric of the blend based OFETs was replaced by an ultra-thin solution processed layer of poly(vinyl formal)(PVF). With that, operating voltages have been reduced down to 5 V and the device thermal stability was improved even for the shortest channels on insulating substrates. However, due to the increased dielectric capacitance, the parasitism associated to the overlap are inevitably increased, degrading the final frequency response. To face this problem, an attempt in developing novel strategies to keep low overlap parasitism without compromising injection properties was done, to alleviate the AC-performance degradation. The third part of this work was dedicated to the exploitation of either direct-written or self-aligned methods, which are the most appealing ones for a scaling-up, to fabricate downscaled and high performing OFETs for HF operation. This is important because the techniques typically used for material patterning in solution based OFETs, are characterized by a low spatial resolution, in the range of few tens of μm , at most. This is not sufficient for high frequency applications, in which the target resolution for critical dimensions like channel and overlap length is around few μm . Some strategies have been already developed to overcome this limitation, such as electro hydro-dynamic ink-jet printing

and fs-laser assisted printing. However, some constraints make still difficult the scaling up of these techniques at industrial level. In this work, printed direct-written metal contacts deposited with the novel ultra-precise deposition (UPD) technique were tested with well-studied semiconductors. Thanks to a combination of contact treatment and mild doping, it was possible to demonstrate HF operation, despite of the unusual high electrode thickens and high roughness. Self-aligned plasma etching and self-aligned printing were also exploited for the fabrication of sub-micrometre channel OFETs, as alternative strategies for high resolution patterning, using simple low-resolution techniques. The results presented in this thesis, show the potentiality of organic electronics, in particular of solution based processes, in becoming a competitive technology for IoT applications, where high performances and simple cost-effective integration of devices are fundamental requisites.

DIFFUSE OPTICAL IMAGING FOR BREAST CANCER: DIAGNOSIS, THERAPY MONITORING AND SURGICAL MARGIN ASSESSMENT

Giulia Maffeis – Supervisor: Paola Taroni

In 2020, breast cancer became the most diffused neoplasia worldwide. Among women, it accounts for 24.5% of cancer cases and 15.5% of cancer deaths. Imaging is the primary tool to detect and characterize breast cancer, by providing information about the morphology or the physiology of the tissue, depending on the specific technique. However, standard imaging techniques (e.g., X-ray mammography, Magnetic Resonance Imaging, Ultrasounds and Positron Emission Tomography) have some relevant limitations: high costs, low efficiency on dense breasts, long examination time or side effects. Diffuse Optical Breast Imaging is an emerging technique that could potentially answer to such unmet clinical needs: it is time- and cost-effective, non-invasive, high-sensitive on dense breasts, and, most importantly, it provides quantitative physiological information about the breast tissue micro-structure and its composition in terms of oxy and deoxy haemoglobin, water, lipid and collagen concentrations. It is an application of Diffuse Optics, that describes photon migration in a turbid medium, just like the breast tissue, according to its absorption and scattering properties. The analytical models chosen to extract the quantities

of interest are the diffusion approximation of the diffusion equation, the Lambert-Beer law and the Mie empirical model. Diffuse optical imaging proved useful for breast cancer risk assessment, lesion diagnosis, therapy monitoring, the prediction of its outcome and surgical resection margin identification. This PhD thesis describes three projects involving experimental activity in laboratory and in clinics about diffuse optical breast imaging: SOLUS, NADOPTIC and implicit calibration. **SOLUS: Lesion characterization** A lesion is usually characterized by a fibrous, dense, high vascularized tissue with respect to healthy tissue, which is more adipose. These properties are generally shared by benign (e.g. fibroadenomas) and malignant (i.e. tumours) lesions. However, according to literature, most tumours have an even stronger angiogenesis, higher water content, less lipids and more collagen. The meaningful differences in terms of composition and micro-structure between tumours, benign lesions and healthy tissue imply that diffuse optical imaging can potentially be used to discriminate lesion type. Indeed, the first instrumentation, developed within the Horizon 2020

project SOLUS, is devoted to the multiparametric non-invasive diagnosis of breast cancer. The project, started in 2016, envisioned the design, development and test in clinics (now ongoing at the San Raffaele Hospital in Milan) of a hand-held probe combining time-resolved Diffuse Optical Tomography (DOT), B-mode ultrasounds (US), Shear Wave Elastography (SWE) and Colour Doppler (CD) sonography. The technological novelty resides in the first ever miniaturization of an 8-wavelength US-guided DOT device in time domain. The outcomes of US-guided DOT about the 16 benign and 6 malignant lesions measured so far have been preliminarily analysed via machine learning to obtain an initial estimate of the performance of the device. Sensitivity is 91% and specificity 75%. The goal is to improve them by including US, SWE and CD findings. **NADOPTIC: Therapy monitoring and prediction of its outcome** Neoadjuvant chemotherapy (NAC) aims at downstaging large tumours before surgery, thus allowing for a more conserving operation. The early assessment of the therapy efficacy would enable the customization of the treatment upon the patient's needs, improving her quality of life. Also, health systems would save

significant amounts of financial resources. Diffuse optical imaging could assess the effectiveness of NAC by estimating the variations induced on the composition. In general, blood, water and scattering properties drop in correspondence of the tumour when the therapy is successful, while they remain unchanged otherwise. Also, responders show higher initial values for saturation and haemoglobin in the tumour with respect to non-responders. Together with therapy monitoring, diffuse optical imaging is thus suitable also for the prediction of its outcome. These are the purposes of the clinical trial that currently involves the second instrumentation, a 7-wavelength (635–1060 nm) optical mammograph developed at the Physics Department of Politecnico di Milano, that operates in time domain and acquires projection images in transmittance geometry. The extension of the spectral range up to 1060 nm allows for the first systematic assessment of collagen (reported to have an important role in carcinogenesis). Preliminary attempts of correlation between the optical data, now measured in terms of average constituents' concentrations, and the patient's response to therapy, evaluated by means of histopathology, of the 8/20 patients completed so far have been made. Each patient is subject to 6 measurements over about 6 months, from first infusion to surgery. For responders to therapy, the initial concentration for water (-5%/-62% range variation from start to end over patients), blood

(+9%/-64%) and collagen (-32%/-71%) in correspondence of the lesion is generally higher than the final one, while lipids exhibit the opposite behaviour (+3%/+272%). **Implicit calibration: Intraoperative resection margin assessment** Worldwide, on average 37% of the breast conserving operations require additional surgeries due to positive resection margins. This has a negative impact on the patients' wellbeing and health care costs. Now-a-days, the most accurate resection margin assessment is via histopathology, that might require several days. Intraoperatively, the main techniques are palpation, touch preparation cytology, US and specimen radiography. However, these methods are time-consuming or not enough precise. Diffuse optical measurements have already found a very good differentiation between breast invasive carcinoma, ductal carcinoma in situ, connective tissue (i.e. healthy glandular tissue), and adipose tissue, mainly based on the lipids and water concentrations on ex vivo specimens. Indeed, the third instrumentation of this thesis work is a hyperspectral imaging setup ranging from 400 to 1600 nm, based on continuous wave devices. It has been used in the framework of a secondment at The Netherlands Cancer Institute (Amsterdam), whose goal was to define and validate an innovative method to pre-process hyperspectral images without the use of reflection standard tiles, impossible to use in sterile conditions, thus enabling its

application intraoperatively. Its name is "implicit calibration", being based on the optical data already contained in the hyperspectral image of the sample itself. After its coding, the software has been successfully tested on simulations and coconut homogeneous phantoms. It correctly recognized the composition of the sample with an error below 0.5%. The three architectures share the principles of diffuse optics, but differ in implementation and spectral range, thus offering different trades off between optical data informative content and experimental setup complexity. During the PhD, efforts were made to acquire expertise to optimize and validate these novel technologies. In particular, SOLUS and NADOPTIC offered the possibility to gain competences in managing a clinical study, while the implicit calibration method is at an earlier development stage, still in laboratory. Even if promising, findings are not conclusive: the clinical trials and the validation of implicit calibration have not been completed yet. Future analysis (a multimodal approach for SOLUS, a more accurate model for the data analysis of NADOPTIC and a systematic validation on specimens for implicit calibration) then could highlight even more the potential of diffuse optical breast imaging.

THE PHOTOPHYSICS OF CELL MEMBRANE-TARGETING PHOTOTRANSDUCCERS

Arianna Magni – Supervisor: Guglielmo Lanzani

Nowadays, understanding how bioelectrical signals regulate cell behaviour is crucial in biological sciences, due to the strong implications that bioelectricity and signalling have in neuroscience and medicine. The first experiments of Luigi Galvani, performed at the end of the XVIII century, demonstrated that it was possible inducing a muscle twitch on a detached frog leg by applying small voltages. Since then, different strategies have been implemented to monitor and control cell and tissue activity, giving raise to the field of bioelectronics.

Endogenous bioelectricity originates in selectively permeable cellular membranes due to the activity of ion channels and pumps. These elements are responsible for the rise of potential differences across the membrane. For instance, in electrically excitable cells, such as cardiomyocytes and neurons, fast changes in membrane potential respectively monitor the heartbeat and propagate the electrical signals that brain cells use to communicate. Membrane potentials are also crucial in non-electrically excitable cells, as they are involved in numerous essential cellular processes including proliferation, differentiation, migration, shape change, and programmed cell death. It is thus

clear that cell membrane and its electrical potential represent the core of bioelectricity, hence representing an ideal target for the exogenous modulation of signalling. However, the hardest issue to tackle in bioelectronics is interfacing cell membrane with exogenous materials, without compromising its functioning. This thesis investigates the use of light as a tool for modulating membrane potential and bioelectricity, with the broad aim to establish life-machine symbiosis that can help in healing disorders and restore biological functions. An approach to induce light sensitivity in animal cells, which are usually transparent to visible light, is the use of photoactuators. These are photoactive materials that can decorate or attach to the cell membrane and are able to transduce light into a signal that can be processed by the cells. A variety of materials are suitable for cell opto-stimulation, ranging from inorganic nanoparticles to organic polymer films and nanostructures. Here, I make use of different small membrane-targeting molecules, with emphasis on the study of the photostimulation mechanism. The goal is to link the photophysical changes, occurring in the molecular photoactuator after light absorption, to the different biological effects observed in cells.

I studied three different molecules, which all have some common characteristics, namely: *(i)* they are amphiphilic in order to spontaneously partition within the cell membrane; *(ii)* they absorb light in the visible part of the spectrum due to their conjugated moieties and transduce the light energy into a membrane perturbation; *(iii)* they have low toxicity, especially in dark conditions. In terms of experimental techniques, I employed confocal fluorescence microscopy to track the localization of the molecules within the cell membrane, while I exploited the patch-clamp technique to evaluate the performance of the photoactuator and record the variations in the membrane potential upon light excitation. Additional experiments were performed on artificial lipid bilayers to elucidate the mechanisms in more simple systems. The photophysical characterization of the different compounds was performed using both steady-state and time-resolved optical spectroscopies, backed by quantum chemistry calculations. The cell response was simulated by modelling the cell membrane with a simple RC circuit, whose characteristic parameters can vary because of the action of the activated photoactuator. The first photoactuator I

investigated is Ziapin2, an azobenzene-based molecule with an azepane ring on one side and two alkyl chains on the other side. Ziapin2 is able to switch between two isomers, a stable *trans* form and a metastable *cis* one. The *trans-to-cis* isomerization is driven by blue light, while the reverse transition occurs spontaneously. This molecule has been shown to efficiently partition within lipid bilayers and to trigger the hyperpolarization of the cell membrane at light onset and the depolarization at the light offset. The mechanism behind it is the following: molecules internalized within the cell membrane tend to form dimers, producing a thinning of the membrane. When light is absorbed, the molecules isomerize, the dimers are broken, and the membrane goes back to its original thickness. Changes in membrane thickness directly reflect on the membrane capacitance, as the two quantities are inversely proportional. Fast modulation of membrane capacitance can perturb the membrane potential. I was able to relate the light intensity shined onto *in vitro* cells to the number of molecules that isomerize and therefore to the change in capacitance. Combining these data in an adequate RC circuit, I quantitatively reproduced the variations in the membrane potential. Moreover, the isomerization process of Ziapin2 is influenced by the environment experienced by the molecule. One key parameter in this scenario is the viscosity, as I found that high-viscosity solvents hinder the *trans-to-cis* isomerization. I correlate the fluorescence lifetime of Ziapin2 to

the viscosity of the environment and exploited its amphiphilicity to build a viscosity sensor able to estimate the viscosity of lipid membranes on the nanoscale. The second molecule I considered is again an azobenzene-based molecule. This system however has two alkyl chains on one side and a nitro group on the other side, with the latter being a strong electron-withdrawing group, which makes the molecule a push-pull system with a strong dipole moment, which reduces by about 30% upon illumination, i.e. the *cis* form has a lower dipole moment than the *trans* one. Also in this case, the isomerization process is able to modulate the membrane potential: a depolarization signal is detected when I shine light on cells loaded with the push-pull molecule. As no variation in membrane capacitance is identified, I hypothesized a completely different mechanism. Indeed, the photo-induced dipole moment modification occurring within the cell membrane provokes a rearrangement of the charges in its neighbourhood. This results in changes in the charges present on the two leaflets of the lipid bilayer and in an inward current across the membrane.

The last examined photoactuator is a donor-acceptor terphenyl-based compound, named BV-1. When I shine light on cells treated with BV-1 I observe a drop in the membrane resistance due to increased permeability of the cell membrane. The phenomenon, which is dose-dependent, leads eventually to cell swelling. The photophysical characterization of BV-1 showed that the molecule is a photosensitizer. The efficiency

of the singlet oxygen generation is enhanced in low-polarity environments such as the cell membrane. The generation of singlet oxygen within the cell membrane brings to the peroxidation of lipids, leading to membrane disruption. This phenomenon was spotted also on artificial lipid bilayers, and thus is non-specific and does not involve any membrane proteins or channels.

In conclusion, I was able to build a relationship between molecular excitations and cell electrical potential photomodulation. I identified three different mechanisms, namely: *(i)* the photoinduced mechanical modulation of the membrane capacitance; *(ii)* the photoinduced charge displacement across the cell membrane; and *(iii)* the photo-induced reduction of the membrane resistance. These findings bring new knowledge to the field of non-genetic cell photostimulation and open up a path for designing and engineering novel photoactuators.

SPIN DYNAMICS, ORBITAL EXCITATIONS AND CHARGE ORDER IN INFINITE-LAYER COPPER AND NICKEL OXIDES

Leonardo Martinelli – Supervisor: Giacomo Claudio Ghiringhelli

My PhD activity has been devoted to the investigation of the peculiar properties displayed by infinite-layer cuprates and nickelates, which I carried out during my Ph.D. activity in the group of Prof. G. Ghiringhelli, at the Physics Department Politecnico di Milano (Italy). It has been carried out with the use of soft x-ray spectroscopies, mostly using X-ray absorption spectroscopy (XAS) and Resonant Inelastic X-ray Scattering (RIXS). These materials are related to the famous class of high-temperature superconducting cuprates, which still hold the record for the highest critical temperature at ambient pressure. Despite several years of intensive research, many aspects of physics of these materials remain unexplained. In particular, a microscopic description of the pairing interaction is still lacking. Although it is known that magnetic fluctuations play a key role, no model can yet give a first-principles description of it. At the same time, the phenomenology outside the superconducting phase is little understood as well, and is possibly the manifestation of a super-entangled state of matter. The fundamental reason is the complexity of the main building block of cuprates: the two-dimensional CuO_2 planes, arranged as a square-lattice of

spin-1/2 sites. This complexity arises, in essence, from three factors. First, the exceptionally strong correlation between electrons, which lose their single-particle character. Secondly, by the reduced dimensionality, which enhances the effect of quantum fluctuations in the several broken-symmetry phases host by cuprates. Third, by the large long-range superexchange couplings which arise from a strong covalency of the planes. We contributed to the topic by studying infinite-layer cuprates, where the peculiar crystal structure pushes the oxygen-mediate superexchange to the extreme. First, we present a detailed investigation of the magnetic excitations in the infinite-layer

cuprate CaCuO_2 . Using RIXS at the Copper L_3 edge, we provide evidence of an anomaly in the magnetic spectrum close to the antinodal point $(1/2, 0)$ in reciprocal space. We investigate its nature through an innovative combination of measurements, including ultra-high-resolution, polarimetric and detuning RIXS measurements. Referring to recent theoretical work, our results present strong evidence in favour of the fractionalization of magnons into spinon pairs. We correlate this behaviour with the exceptionally strong ring-exchange, whose value is enhanced by the large covalency of the system. Our results provide the first reliable observation of fractionalized magnetic excitations in a two-dimensional

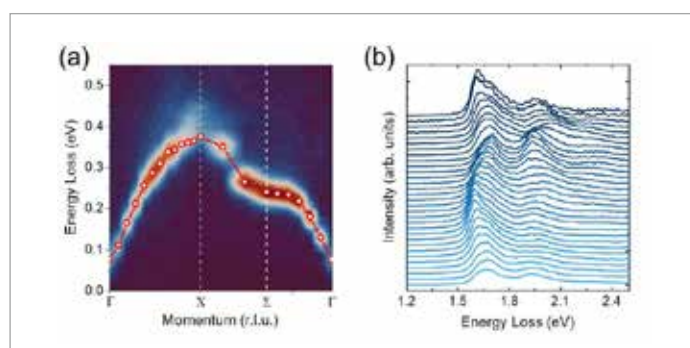


Fig.1 - (a) Magnetic spectrum of infinite-layer cuprate CaCuO_2 . Red dots report the energy of spin waves. (b) Stack of RIXS scans showing the orbital spectrum of the same compound as a function of momentum. Evident is the dispersion of the first two peaks, corresponding to xy and xz/yz orbital excitations.

square lattice. The orbital spectrum of infinite-layer cuprates shows fascinating physics as well. In correlated materials, dd excitations usually behave as localized, atomic-like transitions, with the exception of a handful of one-dimensional cuprate chains. Using RIXS at the Copper L_3 edge on CaCuO_2 and Nd_2CuO_4 , we report for the first time the presence of collective orbital excitation in a two-dimensional $3d$ material, i.e. of mobile quasi-particles called orbitons. Moreover, we show that our experimental observations are incompatible with the current Kugel-Khomskii (KK) model of orbitons in correlated materials. Using an Emery-type charge-transfer model, we construct an extension of the KK model, introducing a next-nearest neighbours orbiton

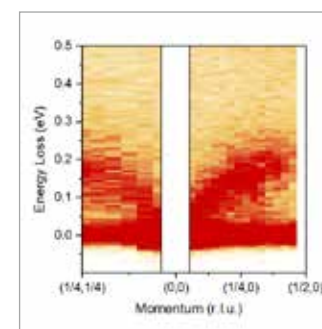


Fig.2 - Dispersion of magnons in infinite-layer nickelate NdNiO_2

super-exchange. We show that this model nicely reproduces our experimental findings, and can naturally explain the different behaviour shown by cuprates with and without the apical oxygens. The reason can be traced back once again to a prominent role of the oxygen bands, which enhance longer-range exchange interactions. I dedicated the second part of my activity to the family of infinite-layer nickelate superconductors, which were first synthesized in 2019. These materials are structurally identical to infinite-layer cuprates: they are composed by a stack of two-dimensional NiO_2 planes, arranged in a square-lattice and with monovalent Ni^{1+} in a $3d^9$ state. Due to their recent discovery, still much is unknown about this class of compounds.

First, we thoroughly investigate their electronic structure using XAS and RIXS at the Ni L_3 and O K edges. In agreement with other recent works, we show that the charge-transfer energy is larger than in cuprates, and that three-dimensional $\text{Nd } 5d$ bands are active at the Fermi level. Consequently, we argue that nickelates present a mixed Mott-Hubbard - Charge-transfer character.

Additionally, we analyse the

different phenomenology displayed by samples with and without an epitaxial SrTiO_3 (STO) capping layer. In the former, we report the second independent observation of dispersing magnons, and the first polarimetric measurements revealing unambiguously their magnetic nature. We show that the characteristic energy of magnetic fluctuations softens with doping, in stark contrast to cuprates. Thanks to preliminary calculations, we also correlated this behaviour with the reduced t/U value in the single-band Hubbard picture. In capping-free samples, we discover a much stronger hybridization with $3D$ Nd - bands, which reduces the electronic anisotropy. We find that this increased three-dimensionality is accompanied by the formation of a charge-ordered phase.

Overall, our results highlight the importance of two crucial properties in determining the physics of cuprates and nickelates: the strong hybridization between the transition metal and oxygen bands, and the degree of two-dimensionality.

FROM THERMAL TO MECHANICAL: SHEDDING LIGHT ON NOVEL WAYS TO CONTROL CELL FATE

Leonardo Maver – Supervisor: Maria Rosa Antognazza

It is of vital importance for cells to be able to communicate with – and receive inputs from – the surrounding environment, as well as with each other in a precise and efficient way. In order to properly react to external stimuli, cells have developed advanced mechanisms of communication so that they can receive an information, transfer the message across the plasma membrane, and finally respond by producing changes within the cell. Cells are sensitive to a range of different cues, depending on the type of cell and the environment they are supposed to survive in. These stimuli include, among the others:

- Chemical cues that are the typical ones used by cells to communicate with one another, by releasing molecules that are then sensed by other cells' receptors;
- Thermal stimuli as thermoregulation is critical in many living beings, cells are sensitive to the temperature variations of the environment, with receptors for the heat and the cold;
- Electromagnetic stimuli of different kind, including light sensitivity for some specialised cells like the retina ones;
- Mechanical cues as the mechanical stress and stiffness of the environment are critical

stimuli for a number of cellular processes, from growth to differentiation to death.

The chemical way of stimulation and signalling was the subject of the earliest studies in medicine and biology, thus becoming the classical path of research for the development of ways to stimulate and control the cell fate. Large effort was put in the development and optimisation of media, factors, chemical agents and protocols to direct and affect cell growth, differentiation, migration and all biological processes.

Nowadays these techniques and protocols are largely assessed, both reliable and effective, but they still have drawbacks. The most important ones are the lack of reversibility of such cues, and the poor control and precision in the spatiotemporal domain: *e.g.*, it's impossible to target specific cell sub-population within the same *in vitro* culture. An improvement on these techniques would require a dynamic control of the extracellular environment, thus offering the possibility to provide precise stimuli at selected time-points in a more versatile way. As a consequence – especially in the last decades – an increasing interest and effort was put in the research field

of biophysical cues, besides biochemical ones, to exploit all the spectrum of stimuli that can be sensed by different kinds of cells.

Among other cues, the use of light could offer a huge improvement in control and resolution, both in the spatial and temporal domain. The last decades saw important technological advancements in the field (*e.g.*, two-photon microscopy and laser) that paved the way for advanced ways to control cells using light, with high spatial and temporal resolution (down to $< 1\mu\text{m}$ and $< 1\text{ms}$, respectively).

Cell photostimulation, however, presents one huge limitation: mammalian cells do not present any specific sensitivity to light (with some exceptions, as the photoreceptors in the retina). Research has thus been mainly focused on overcoming this limitation, by employing external light absorbing elements that could act as phototransducers – converting light signals into stimulation of cell activity. A number of such systems, different in size, shape, material and working principle, has been consequently developed.

In this PhD thesis work I studied different ways to obtain an

effective photostimulation of living cells. The different steps of my research pathway exploit different elements among the spectra of possibilities given by the (photo)active material, the cell type and the stimulation pathway to be targeted. In particular:

- in the first branch we used an organic semiconducting polymer, namely poly(3-hexylthiophene-2,5-diyl)(P3HT), as a culturing, light-sensitive substrate to affect human adipose-derived stem cells (hASCs) fate;
- in the second branch a new biomaterial, inorganic indium selenide (InSe), was tested as a substrate, with the idea that the mix of electrical and morphological properties could affect significantly the cell biology;
- in the last branch the interest in mechanical properties of the substrate for cell stimulation (introduced previously) is further developed, from the biological study on the PIEZO1 channel, to the effective stimulation of cells with an electrically controlled swelling polymer, towards the use of azobenzene-based photodeformable substrates.

The focus of this research work started on stem cells stimulation with light, and then progressively shifted towards one stimulation pathway less explored to date, that is mechanotransduction. There is a double *fil rouge* connecting the different chapters:

- light is proposed as the primary controller of stimulation in this research. This is the starting point in the first two

lines, where we select the photoactive material as the first step; while in the last project we solely end with the idea of using a photoactive material to photomodulate our stimulation.

- stem cells stimulation and fate control is also present as the motivation of most research, at least as the leading drive of the studies. The first section is directly about hASC stimulation with our materials, while the following chapters are not explicitly about stem cells; however, the mechanical stimuli coming from the environment, be them passive (like in the second section for the morphology) or active (like all we achieved in the last section) play a key role in the control of cell fate for a huge number of different kinds of cells, including stem cells.

All in all, this PhD thesis research work developed with the ambition to widen the spectrum of different techniques, materials and biological applications to which light as the initial controller could be applied. As compared to the other approaches in the field of biophysical cues, the use of light presents some clear advantages:

- it is minimally invasive, as there is no wiring or contact needed between the cells and the stimulating setup;
- it is spatially confined, as the resolution that could be achieved with a light beam is $< 1\mu\text{m}$;
- it is highly versatile, since the parameters of the light stimulation protocols can be optimized *ad hoc*.

Also, in principle the techniques that we reported here are mostly easily applicable to any *in vitro* cell culture facility, in incubating conditions, with no needs for expensive or bulky instrumentation, and in a remotely controlled way.

This is not totally true (yet) for the results we reported for mechanotransduction, but research on that project is going toward that direction.

We thus believe that our results could be promising enough to offer novel approaches on the old problems that the world of biophysical cues is trying to solve:

- we deepened the knowledge on the photothermal effect, reporting its consequences on stem cells;
- we added a novel material to the spectrum of biomaterials, so that it could be employed in more advanced applications and devices;
- we proposed a novel, rarely studied pathway for cell stimulation, that could offer a possible breakthrough in the research on biophysical cues.

For these reasons, we are confident that our results represent a useful and promising basis for further studies, aimed at investigating in detail the opportunity to use light for controlling a number of processes in different cell models, like the differentiation status of *in vitro* stem cells.

This could open the way to unprecedented tools in the field of regenerative medicine.

ULTRAFAST LIGHT-CONVERSION PROCESSES: FROM THERMO-OPTIC AND OPTO-MECHANICAL SWITCHES AND MODULATORS BY FEMTOSECOND LASER MICROMACHINING

Roberto Memeo – Supervisor: Roberto Osellame

In the last decades, integrated photonics has played an always-increasing role in the development of new technologies and devices, with applications not only in the field of optical communications but, more recently, also in linear-optical quantum computing and simulations. Actually, the possibility of integrating a highly-engineered photonic circuit inside a small glass chip allows to develop ultra-stable platforms for the large-scale processing of classical and quantum optical signals.

A key feature of integrated photonic devices is reconfigurability, i.e. the capability of tuning the functionality of the device by means of externally-applied control signals, e.g. for implementing fast optical switches or active routers which can be operated in a flexible and dynamical fashion. The reconfigurability of integrated devices is often implemented by means of thermal shifters, i.e. electrically-driven resistors which induce a local temperature change in some specific points of the circuit, to modulate the waveguides effective index through the thermo-optic effect, thus imposing a controlled phase shift to the propagating

light. Inserted in Mach-Zehnder interferometric rings, these components enable to arbitrary route the optical signals through the circuit. Currently, the most advanced reconfigurable integrated photonic chips are realised through lithographic techniques, which provide high precision, miniaturisation and low-loss switching. However, fabrication time is generally long and the requirement of a clean room environment makes these methods less effective in the prototyping of optical circuits with innovative geometries. In the last twenty years, Femtosecond Laser Micromachining (FLM) has progressively attained a relevant role as fabrication technique for integrated optical circuits due to its advantages. It consists in the direct writing of optical circuits by means of focused femtosecond laser pulses. FLM relies on a maskless approach which does not require a clean room environment, and it allows for the fast prototyping of high-quality integrated photonic circuits on glass substrates. Moreover, FLM is intrinsically a 3D fabrication technique as it exploits non-linear absorption phenomena taking place only at the focal point, whose depth in the substrate is chosen freely.

In recent years, FLM has been exploited to fabricate integrated photonic devices for numerous applications, including beam dividers, directional couplers, polarisation sensitive elements and wavelength division multiplexers. Furthermore, thermal phase shifting elements can be also fabricated by FLM, by depositing metallic films on the substrate and then ablating them with the femtosecond laser. The choice of thermal tuning to reconfigure integrated circuits is related to its high stability and reliability and to the simplicity of its implementation. Nevertheless, this approach has two main limitations: I) heaters should not be placed too close one with respect to the others in order not to induce excessive cross-talks. II) The temporal response of such devices is limited to the millisecond scale, due to the intrinsic slowness of thermal diffusion processes. Thus, the switching time limits the device operation at frequencies lower than hundreds of Hz. On the other hand, lithium niobate devices find widespread application in the optical communications field, for signal switching and modulation purposes. They provide very high frequency operations (up to 100 GHz) but suffers from significant

insertion losses (~ 7 – 8 dB), which make them not suitable for those applications where the optical signal can not be regenerated or amplified (e.g. quantum optics). A possible way to circumvent the previous limitations could be to take advantage of a different effect for altering the refractive index of the substrate. Specifically, the elasto-optic effect, which produces a refractive index change in response to an applied mechanical stress, looks particularly promising, since it can be exploited in a wide variety of substrates, including glass. Moreover, low-loss optical waveguides have been extensively demonstrated in glass and can be coupled to micromechanical elements thanks to the versatility of FLM. The realisation of integrated opto-mechanical phase shifters would indeed allow to push the operational frequency of the devices up to the MHz regime, in principle with

negligible cross-talk between different elements. However, the fabrication of such components is challenging, as it requires the carving of complex 3D mechanical resonating structures inside the bulk substrate, with micrometric resolution.

This work aims at improving the temporal response of the existing methods, based on the thermo-optic effect, for signal modulation in reconfigurable photonic circuits on glass substrates and at proposing new alternatives to them, by exploiting the elasto-optic effect to induce controlled refractive index variations related to localised stresses in the material due to the oscillation of micro-mechanical structures. In this context, two different devices have been optimised and fabricated.

The first device consists in a thermally-reconfigurable optical circuit relying on a micro-resistor patterned on the top of the glass substrate, in correspondence

of one arm of an integrated Mach-Zehnder interferometer (see Figure 1a). Thanks to a novel lateral multiscan writing approach, the circuit waveguides are inscribed very close to the sample top surface, helping to improve the temporal response of the device which shows a cut-off bandwidth of 1.5 kHz (see figure 1b), one order of magnitude better than other thermo-optical modulators fabricated by FLM. The second device exploits the resonant oscillations of integrated microstructures, acting on a single-mode optical waveguide which is directly inscribed within them. These embedded structures are fabricated by FLM and operate periodically at a fixed frequency, modulating the effective refractive index of the circuit waveguides through the elasto-optic effect. Depending on the device geometry, the resonance frequency of micro-mechanical structures can be tailored from tens of kHz to approximately 1 MHz, markedly overcoming the performances of other glass-based integrated modulators, which rely on the thermo-optic effect. Figures 1c and 1d report the scheme of a fabricated microstructure together with its polarisation-dependent switching capabilities at a frequency of 1.024 MHz.

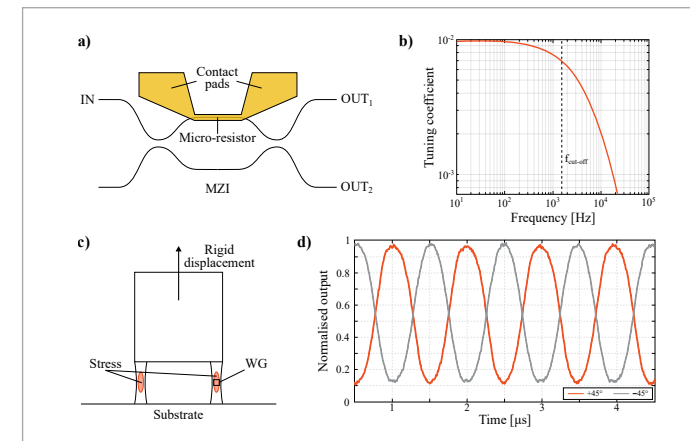


Fig.1 - (a) Schematic representation of an integrated Mach-Zehnder interferometer (MZI) with a patterned micro-resistor and (b) its measured frequency response. (c) Schematic cross-section of the micro-mechanical resonator, highlighting the stress concentration regions and the waveguide (WG) position, and (d) the signal modulation at its output for two orthogonal polarisation input states.

MOLECULAR SENSING WITH SURFACE WAVES

Erika Mogni – Supervisor: Paolo Biagioni

Optical sensors are well-established tools in today's life. The specific detection of small quantities of analytes has a huge importance due to its application in medicine and life science so sensing tools that allow enhancing the molecular signals are of great interest. Bloch Surface Waves (BSWs) generated at the surface of a semi-infinite one-dimensional photonic crystal (1DPC) are nowadays a well-known tool for surface-enhanced spectroscopies. BSWs are complementary to Surface Plasmon Polaritons (SPPs): they share the evanescent behavior of the electromagnetic field in the direction perpendicular to the surface while propagating along the plane of the surface itself but have some crucial differences. SPPs can be generated by the illumination with red/near-infrared light of a thin metallic layer, allowing for the refractometric sensing of analytes present on top of the surface. The design of 1DPCs sustaining BSWs can instead be fine-tuned to have resonances in the visible/UV region of the spectrum, as in our case of study, to investigate also electronic transitions. Moreover, SPPs can only be excited with transverse magnetic (TM) polarized light because collective oscillations of

surface electrons are involved, while 1DPCs can sustain both TM and TE (transverse electric) polarization of surface modes. In general, TE and TM surface modes have different phase velocities, so it is not possible to generate an arbitrary defined polarization state resulting from a combination of the two modes. A further step in the field of surface-enhanced spectroscopy would be to control the polarization state of BSWs. This goal can be realized by engineering the structure of the 1DPC to obtain overlapping dispersion relations for TE and TM modes. TE and TM modes with the same phase velocities allow for simultaneous measurements of the two polarization responses, at the same angle and at the same wavelength, and the differential signal could be used for the investigation of the birefringence of a top molecular layer over a broadband spectral range,

adding the ability to distinguish between randomly disposed and oriented molecules anchored to the surface. Moreover, the superposition of the TE and TM modes enables linear and circular dichroism spectroscopy since it is possible to combine them in a controlled way, to obtain for example circular or elliptical polarization states over a broadband spectral range. This feature can be experimentally tested with the acquisition of reflectivity maps as a function of the illumination wavelength and the angle of illumination in a total internal reflection geometry. We have worked on a design that can exploit this feature and ended with the structure illustrated in Figure 1.

Alternating layers of SiO_2 and Ta_2O_5 are fabricated by reactive magnetron sputtering. The overlap between TE and TM dispersion relations is obtained by inserting a high refractive

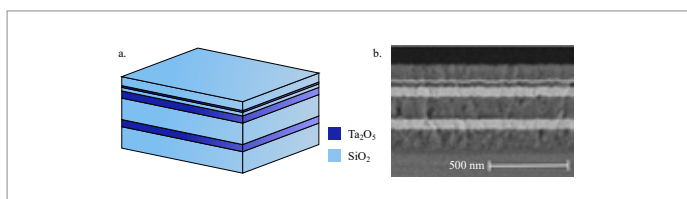


Fig.1 - a) 3D sketch of the 1DPC with a high refractive index inclusion into the last SiO_2 layer that allows for TE and TM dispersion relations overlapping over a broadband spectral range. b) SEM image of the cross-section of one of the fabricated 1DPC.

index inclusion in the topmost layer.

My first activity has been the optical characterization of TE and TM surface modes of the 1DPC to demonstrate their overlap. This was obtained by acquiring reflectivity maps for TE and TM illumination of the sample as a function of the illumination wavelength and of the angle of incidence in aqueous-based environment. Results are shown in Figure 2.

Panel a shows the dispersion of the TE mode, that appears in the map as a narrow dip. Panel b shows instead the TM response of the sample, and the mode is visible only as a weak halo. This behavior is confirmed by looking at sections at fixed wavelength of both maps, as shown in panel c. From here, it is possible to observe the partial overlap of the

modes, with the sharp TE mode positioned around the tail of the broad TM mode. This overlap is enough to perform polarization sensitive spectroscopy, as I did as a second activity. The idea is to follow the functionalization of the crystal surface collecting the spectral position of the two modes and their shifts as a function of the refractive index of the top layer. I followed the development of single-stranded DNA (ss-DNA) brushes, obtained by the Rolling Circle Amplification (RCA) process. This procedure is applied to study the optical birefringence of ss-DNA arms through the comparison between the TE and TM response. The tracking of the shift of TE and TM modes is shown in Figure 3, where the principal steps of the process are highlighted. Comparing the TE and TM signals we can assess the anisotropic

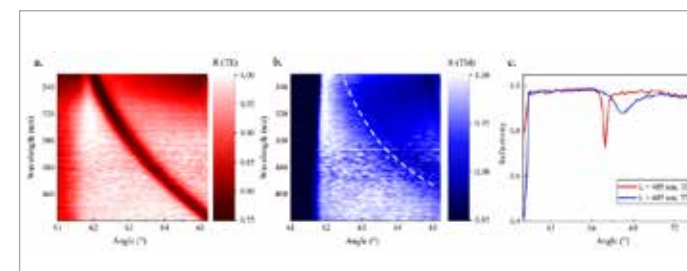


Fig.2 - a) Reflectivity map obtained with TE illumination. b) Reflectivity map obtained with TM illumination. c) Angular scan at 405 nm wavelength.

effective index of the aligned ss-DNA strands, paving the way for polarization-resolved surface-enhanced spectroscopy techniques.

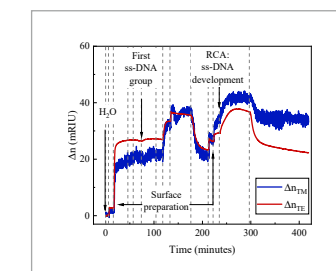


Fig.3 - Time evolution of the preparation of the sample for the RCA process

TRANSIENT ABSORPTION SPECTROSCOPY ON 2D SEMICONDUCTING MATERIALS FROM LIQUID PHASE EXFOLIATION FOR OPTOELECTRONIC APPLICATIONS

Floriana Morabito – Supervisor: Christoph Gadermaier

The global energy crisis and climate change are two crucial challenges that scientific research must face. Much effort is put into finding new sustainable sources for clean and green energy. Moreover, the lack of raw materials and need for low-cost technologies boost interest in new promising nanomaterials for these purposes. By reducing material dimensions, new physical and chemical properties can be exploited for potential applications. Of course, reaching the low-dimensional limit is challenging and implies the investigation of new phenomena related to size-effects or quantum mechanisms. The full understanding of these new physical effects is crucial to find a proper potential application, such as new commercial devices. Nanomaterials are classified according to their geometry as a result of the quantum confinement zero-dimensional (quantum dots), one-dimensional (nanotubes, nanowires) and two-dimensional (2D) (surfaces, nanolayers, quantum wells) materials can be studied. One particular group of 2D materials, known as van der Waals crystals, have been studied extensively since the isolation of graphene in 2004 by A. Geim and K. Novoselov. Graphene is a single layer of

two-dimensionally arranged sp^2 hybridised carbon atoms. Due to their chemical structure, weak van der Waals interactions between atomic planes and strong covalent or mixed covalent/ionic bonds in plane, 2D nanomaterials can be easily exfoliated, that is delaminated into single layers. Nowadays, their fabrication can be obtained according to different methods, which can be divided into two main approaches: bottom-up or top-down methods. Many 2D material growth techniques, such as chemical vapour deposition (CVD), molecular beam epitaxy (MBE), pulsed laser deposition (PLD) and many others, belong to the class of bottom-up methods. On the contrary, a top-down approach refers to mechanical microcleavage, for example the scotch tape method, or liquid phase exfoliation (LPE). LPE gives rise to a dispersion in the form of an ink, where the nanosheets are polydisperse both in thickness and lateral size. Nevertheless, by following steps of the so called liquid cascade centrifugation (LCC), it is possible to enrich the dispersion of flakes of desired thickness, e.g. monolayer flakes. With particular attention to the class of transition metal dichalcogenides (TMDs), LPE can yield semiconducting 2H-polytype

nanosheets with characteristic narrow exciton fluorescence linewidth. Recently, LPE has gained increasing attention for potential applications at industrial scale due to its scalability, high production rates, low cost, and ease of fabrication. It shows huge versatility for the exfoliation of a broad range of materials, for example TMDs, hexagonal boron nitride, metal phosphorus trisulfides, MXenes, and many others. LPE is achieved through two main steps: sonication, aiming to break weak van der Waals interactions using ultrasonic energy, followed by LCC, in order to perform a good enough size selection on the resulting dispersion. Suitable solvents and surfactants are used as stabilisers to prevent nanosheet reaggregation. Investigation of their optical properties is performed before and after deposition, either in dispersion or in film. This PhD thesis focuses on the study of the optoelectronic properties of semiconducting 2D materials belonging to the class of TMDs. The research activity consists of the exfoliation and microscopic and optical static characterisation of the materials. The photophysical understanding is achieved by means of a time resolved

spectroscopy technique known as pump-probe (PP) or transient absorption (TA). In previous works, exciton formation and relaxation within 1 nanosecond has been widely investigated and reported, mainly focusing the attention on monolayer flakes made by mechanical exfoliation. The novelty of this research activity is about the measurement and understanding of how the nonlinear response of the few-layer flakes exfoliated via LPE evolves in time from 1 nanosecond up to tens of microseconds. The goal of the research activity described in this PhD thesis work is to provide useful insights for technological applications where 2D materials made by LPE can be implemented in optoelectronic devices. This aim is achieved via the investigation of charge recombination mechanisms occurring in these materials after photoexcitation. The understanding of the fate of photogenerated species is crucial for all those applications where a good charge extraction and collection at electrodes are needed. In particular, in this PhD thesis two main materials belonging to TMDs were widely studied: molybdenum disulphide (MoS_2), and tungsten disulphide (WS_2). For the first time a heterojunction (HJ) from both

materials has been made via LPE and studied. The design of heterostructures (HSs) has been addressed as a promising solution to increase the recombination time of the photogenerated carriers by inducing the formation of the interlayer excitons, that are the electron-hole bound states where the two charges belong to different layers. The nonlinear optical response of the HJ via LPE is compared to the same materials stacked forming a HS made by mechanical exfoliation. Moreover, a thickness dependence study was performed on these materials, in order to understand the role of dimensionality, i.e. lateral size decreases by decreasing nanosheet thickness, on the charge carrier mobility and recombination time constants. The much longer carrier lifetimes compared to monolayers obtained with different techniques make few-layer flakes from LPE particularly promising for light-harvesting applications such as photovoltaics and photocatalysis. The formation of a HJ, while an important advancement of the processing of 2D materials for future devices based on multilayer structures, has proven unnecessary in this particular case, since the simpler material from a single-step

deposition already exhibits competitive carrier lifetimes. In the final Chapter, results on another new 2D semiconducting material are presented. Methyl-terminated germanane $GeCH_3$ is a promising alternative to graphene and good candidate for LEDs applications due to its anisotropy and significant photoluminescence. It has been proven that its strong emission in the visible range, i.e. peak around 670 nm, does not dramatically depend on the thickness of the layer. In contrast to the direct-to-indirect bandgap transition occurring in TMDs which results in a rapid quenching of emission for layers thicker than a monolayer, $GeCH_3$ emits for thicknesses up to tens of nanometres. As a result, the monolayer limit is not a constraint. This is very interesting, because it implies that LPE could be an excellent fabrication method for this kind of material at the industrial scale.

ULTRAFAST LIGHT-CONVERSION PROCESSES: FROM FUNDAMENTALS TO PHOTOCHEMISTRY

Vasileios Petropoulos – Supervisor: Giulio Cerullo

The abundance of sunlight energy, coupled with the current energy challenges facing the Earth, highlights the pressing need for the development of environmentally-friendly photoconverting technologies. To this regard, the research outlined in my Thesis explores light-driven pathways found in natural and artificial photo-conversion complexes. The study aims to elucidate the primary photo-physical processes, occurring within tens of femtoseconds to nanosecond timescales, controlling the yield of the light-converting response. To achieve this, we employ sub-10 fs pulses in combination with both conventional transient absorption spectroscopy and advanced multidimensional spectroscopic approaches.

Free-base porphyrins, like pheophytins, are instrumental for energy transport and charge separation processes in Photosystems (Figure 1a). Their efficiency in light-converting processes relies on the ultrafast sub-ps internal conversion mechanisms that direct the energy to the minima of the Q-band. In this work, we resolve the 60 fs internal conversion process within the Q-states in a functionalized free-base porphyrin. We observe

high frequency vibrational modes coupled to the internal conversion, with tuning (1514 cm^{-1}) and coupling modes (1270 cm^{-1} and 1350 cm^{-1}) promoting the population transfer. Theoretical calculations reveal a touching seam region within the Q-states, accessible by the interplay of high frequency vibrations. The touching seam region is directly related to the motions of the attached functional groups, as it is absent in an unsubstituted free-base porphyrin. These findings pave the way towards a predictive design of the population transfer within the Q-states by the facile attachment of functional groups to the free-base porphyrin core. On the other hand, eumelanin plays in Nature a fundamental role as photo-protecting agent (Figure 1b). In principle, this essential function results from the ability

to (i) absorb light in a broad energy range, and (ii) dissipate the adsorbed energy fast in the form of heat. Despite its importance, even the origin of eumelanin's broadband absorption spectrum is still debated. We reveal sub-50 fs formation of charge transfer states in melanin-like materials, which is the principal pathway of their efficient de-activation in sub-10 ps timescale. Their photothermal efficiency relies on charge transfer states that are immobile after their birth, without undergoing cascade charge transfer events that could possibly lead to long-lived charges. Interestingly, we observe excitation wavelength-dependent dynamics on the charge transfer and recombination events. UV excitation leads to faster formation of charge transfer states and subsequently to a

slower recombination compared to visible excitation dynamics. The excitation wavelength-dependent dynamics act as a molecular ruler of the formed charges, highlighting the efficient photoprotection of melanin-like materials upon visible excitation while giving an insight into the possible photodamaging effects of UV excitation.

Furthermore, inspired by the minimal photosynthetic unit needed to drive photo-synthesis in photosynthetic organisms, defined as Quantasome, artificial Quantasomes in this work rely on perylene-based self-assembly supramolecular complexes (Figure 1c). The structural information reveals that the artificial Quantasome accurately replicates the arrangement of chlorophylls in the thylakoid of chloroplasts. By introducing either a redox-active or a redox-inactive catalyst as a guest in the Quantasome framework, we can control the outcome of photo-conversion to either utilize free charge carriers or perform water oxidation, respectively. We review the photophysical aspects behind the outstanding performance of the Quantasome aggregation topology with respect to well-known topologies of aggregated perylenes reviewed in literature. Surprisingly, the very first event of symmetry breaking charge separation, mimicking bacteriochlorophylls, is taking place in ultrafast sub-100 fs timescales. In addition, transient absorption anisotropy suggests that the anion is rapidly moving in space after its birth preventing its fast recombination, leading

to long-lived separated charges. Our photo-converting machinery illustrates a charge separation event that lies close to the barrierless regime of the normal Marcus region and a charge recombination event that lies far into the inverted region of Marcus theory, optimal for efficient light-conversion.

Last but not least, in contrast to BODIPYs well known photostability, we observe aggregation catalysed photochemistry in a BODIPY model system (Figure 1d). The light-driven reaction can take place under ambient laboratory light, without the presence of catalysts or redox agents while leading to novel monomeric and dimeric photoproducts not previously synthesized chemically. This novel photochemistry takes place through electron transfer processes, following the symmetry breaking charge separation event of the aggregated BODIPY occurring within 3 ps after light-absorption. The alternative Z-scheme drives the observed photochemistry by activating novel C-H functionalization of BODIPYs in water and generating reactive radical species. While, the photochemistry is directly related with the recorded selective aggregation of the main photoproduct within dimers, exhibiting CT-mediated characteristics. This innovative aggregated photoproduct boasts a huge 180-nm Stokes shift of the NIR emissive state and long-lived charge separation, being an

optimal candidate for bio-imaging and artificial photosynthetic applications respectively. Overall, the research work presented in this Thesis explores the fundamental aspects of light-conversion mechanisms found in natural and artificial systems with the perspective to be applied in future generation materials. The concept of functionalizing the porphyrin core to control internal conversion reactions holds significant relevance in the fields of biology and chemistry. Vibronic coherences have been proven to control the fate of energy and charge transfer reaction pathways, eventually suppressing or enhancing specific functions. Furthermore, it is astonishing that such a crucial biological system as melanin remains largely unexplored despite its importance. Grasping the knowledge of melanin/like materials, can pave the way towards the design principles of next generation sunscreens. On the other hand, artificial Quantasomes possessing similar photophysics as the natural photosystems can optimally supplement some functions found in natural systems by producing additional fuels of interest. Lastly, we hope that the novel BODIPY photochemistry reported here for the first time will spark research towards catalyzing green photochemistry through aggregation-induced molecular systems.

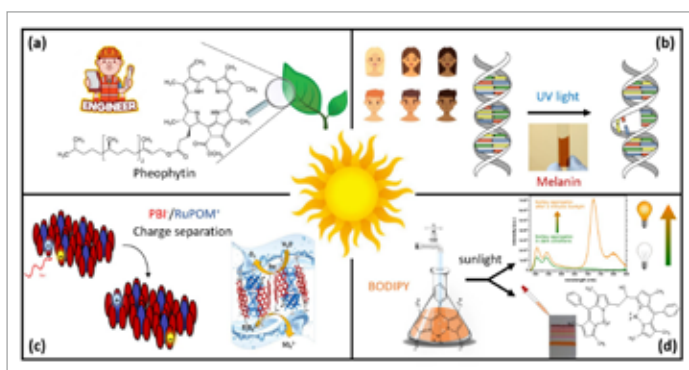


Fig.1 - A graphical abstract of the light-converting molecular systems studied in this research work.

ELECTROCHEMICAL SENSING AT THE GRAPHENE EDGES OF VAN DER WAALS HETEROSTRUCTURES

Aleksandra Plackic - Supervisor: Roman Sordan

Two dimensional materials, especially graphene, provided many innovative possibilities in the realization of electronic devices. My PhD research was focused on the development of the electrochemical sensors based on graphene. For this purpose, two graphene field-effect transistor (GFET) types were realized and electrochemically characterized: GFETs based on van der Waals (VDW) heterostructures (HSs), and GFETs based on graphene grown by chemical vapour deposition (CVD)(figure 1). Electrochemical sensing was performed at the exposed edges of graphene in both types of devices. In the case of GFETs based on VDW HSs, graphene was encapsulated between the top and bottom hBN flake, while in the case of CVD graphene GFET, graphene was not encapsulated. Due to the hBN encapsulation of graphene in GFETs based on VDW HSs, it was possible to realize one dimensional edge contacts in these devices. In the case of CVD graphene GFETs, only surface contacts were fabricated because of the lack of graphene encapsulation. Additionally, the source (S) and drain (D) contacts were made of solid material (80 nm of Au), while the gate (G) contact was liquid for the

purposes of the electrochemical sensing. Liquid gating of the GFETs was performed before the measurements. Both GFET types were investigated as electrochemical electrodes. These devices were found to operate as ultramicroelectrodes (UMEs), i.e., nanoband electrodes, by slow scan cyclic voltammetry (SSCV)(figure 2), and fast scan cyclic voltammetry (FSCV) measurements. As shown in

figure 2, measured $I-E$ curves exhibit sigmoidal profile, which is an indication of the UME. The electrochemical sensing was performed with seven redox probes: ferrocenemethanol, ferrocenedimethanol, dopamine, hexaammineruthenium, methylene blue, ascorbic acid, and ferrocyanide. Given the confirmation of graphene edge nanoelectrodes, new layout of devices was realized, so-called

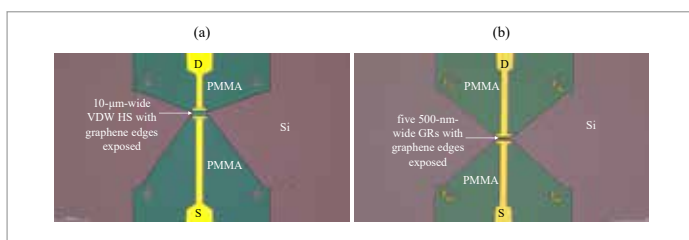


Fig.1 - Optical images of the realized GFETs. (a) S and D contact the graphene channel, i.e., 10- μm -wide graphene ribbon (GR) based on a VDW HS. (b) S and D contact the graphene channel which comprised five 500-nm-wide GRs made of CVD graphene.

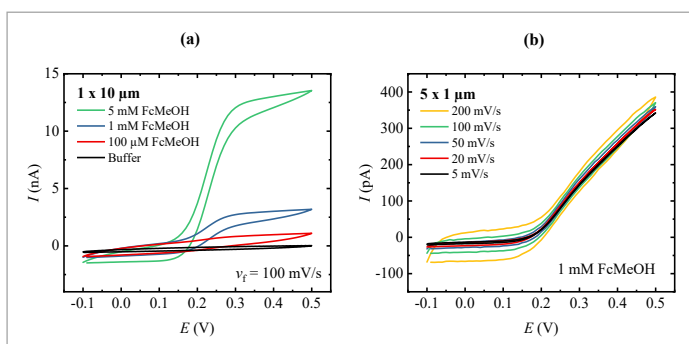


Fig. 2 -SSCV plots obtained with GFETs based on VDW HSs in the presence of FcMeOH. (a) Concentration dependence obtained with the GFET comprising one 10- μm -wide GR. (b) Scan rate dependence obtained with the GFET comprising five 1- μm -wide GRs.

nanogap GFET, where ≥ 2 graphene edge nanoelectrodes were separated by a nanogap (length from 100 to 250 nm). Nanogap GFETs allowed electrochemical sensing and redox cycling in water and supporting electrolyte, and single entity electrochemical detection of silver nanoparticles in water. Nanogap GFETs based on VDW HSs provided the access to the redox cycling effect, because it was possible to keep one nanoelectrode at the positive voltage, while having the other nanoelectrode at the negative voltage. In this configuration, one electrode acts as a generator while the other as a collector. The basic idea behind the redox cycling is the amplification of the generated Faradaic current, thus providing the possibility to detect very low concentrations of used

redox species. Figure 3 shows the obtained data in the case of redox cycling of FDM in water (figure 3.a) and background electrolyte 0.1 M KCl (figure 3.b and c). As shown in figure 3.a, achieved amplification factor with a nanogap GFET based on VDW HSs is ~ 2 , which can be easily explained from figure 3.c. The diffusion factor of 20 % (i.e., only 20 % of the species generated at the generator reached the collector) was estimated based on the data shown in figure 3.b. Graphene edge nanoelectrodes exhibited stable device response during the electrochemical characterizations. Since they are UMEs, it was possible to investigate the fast electron transfer and fundamental electrochemical reactions with these devices. Due to the possibility to detect 4 dopamine

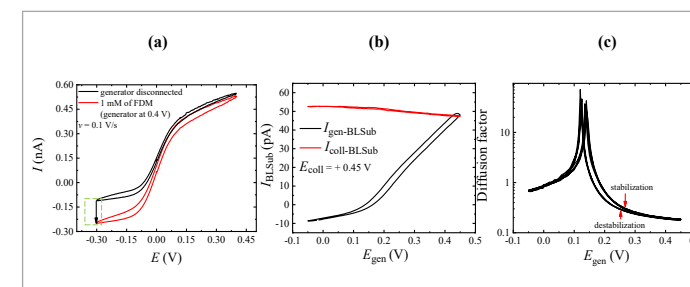


Fig.3 - Redox cycling of FDM measured with nanogap GFETs based on VDW HSs. (a) CV plot obtained in the presence of 1 mM FDM in water (black arrow in the green rectangle marks the $|I|$ increase). (b) Oxidation (I_{col}) and reduction (I_{gen}) current measured while the collector electrode was fixed at + 0.45 V. (c) Diffusion factor calculated based on the data shown in (b).

during the FSCV, clinical applications in the future could be considered. Eventually, these devices could be optimized for the detection of natural agents.

STRUCTURE-PROPERTY RELATIONSHIPS IN N-TYPE DOPED ORGANIC SEMICONDUCTORS FOR THERMOELECTRICS

Pietro Rossi – Supervisor: Mario Caironi

The web of distributed and connected devices known as the Internet of Things (IoT) is rapidly expanding, likewise, the request for sustainable micro-power sources is tremendously increasing. Most IoT devices are characterized by a limited power demand, in the range between a few nano- to milliwatts. Nonetheless, summing hundreds of billions of them accounts for a massive energy budget. Considering the diffuse character of this network, solid-state energy harvesting systems which, unlike batteries, do not require recharging or substitution are highly appealing. Photovoltaics currently play a major role, since they rely on the almost inexhaustible energy reservoir provided by the Sun. However, in dark conditions alternatives need to be evaluated. Thermoelectric generators (TEGs) exploit waste heat by converting thermal gradients into electrical potential differences, through the Seebeck effect. TEGs can therefore supply electrical power to an externally connected load. The thermoelectric properties of a material are summarized in the figure-of-merit $zT = (\sigma S^2 / \kappa) T$, which is directly proportional to the product between the electrical conductivity σ and the Seebeck coefficient S

and inversely dependent on the thermal conductivity κ . To complement standard TEGs based on expensive inorganic semiconductor alloys, conjugated carbon-based materials are currently being investigated due to their promising characteristics in harvesting low-grade heat, ideal to power distributed wearable devices and healthcare monitoring systems. Organic semiconducting materials (OSCs) are considered a less performing but greener alternative, not an equivalent replacement of conventional technology. These non-toxic and light-weighted materials offer good mechanical flexibility and conformability and are compatible with low-cost solution-based fabrication techniques. Moreover, their optoelectronic properties can be easily tuned through chemical structure engineering and functionalization. Fabricating thermocouples – the basic thermoelectric units – requires p- and n-type materials with matching properties. At present, the main bottleneck towards the realization of organic TEGs is the lack of n-type materials with adequate performances, especially considering their scarce air stability and poor electrical conductivity. My research mainly

focused on exploring molecular doping strategies to improve the thermoelectric characteristics of OSCs. Solution-based processes were investigated since these can be efficiently integrated with high throughput direct-writing fabrication techniques, such as printing technologies. In OSCs doping occurs by blending the semiconductor with reducing (n-doping) or oxidizing (p-doping) chemical compounds, forming a multiphase semiconductor-dopant system with enhanced charge carrier density. In conjugated materials, charge transport is strictly linked to the microstructure, particularly the interconnectivity between more and less ordered regions. Introducing an additional component, such as dopant molecules, can significantly alter the morphology of the pristine material, possibly inducing structural reorganization, phase segregation and related charge-trapping effects, affecting the electronic transport properties. Considering n-doping, benzimidazolines represent the most widely employed family of dopants, thanks to their good solubility in commonly used processing solvents and their compatibility with both polymeric and small molecule semiconductors.

A factor strongly limiting the performances of these compounds is their scarce miscibility inside the semiconductor matrix. Chemical functionalization of the benzimidazoline structure is an established strategy to improve solid-state solubility. Herein, I present the study of a novel derivative bearing an iminostilbene moiety, which does not significantly modify the electron-donating properties of the benzimidazoline-core, as electrochemical measurements demonstrate. Introducing a rigid and planarized, yet π -conjugated, substituent leads to more efficient intercalation of the dopant molecules inside the crystalline domains of the benchmark n-type copolymer P(NDI2OD-T2). Synchrotron-based X-ray diffraction techniques and atomic force microscopy, performed on thin films, showed that, despite the disruption of the long-range crystalline order, supramolecular connectivity is maintained, thus preserving efficient charge percolation pathways. As a result, the highest electrical conductivity value of $1.1 \times 10^{-2} \text{ S cm}^{-1}$ for solution-doped P(NDI2OD-T2) was recorded, showing an improvement of almost one order of magnitude compared to the parent and commercially available dimethylaniline substituted benzimidazoline N-DMBI. The thermoelectric figure of merit is also improved compared to values reported in the literature. These findings support the claim that a careful tuning of the dopant chemical structure leads

to an improvement of the solid-state miscibility between the components. Even if benzimidazolines are generally regarded in the literature as air-stable molecules, experimental evidence led to question this statement. Indeed, it was possible to isolate N-DMBI main degradation product, forming due to the interaction with environmental oxygen and moisture. Surprisingly, progressive dopant oxidation did not directly lead to a deterioration of its doping capabilities, as shown by the electrical conductivity measurements performed on thin films of P(NDI2OD-T2). Thermal analysis of the N-DMBI samples allowed disclosing the role played by the generated by-product, serving as a nucleating agent for a new N-DMBI crystalline phase. If the mechanistic details are currently still under study, heterogeneous nucleation appears to effectively mediate dopant reactivity, allowing a more efficient doping interaction with the polymeric matrix. Further experiments involving the introduction in the semiconductor-dopant blend of an exogenous nucleating agent confirm a boosting effect on the electrical conductivity, leading to a 3.5 times enhancement compared to pure N-DMBI. Considering doped OSCs not as simple binary mixtures but as complex multiphase systems, allows a better comprehension of their transport properties. These findings pave the way for improved doping strategies focusing both on the synthesis of novel dopants and additives and

on the processing steps. These experimental investigations emphasise the fundamental role played by the microstructure of doped OSC samples on electronic transport. Achieving fine control over the interaction among the involved phases is essential to realize organic blends with enhanced zT . The results obtained in the current experimental framework have a more fundamental character since the formulated doped OSCs could not be implemented into fully operating TEGs. This is mainly ascribed to the intrinsic limited charge transport characteristics of P(NDI2OD-T2), which instead provides a large set of published data for comparison. Starting from a solid understanding of the thermoelectric properties of OSCs, the research community must transition towards an application-oriented approach, focusing also on novel designs, fabrication techniques and device integration. Combining materials development with the know-how derived from prototype fabrication will enable organic thermoelectrics to play a relevant role towards a sustainable technological future.

PREDICTIVE MODELLING OF ULTRAFAST HOT CARRIER DYNAMICS AND NONLINEAR PHOTOTHERMAL PHENOMENA IN DESIGNER NANOPHOTONIC STRUCTURES

Andrea Schirato – Supervisors: Giuseppe Della Valle, Remo Proietti Zaccaria

The recent outstanding advances in nanofabrication have enabled to shrink optical materials down to the nanoscale, leading to a transformative change in optical sciences. The new field of nanophotonics has emerged, aimed at investigating the unparalleled conditions of interaction between light and nanostructured materials, as well as at manipulating such conditions to develop forefront nanometric optical technologies.

Radically different paradigms of interaction between electromagnetic radiation and matter have been proposed beyond the conventional rules of optics, based on new phenomena arising at the nanoscale and unattainable in bulk materials. Among the most notable examples, *metasurfaces* represent a particularly exemplifying illustration. These are ultrathin optical components consisting of planar sub-wavelength arrangements of resonant nanostructures (meta-atoms). Thanks to their quasi two-dimensional (2D) configuration, these nanopatterned layers exhibit extraordinary optical properties, with no counterparts among naturally available materials. Negative refraction, cloaking and sub-wavelength focusing are few of the intriguing functionalities achieved by optical metasurfaces,

which have opened the way to the era of flat optics. Additionally, since the response of these nanostructures is dominated by that of their meta-atoms and, specifically, by the meta-atom resonances, metasurfaces offer exceptional flexibility. Rational design of the individual nanoresonators making up the array enables full control over the metamaterial behaviour. This allows for engineering electromagnetic fields at the nanoscale, tailoring light-matter interactions, manipulating properties of light with completely new tools.

In parallel to phenomena otherwise impossible, nanophotonics has disclosed novel routes to achieve already existing functionalities in nanometric volumes. Such findings have concerned linear functionalities, as beam steering or wavefront shaping, as well as nonlinear functionalities, for which optical nanostructures are highly attractive. The efficient coupling with light, localised resonances and strong field enhancements on deep sub-wavelength scales which characterise nanophotonic systems make them ideal to induce, intensify and engineer nonlinear optical effects, offering substantial advantages compared to conventional set-ups. This is

especially true when ultrashort lasers are involved. Femtosecond light pulses are able to trigger nonlinear optical phenomena more efficiently than continuous illumination, due to the higher peak intensities. As such, when photoexcited with ultrashort optical pulses, nanostructures experience a light-induced modification of their properties on the characteristic time scale of the interaction, typically from tens of femtoseconds to several tens of picoseconds. This offers opportunities to exploit enhanced nonlinear effects and manipulate light with unprecedented speed in ultracompact platforms.

In the plethora of nanostructures explored, plasmonic metals have taken on particular significance, owing to the unique properties of metals at the nanoscale, resulting from the spatial confinement of their free electrons. Light interacts strongly with the metal conduction-band electrons, resonantly exciting localized surface plasmons (LSPs), i.e. collective charge oscillations coupled to the electromagnetic modes bound to the conductor/dielectric interface. The phenomenon is known as LSP resonance, and enables a high light mode confinement in nanometric volumes. Plasmonic nanostructures have thus been

extensively studied and exploited in a variety of contexts benefiting from the enhanced coupling with light, as photodetection, solar energy harvesting, nonlinear optics and sensing.

In the ultrafast, nonlinear regime, plasmonic nanostructures have also been shown to hold promises. In these conditions, their response is dictated by a giant optical nonlinearity driven by nonequilibrium electronic states. Specifically, following ultrafast illumination, the LSP dephases quickly and releases energy to create *hot* electron-hole pairs with high energies. In their higher-energy states, hot electrons and holes promote processes otherwise unattainable. Driving photochemical reactions to increase catalytic yields, collecting carriers to enhance photovoltaics, or modulating light with unprecedented speed are few of the applications explored so far. Yet, such opportunities are limited by the carrier ultrafast relaxation, which dissipate the absorbed light energy by equilibrating with the environment and converting it into heat. This process promotes an ultrafast (picosecond) temperature increase of the metal and its surroundings, providing a local heating which can be exploited for several applications, as photothermal therapy of tumours. Due to their ability to combine light capture and energy conversion at the nanoscale, hot electrons in plasmonic nanostructures have attracted increasing attention and opened routes in science and technology.

The promising advances in hot carrier physics and hot carrier-based nanophotonic technologies rely on the understanding of the nonequilibrium mechanisms regulating the interaction between light, electrons in the material and the environment. For this purpose, accompanying experimental investigations with advanced theoretical and numerical tools is paramount. Accurate simulations are essential to determine the optical behaviour of systems of arbitrary complexity and to gain insight into light-matter interactions at the nanoscale. Moreover, a comprehensive picture of the effects of hot carrier relaxation requires multiscale, multiphysics numerical tools, to fit the interdisciplinary contexts where nonequilibrium electrons are exploited. Advantages of a predictive modelling of these phenomena are not limited to understanding the fundamentals of hot carrier-based nanophotonics. The development of holistic simulations, ideally balancing accuracy and computational complexity, would indeed enable the design of optimal nanophotonic systems and nanodevices implementing hot-carrier-driven functionalities. Quantitative predictions of the response of such systems would allow one to engineer the hot carrier photophysics, in view of real-world applications.

In the sparkling landscape of efforts to propose blueprints for advanced nanophotonic systems exploiting engineered light-matter interaction, the research activities summarised in this thesis are ascribed. This

manuscript has the two-fold aim of presenting suitable approaches to model light-matter interaction at the nanoscale, and of showing that a rational design of nanophotonic structures is possible and enables to achieve advanced optical functionalities. The techniques to describe i) the ultrafast dynamics of hot carriers in nanostructures, with particular emphasis on plasmonic materials, ii) the electromagnetic and (photo)thermal phenomena at the nano- and macroscale, iii) the optical nonlinearities driven by nonequilibrium electrons are first introduced. Details on the modelling approaches are followed by an overview of our contributions to the field of hot carrier-based nanophotonics. Examples are reported of nanophotonic systems, mainly in metastructure configuration, designed to achieve various functionalities, encompassing ultrafast control of light, all-optical reconfiguration, photothermal drug release, solar-driven steam generation, photocatalysis.

Taken together, this work aims at indicating a possible route to conceive hot carrier-based nanodevices for real-world applications. The presented segregated multiphysics modelling, validated by ultrafast spectroscopy techniques, can provide us with valuable tools to understand and rationally manipulate the complex mechanisms of light-matter interaction at the nanoscale, paving the way for a novel class of nanophotonic devices fully exploiting the potential of hot carriers.

NOVEL SEMICONDUCTOR PHOTON SOURCES FOR QUANTUM APPLICATIONS

Giulio Tavani - Supervisor: Monica Bollani

Over the last few years, quantum communication has become increasingly important from a technological and pure research perspective. For this reason, a great effort has been made to design and fabricate novel light sources pivotal for quantum optics experiments.

In this PhD activity, we present the fabrication and the optical characterization of two novel light sources to implement the quantum key distribution (QKD) protocol. QKD is perhaps the most known quantum communication achievement. It enables two users (Alice and Bob) to share a secret key that will be later used to encrypt a message. Being based on quantum principles, QKD permits Alice and Bob to notice the presence of an eavesdropper during the communication of the key whereas this is impossible using a classical data transmission system.

The first implementation of QKD is the so-called BB84 protocol. This protocol is based on single photon sources. Many years of research have been spent on their design. Today, for the challenges in their implementation, they are commonly replaced with attenuated laser pulses in the QKD experiments.

A physical effect that is frequently adopted to implement single

photon sources is spontaneous parametric down-conversion (SPDC). This is a second-order non-linear effect present in systems that lack inversion symmetry. In SPDC, a photon is converted into two photons with lower energies. As it is well-known, non-linear effects are poorly efficient and usually, the approaches to tackle this problem are two: either a brute force approach based on the amplification of the optical pump or the adoption of an optical cavity where the incoming light is confined and therefore, the electric field interaction with the material is boosted. Several optical systems have been proposed as optical cavities. One of the most widely used is photonic crystals. Indeed, it is possible to engineer the

band structure of the photonic crystal and to confine light at the fundamental harmonic wavelength. In this thesis, we are going to present a doubly resonant AlGaAs photonic crystal meaning that both the fundamental and the second harmonic wavelength are spatially and temporally confined in the cavity. Such a condition is forbidden using the classical band structure engineering mentioned before but a more complex approach has to be applied. In our case, the second harmonic wavelength is confined using a bound state in the continuum (BIC). Such a state falls into the light cone of the photonic structure and yet, it does not emit light for symmetry reasons, thus it creates a resonance in the cavity. In the first part of the thesis,

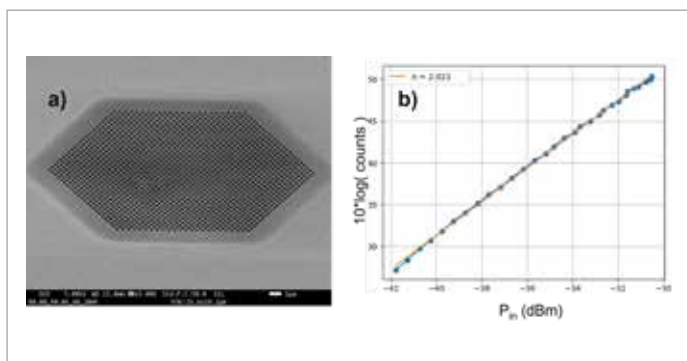


Fig.1 - In figure a) a tilted SEM view of the doubly photonic crystal. The dark border around the cavity is due to the suspension. In figure b) the counts generated at the second harmonic wavelength versus the input power at the fundamental harmonic. The slope of the linear fit is equal to 2 as expected from the theory.

we introduce the design of the photonic crystal cavity, its fabrication, and preliminary optical characterization. Resonant scattering measurements are presented to study the resonances of the fabricated structures. Since the position of the resonances strongly depends on the fabrication parameters, lithographic tuning was carried out. Among the cavities that we have fabricated and characterized, we have found one that is doubly resonant at 1566 nm. We present its second harmonic (SHG) characterization, showing the quadratic dependence of SHG intensity on the fundamental wavelength power. Finally, we compute the second harmonic conversion efficiency. SPDC measurements are in process.

The second part of the thesis is centered on the possibility to implement a quantum key distribution protocol using a silicon photonic platform. It is quite well known that silicon photonics is catching on since it is pivotal to integrate several optical

components on the same chip and to pave the way to photonic quantum computers, improved LIDARs, and quantum sensing. Silicon performs very well for passive optical components in the near-infrared wavelength range and a lot of effort was spent to implement active optical components. In the specific, germanium photodetectors have been implemented in silicon and despite lacking the possibility to exploit the Pockels effect, optical modulators have been fabricated thanks to the plasma dispersion effect.

Unfortunately, single photon and laser sources on silicon are still missing. Today, the most common approaches to implementing light sources on silicon are hybrid or heterogeneous integrations with other materials.

In this work, we would like to tackle this problem from a different perspective. Recently, it was demonstrated that it is possible to implement a secure version of quantum key distribution using an arbitrary photon statistic distribution. Given this, we conceived a fully

CMOS-compatible light source. The proposed device is a silicon p-n junction where an erbium-oxygen co-doping is introduced near the depletion region. Upon setting a potential difference between the two pads of the device, electron-hole pairs are created and their recombination excites the erbium ions that will eventually emit.

In the second part of the thesis, we are going to provide a comprehensive view of the physical background of this light source, its nano-fabrication, and electrical and optical characterization. Special attention is given to the analysis of oxygen-erbium doping since it has a strong impact on the luminescence of the device. In the optical characterization part, we present two kinds of devices: the first is characterized in open space whereas the second has an embedded waveguide, and the emitted photons by the erbium ions are guided, collected, and measured.

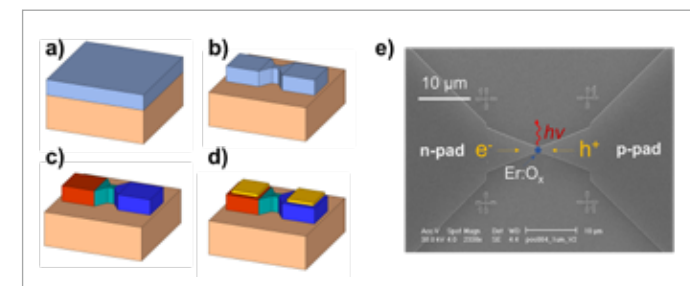


Fig.2 - (a) Silicon on insulator wafer, the silicon layer is 220 nm-thick and it lies on a 3 μm-thick SiO₂ buried layer. (b) Mesa of the device defined by electron beam lithography (30 keV) using a positive resist (PMMA). The etching is performed via a Bosch process. (c) Sketch illustrating the doping of the device. In red, the p-area doped with boron, in blue, the one doped with phosphorous, and, in green, the region co-doped with erbium and oxygen. (d) Final device. In yellow, the electrical contacts made of titanium and gold.

UNRAVELLING THE OPTOELECTRONIC PROPERTIES OF TIN HALIDE PEROVSKITES FOR INNOVATIVE DEVICE ARCHITECTURES

Antonella Treglia – Supervisor: Annamaria Petrozza

Metal halide perovskites are currently in the spotlight due to the impressive evolution of their application in photovoltaics. Recently, solar cells based on lead halide perovskites (LHPs) have reached conversion efficiencies over 25%. Besides, other promising applications, such as light emitting diodes, photodetectors and lasers have been demonstrated. The main reasons for this success are the high absorption coefficients, long carrier diffusion lengths and long carrier lifetimes, but also the promise of inexpensive fabrication. Over the last few years, tin halide perovskites (THPs) have emerged as highly promising materials for efficient single junction solar cells thanks to the achievable bandgap of 1.35-1.4 eV with ASnI_3 compositions. Absorbers with this bandgap result to be optimally matched to the solar spectrum and potentially produce devices with power conversion efficiencies of up to 30%. This has attracted great attention for its potential applications in tandem devices, single-junction solar cell, light emitting diodes and lasers. THPs indeed feature large absorption coefficients, sharp absorption onsets, low exciton binding energies and high photoluminescence

quantum yields. Nonetheless, THP solar cells lag far behind their lead-based counterparts in terms of efficiency (up to ~13 %) and operational stability. The main reason is that THPs are p-doped semiconductors with limited carrier diffusion lengths and short lifetimes, while the foremost studied LHPs are intrinsic. Such p-doping is induced by highly stable shallow Sn vacancy defects and by the tendency of tin to oxidize to the 4+ state. Much effort has been invested into controlling the main disparities with LHPs, focusing especially on reducing the self-doping of the material and avoiding tin oxidation. However, an in depth understanding of the effect of these features on the optoelectronic properties of THPs would allow to not just tolerate, but even exploit them for innovative device operation and architectures. For both photovoltaic and light emission applications, high rates of radiative recombination of carriers are essential for efficient device operation. Such a process competes with the trapping of the carriers at defects. The trap-limited recombination is usually investigated by monitoring the quantum yields and dynamics of the photoluminescence (PL). This approach allows to investigate

the intrinsic properties of perovskites, without the influence of complex interfaces and electrodes. The fundamental optoelectronic properties related to radiative and non-radiative recombination processes are explored to establish the interplay between doping and trapping in $\text{FA}_{0.85}\text{Cs}_{0.15}\text{SnI}_3$. We use a combination of steady-state optical characterization, time-resolved photoluminescence (TRPL) and pump-probe ultrafast transient absorption spectroscopy (TAS) to explore the recombination dynamics. The dominant processes taking place in different photoexcitation conditions are studied as a result of electronic and chemical doping, oxidation, and density of surface to bulk trap states. We support experimental results with carrier dynamics simulations and DFT calculations of defects. Our findings show that the dominant recombination path for electrons in THPs is either with traps or with dopant holes *via* monomolecular processes, depending on their relative value and the range of excitation density considered. If doping is sufficiently low monomolecular trap-assisted recombination is the limiting process, inducing excitation-dependent lifetime and low PLQY values at low

injection levels. When doping dominates both lifetime and PLQY results to be independent on excitation density. Up to a reasonable density (in the order of 10^{18} cm^{-3}) doping boosts the emission thanks to the radiative recombination of dopant holes with photogenerated electrons. For higher doping density, Auger non-radiative recombination becomes the limiting recombination path decreasing performances even at low photoexcitation density due to the high probability of the hole-hole-electron recombination to happen. The Auger induced reduction of PLQY even at low excitation density (typical of device operating conditions) must be carefully considered when optimizing material performances. Different strategies have been studied to control the intrinsic doping, such as the use of reducing agents, alternative solvents, passivating additives and the addition of extra Sn^{2+} compensation. Up to now, tin fluoride (SnF_2) is the most commonly used additive to improve the film quality and to avoid the formation of Sn vacancies, leading to reduced background hole densities, during the film formation. The introduction of SnF_2 increases the

lifetime and radiative efficiency by reducing the background doping and passivating electronic trap states. Computational studies show how upon addition of a molar fraction of SnF_2 , self-p doping is mitigated. Simultaneously, surface hole and electron traps are passivated, thus justifying the experimental observations. We finally investigate the fundamental optoelectronic properties of THPs when integrated in a device. The currently used architecture of lead-based solar cells, where an intrinsic absorber is sandwiched between two organic extraction layers (pin), is intrinsically not suitable for THPs. Indeed, it would result in a p-p-n structure (as long as the THP remains intrinsically p doped) with inefficient charge extraction. The short carrier lifetimes deriving from the intrinsic p-doping and the upshifted valence and conduction bands result in a reduced extraction capability. The free carrier dynamics in presence of extraction layers are probed with TAS from the fs to μs time scales. We evidence changes in the extraction of electrons and holes in different temporal regimes and identify the effect of long-lived trap states. The band alignment, surface

trap distribution and charge transfer are probed for mixed $\text{FA}_{0.85}\text{Cs}_{0.15}\text{Pb}_{1-x}\text{Sn}_x\text{I}_3$. As lead-based perovskite is alloyed with tin, its doping density, valence band position and bandgap can be gradually tuned, resulting in a modified energetic landscape of photogenerated carriers affecting carrier extraction.

HIGH-SPEED MULTIPLEX CARS MICROSCOPY IN THE ENTIRE RAMAN ACTIVE REGION THROUGH SUPERCONTINUUM GENERATION IN BULK MEDIA

Federico Vernuccio – Supervisor: Dario Polli

Introduction

Raman microscopy is a powerful vibrational technique for life sciences delivering chemical maps of cells and tissue in a label-free and non-invasive manner. Despite its high specificity and sensitivity, spontaneous Raman (SR) features a small Raman cross-section preventing high-speed imaging. Coherent anti-Stokes Raman scattering (CARS) provides several orders of magnitude higher speed exploiting third-order nonlinear optical processes. In its simplest implementation, CARS delivers to the sample two spatially and temporally overlapped picosecond pulses, pump and Stokes, at frequency ω_p and ω_s , respectively, whose frequency difference $\Omega = \omega_p - \omega_s$ is resonant with a vibrational mode Ω_r of the scrutinized sample. The signal arises in correspondence with the anti-Stokes frequencies region, blue-shifted with respect to the pump and Stokes beams. This approach, known as narrowband CARS, allows us to acquire a single vibrational mode at a time. Broadband CARS (BCARS) employs a narrowband pump beam with a broadband Stokes beam thus merging the high acquisition speed of narrowband CARS with the high chemical specificity of SR.

CARS suffers from the presence of the so-called non-resonant background (NRB), a nonlinear signal generated by out-of-resonance four-wave mixing that distorts the vibrational line-shapes. While, in the narrowband configuration, NRB limits the sensitivity and specificity of the technique, in the broadband approach, NRB can be exploited to amplify the weak Raman modes of the fingerprint region ($400\text{--}1800\text{ cm}^{-1}$). The line-shape distortions can be removed in post-processing, exploiting either numerical methods or deep-learning approaches. Despite many improvements in the last decade, BCARS approaches struggle to entirely cover the biologically relevant Raman window ($400\text{--}3200\text{ cm}^{-1}$), spanning from the fingerprint spectral region to high-frequency region ($2800\text{--}3100\text{ cm}^{-1}$).

I demonstrated a novel and high-speed approach to BCARS that answers this need. The BCARS microscopy platform (Fig. 1) starts with a 2-MHz repetition rate amplified Ytterbium laser system at 1035 nm . The system produces 3.7 ps narrowband pump pulses, determining the spectral resolution of the system ($\approx 9\text{ cm}^{-1}$), and broadband Stokes pulses ($1200\text{--}1600\text{ nm}$) through white-light supercontinuum in bulk media. I pre-compressed the Stokes pulses through a prism compressor to sub-20 fs pulses at the sample, thus compensating for the positive group delay dispersion mainly introduced by the first microscope objective. A mask is inserted after the second prism of the compressor to finely tune the spectral bandwidth of the Stokes beam. The two beams are spatio-temporally combined using a dichroic mirror

and a mechanical delay stage, and then sent to a home-made vertical transmission microscope, designed in upright configuration. The sample is raster-scanned with an XYZ stage, while sample illumination and collection are performed with two 0.85-NA air objectives. After the microscope, the anti-Stokes component is detected with a spectrometer equipped with a CCD camera. Compared to conventional systems based on multiplex CARS operating with a higher ($40\text{--}80\text{ MHz}$) repetition rate, our platform employs high-energy ($\approx 2\text{ }\mu\text{J}$) pulses, enabling us to replace the use of photonic crystal fibers for broadband beam generation with a 10-mm YAG crystal. This solution leads to a more robust, compact,

and alignment insensitive setup configuration. Furthermore, the generated white-light source shows long-term stability and does not suffer from wavelength-dependent intensity fluctuations that may affect the CARS spectral shape. The employment of a low repetition rate also boosts the setup performance in terms of signal quality and acquisition speed. Eventually, the system works in a red-shifted spectral region (1035 nm for the pump and $1200\text{--}1600\text{ nm}$ for the Stokes) with respect to standard CARS setups (800 nm for the pump, $830\text{--}1000\text{ nm}$ for the Stokes), allowing us to employ higher laser intensities on the sample before the onset of photo-damage.

The pre-compressed Stokes pulses enable accessing the first part of the vibrational spectrum (from 500 to 1400 cm^{-1}) through impulsive excitation of the vibrational modes and the remaining part (from 1400 to 3100 cm^{-1}) through inter-pulse excitation between the narrowband pump and the broadband Stokes beam. The combination of these two processes for CARS generation, namely three-color and two-color CARS mechanisms, respectively, generates good quality hyperspectral data when a moderate average power of the Stokes ($< 10\text{ mW}$) and pump ($< 25\text{ mW}$) beams is used to shine the sample. To extrapolate the maximum amount of information from the hypercubes, I designed a novel data-processing pipeline including: (i) a spectral denoiser based on a convolutional neural network architecture; (ii) a NRB removal numerical algorithm based on the time-domain Kramers-Kronig relations, and (iii) spectral unmixing methods to identify the pure spectra and the relative abundances of the different species. I demonstrated state-of-the-art speed ($\approx 0.8\text{ ms/pixel}$, limited by the readout time of the CCD) and unprecedented sensitivity ($\approx 14\text{ mmol/L}$) for multiplex CARS. The BCARS microscope was used to image cancer cells and to deliver large field-of-view ($>600\times 600\text{ }\mu\text{m}^2$) chemical maps of heterogeneous biological samples, detecting tumor in the liver of mouse models (Fig. 2). I envisage that the presented BCARS platform may find important applications in biomedical science, especially in the field of cancer research.

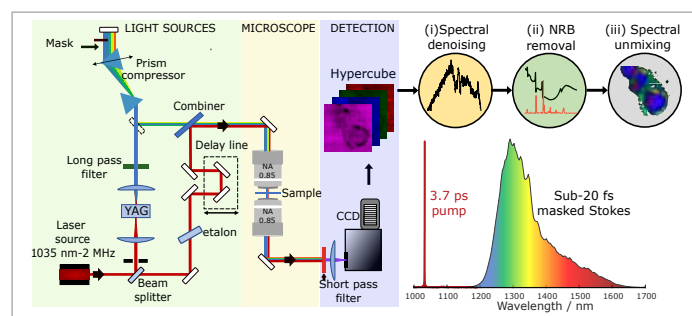


Fig.1 - Scheme of the experimental setup, post-processing pipeline, and pump and Stokes spectra. HWP: half wave-plate. PBS: polarizing beam splitter.

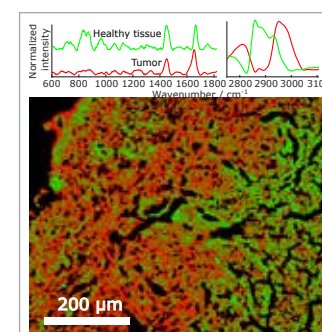


Fig.2 - $600\times 800\text{ }\mu\text{m}^2$ BCARS imaging on a tumoral liver slice of a mouse model with spectra associated with tumor (red) and healthy regions (green). Imaging settings: 300×400 pixels; 3 ms pixel exposure time; $2\text{ }\mu\text{m}$ pixel size.

HIGH REPETITION RATE IR PUMP-PROBE ON DOPED SEMICONDUCTOR NANOCRYSTALS

Andrea Villa – Supervisor: Francesco Scotognella

In the last decades, ultrafast transient absorption (TA) spectroscopy has established itself as one of the most important techniques for the investigation of the photo-physical properties of several different materials, ranging from biomolecules to solid state samples. Recently, the advent of stable, high-repetition-rate femtosecond Yb-based lasers sources has opened the way to the possibility of strongly increasing the speed and signal-to-noise ratio (SNR) of pump-probe measurements, pushing the limits of sensitivity even further and offering a competitive alternative to well-established Ti:Sapphire laser systems. Designing solutions exploiting the high repetition rate offered by said lasers in several different spectral regions, including near- and mid-infrared (NIR/MIR), where fast-readout in-line detectors and dispersive spectrometers are not available, is important to study several materials displaying resonances outside of the visible. Examples of said materials are doped semiconductor nanocrystals (DSNCs), which display IR plasmonic resonances and have aroused interest for photocatalytic and photovoltaic applications due to their tunable carrier densities and interesting

optical properties. Examples of DSNCs include aluminum zinc oxide (AZO), indium tin oxide (ITO), sub-stoichiometric copper chalcogenides (Cu_{2-x}Se , Cu_{2-x}S , etc.) and many others. In this thesis, we present a highly versatile pump-probe setup running at 100 kHz and characterized by ample tunability and high temporal resolution for the pump, and an extended visible and IR coverage for the probe. The pump pulses are obtained either through a mid-infrared two-stage optical parametric amplifier (OPA) or by achieving higher harmonics of the laser fundamental. The probe is instead obtained by stable supercontinuum generation in bulk YAG crystals. Detection is performed through an interferometric spectrometer coupled to suitable detectors, performing detection directly at 50 kHz in both visible and NIR and retrieving the shot-to-shot stability offered by the laser, achieving high SNR and good spectral resolution. The setup has been used to perform several test measurements, determining its maximum sensitivity and temporal resolution. After characterization, the setup has then been used to perform ultrafast transient absorption measurements on dropcast nanocrystalline films

of Cu_9S_5 (digenite), a p-type semiconductor which could be of interest as a suitable alternative to transition metal dichalcogenides for the realization of thin p-n junctions and for integration into IR absorbing photovoltaic cells. Finally, measurements on ITO-MoS₂ heterojunctions have been performed to verify the possibility of achieving hot electron transfer from ITO to MoS₂ after resonant photoexcitation of the ITO plasmon. The setup is supplied by a regeneratively amplified Yb laser running at 100 kHz and providing 100 μJ , 224-fs-long pulses at 1030 nm, of which a 50 μJ fraction is used to realize the pump and probe arms. A small fraction of the energy of 2 μJ is used to achieve the probe beam, obtained by focusing the beam into 0.6- and 1-cm-long YAG crystals respectively, thus covering the 0.52-0.95 μm and 1.15-2.1 μm visible and NIR regions. The remaining energy is modulated at 50 kHz through a Pockels cell and used to achieve the pump beam, which is either the 2nd, 3rd or 4th harmonic of the fundamental (0.515, 0.343 and 0.257 μm respectively), or the output of a widely tunable two-stage OPA spanning the whole 1-10 μm region. The OPA

is constituted by a non-collinear BBO-based first stage pumped at 515 nm and amplifying a 1.15-2.1 μm NIR seed, followed by a collinear second stage pumped at 1030 nm and exploiting either periodically poled lithium niobate (PPLN) or LiGaS₂ (LGS). These crystals allow to achieve further amplification of the seed and the simultaneous generation of an idler spanning the 2-10 μm region. Signal and idler are retrieved through proper optical filters, and the high output powers allow to achieve second harmonic generation (SHG), extending the spectral coverage up to 0.575 μm by frequency doubling of the signal. The signal pulses display broad spectra which can sustain temporal durations comprised between 40 and 100 fs, suggesting the possibility to achieve high temporal resolution also with the idler pulses due to nonlinear phase transfer, although between 2 and 4.3 μm compression is required. SHG-FROG measurements of the signal tuned at 1.6 μm confirmed a temporal duration of 43 fs, while the corresponding idler at 2.85 μm was far from TL, requiring compression through bulk propagation in suitable materials like CaF₂. Detection exploits an interferometric spectrometer followed by suitable single pixel detectors, thus fully exploiting the high repetition rate offered by the setup both in the visible and NIR. Synchronization of the system is achieved by feeding the trigger signal from the laser to a digital delay generator, which is used to create reference signals

for both the Pockels cell and the lock-in amplifier demodulating the detector's signal. Custom photodetectors with tailored electrical response have been realized to maximize the SNR of the system. An avalanche Si photodiode (0.4-1.1 μm) is used in the visible range, while an extended InGaAs (0.9-2.1 μm) photodiode covers the NIR. The probe is spectrally resolved by using a common path birefringent interferometer (GEMINI, Nireos), working in the 0.4-4.2 μm range. The differential measurement is performed by first measuring the static transmission of the sample at negative pump-probe delays, demodulating the signal from the detector at 100 kHz. The same operation is then repeated at 50 kHz to retrieve the differential transmission for several values of the pump-probe delay, reconstructing the pump-probe signal. After proper data processing of the interferential measurements standard spectrally resolved pump-probe maps are retrieved. The system has been tested by measuring interlayer excitons' formation dynamics in WSe₂-MoSe₂ hetero-bilayers after photoexcitation of MoSe₂'s A exciton. Since the interlayer exciton of this heterostructure is characterized by an oscillator's strength 100-1000 times lower than intralayer excitons, measurement of the associated signal at low pump fluences constitutes a good benchmark for the sensitivity of the setup. Even for pump fluences as low as 1 $\mu\text{J}/\text{cm}^2$ it was still possible to resolve the signal, which was found to be

as low as 10⁻⁶ at its peak value. Moreover, characterization of the ultrafast plasmonic response of dropcast nanocrystalline films of Cu_9S_5 produced by reactive annealing of a thin copper foil has been performed. The sample, which displayed a broad plasmonic absorption located in the NIR spectral range and peaking at 2100 nm, was pumped at 1.8 μm , thus performing intraband excitation, and probed in both visible and NIR ranges. The measurements quantified the hole-phonon and phonon-phonon scattering lifetimes, which were respectively found to be $\tau_1=360 \pm 20$ fs and $\tau_2>1$ ns. This was the first step in the characterization of the material before its integration into p-n junction with suitable hole acceptor materials. Finally, measurements on ITO-MoS₂ heterostructures were performed to investigate the possibility of achieving hot electron transfer from ITO to MoS₂ after resonant photoexcitation of the ITO plasmon at 1.75 μm . By probing the region of the A exciton transition of MoS₂, we verified the presence of charge transfer by observing the bleaching of the transition due to partial filling of the conduction band of MoS₂. Even in the presence of a low electron transfer efficiency and at low pump fluence, the high sensitivity of the setup allowed to effectively resolve the signature associated to the charge transfer process.

ULTRAFAST DYNAMICS IN MOLECULES FOR ORGANIC OPTOELECTRONICS

Yingxuan Wu – Supervisor: Rocío Borrego-Varillas

During my Ph.D. I investigated the ultrafast response mechanism inside molecules when they interact with light. These processes, such as photoinduced electron transfer and charge transfer processes, occur in a short timescale of femtosecond (fs) down to a few hundred attoseconds (as). The understanding of these processes is at the basis of core technologies aiming, for example, in organics optoelectronics applications, where the effective conversion of solar energy into electrical energy is sought. Here, we investigated the ultrafast dynamics following photoionization in paranitroaniline (pNa), the simplest donor-acceptor system. As depicted in the top left of Fig. 1, the molecule is characterized by an NH_2 group that can donate an electron called donor and a NO_2 group at the opposite side that attracts electrons called acceptor; a π conjugated system of the benzene ring links these two groups. We explore the role of functionalization of inductive-conjugative effect in metanitroaniline (mNa) by changing the acceptor group's position and the donor group's electron affinity through double methylation in N,N-Dimethyl-paranitroaniline (DmNa). The

chemical structures of the three compounds are represented on the top right panel of Fig. 1. Using a synergetic approach, we combined our effort both using real-time imaging of the electronic-nuclear motion using the attosecond beamline developed in the laboratory at the Physics department of Politecnico di Milano,

schematically represented in the central panel of Fig. 1, with the experimental result by Photo-Electron Photo-Ion COincidence (PEPICO) energy-resolved measurements obtained with the experimental campaign at GasPhase beamline at Elettra Synchrotron facility and quantum simulations provided by our collaborators from the

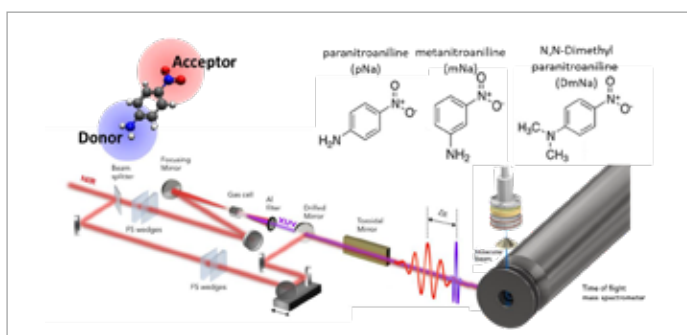


Fig.1 - Top-Left, the structure of push pull molecule; Top-Right, the chemical structure of paranitroaniline (pNa), metanitroaniline (mNa) and N,N-Dimethyl-paranitroaniline (DmNa); Center, the schematic of the attosecond beamline to obtain the time-resolved measurement.

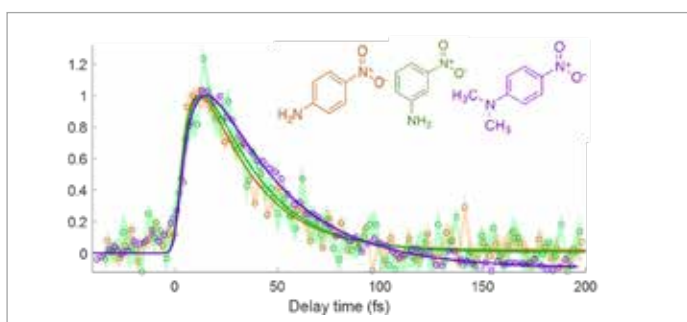


Fig.2 - Relative ion yield of the fragment NO^+ (mass to charge ratio 30) with the corresponding fit for the three different compound obtained using XUV pulses generated in Krypton (20-40 eV).

Universidad Autónoma de Madrid. The combination of the three complementary approaches univocally describes the observed ultrafast dynamics correlated to the wave-packet spreading in the excited states of the cation. In more detail, the time-resolved measurement employed the attosecond eXtreme-UltraViolet (XUV) pump and InfraRed (IR) probe scheme, schematically shown in the main panel of Fig 1. The tunable attosecond XUV pulses, with spectrum ranging from 20 to 50 eV, ionizes the molecules leaving them in an excited state and giving start to the photodissociation process; the following <4 fs IR pulse tracks the evolution initiated by the pump pulse. The resulting positive charged photofragments are measured using a Time of Flight (TOF) mass spectrometer. We followed the change of the different mass fragments as a function of the pump and probe delay. We were able to identify

transient ultrafast dynamics of the dissociation of the positive ion of the acceptor group (NO^+ and NO_2^+) with a formation time around 10 fs and a relaxation decay with a time constant of 24 fs for pNa, 25 fs for mNa and 33 fs for DmNa, shown in Fig 2. Through the distinctive fingerprint of the Coulomb explosion in the shape of these fragments in the mass spectrum and in combination with energy-resolved PEPICO measurements, we can unambiguously assign these dynamics to precise fragmentation pathways through the dication's state of the molecule and mediated by Coulomb explosion. Interestingly, we experimentally find this mechanism to depend on the XUV excitation energy, with higher photon energies leading to slower dynamics, as recorded in Table 1. Numerical simulations, using semi-classical trajectories with the surface-hopping method at the CASSCF level of theory,

m/q = 30	Xenon (15-30 eV)		Krypton (20-40 eV)		Argon (30-45 eV)	
	T rise (fs)	T decay (fs)	T rise (fs)	T decay (fs)	T rise (fs)	T decay (fs)
pNa	12,3±1,6	23,1±1,2	12,0±1,5	23,9±1,4	10,1±1,3	41,4±1,0
mNa	11,2±2,6	23,1±1,4	12,1±1,8	24,6±1,5	12,1±1,8	27,3±1,9
DmNa	12,1±1,8	24,3±1,3	11,5±1,4	33,0±1,2	13,4±1,5	39,8±1,4

Tab. 1 - Table summarizing the fitted decay and rise times of the fragment NO^+ , for the different compounds and the energy of the XUV pump.

demonstrate that the observed transient features are related to an ultrafast and efficient spreading of the cation nuclear wavepacket, which causes a progressively less efficient probing by the IR pulse to excite the wavepacket from the cationic state to the dication as time goes by. These results are pushing further the understanding of the ultrafast coupling among the internal degrees of freedom, which mediates the population transfer between the cationic states on femtosecond time scales. In conclusion, the combination of the ultrafast time-resolved spectroscopy, high energy resolved measurement, and theoretical calculations allowed us to disentangle the complex dynamics following photoexcitation in nitroanilines and shed new light onto the role of ultrafast wavepacket spreading in the internal relaxation of prototype donor-acceptor systems.